UNIVERSIDADE DE COIMBRA

FACULDADE DE CIÊNCIAS E TECNOLOGIA

Departamento de Ciências da Terra

Organic facies variability during the Toarcian Oceanic Anoxic Event recorded in southern France: Grands Causses, Quercy and Pyrenean basins

Carolina Maria Flores Marcelo da Fonseca

Mestrado em Geociências – Área de Especialização em Geologia do Petróleo

Orientadores científicos:

Prof. Doutor Luís Vitor da Fonseca Pinto Duarte, Faculdade de Ciências e Tecnologia da Universidade de Coimbra

Prof. Doutor João Graciano Mendonça Filho, Departamento de Geologia, Instituto de Geociências da Universidade Federal do Rio de Janeiro

Prof.ª Doutora Carine Lézin, Département Biologie et Géosciences, Université Paul Sabatier – Toulouse III

Junho, 2016

Dedico este trabalho
aos meus pais.

“Error never can be consistent, nor can truth fail of having support from the accurate examination of every circumstance.“

— James Hutton

Agradecimentos

Ao meu orientador, Professor Luís Vitor Duarte. Estou muito grato pela sua ajuda e orientação perspicaz ao longo desta dissertação e as suas críticas construtivas. Agradeço toda a confiança que depositou em mim e a oportunidade de desenvolver este trabalho tão desafiante.

Ao meu co-orientador, Professor João Graciano Mendonça Filho, pela oportunidade de trabalhar no Laboratório de Palinofácies e Fácies Orgânicas (LAFO) como membro da sua fantástica equipa. Por todas as discussões frutíferas que ajudaram a melhorar esta dissertação e por todo o apoio e amizade durante a minha estadia no Brasil.

Je voudrais tout d'abord remercier à mon co-directeur, le professeur Carine Lézin, pour toute son aide, sa critique constructive, tout au long de cette thèse. Elle a toujours été là pour me soutenir et me conseiller. Sans votre soutien et votre savoir-faire, ce travail n'aurait pas pu être possible.

À Dr.ª Joalice Mendonça, pela amizade, simpatia, hospitalidade e incansável apoio que me prestou durante a minha passagem pelo Rio de Janeiro e na realização desta dissertação.

Je tiens également à remercier Dr. Philippe Fauré pour m'avoir fourni les informations sur la biostratigraphie d'ammonite des trois sections étudiées.

Ao LAFO, por todo o apoio técnico e a todas as pessoas que lá trabalham por me receberem e me fazerem sentir em casa. Em particular, gostaria de expressar a minha gratidão ao Donizete de Oliveira, Jaqueline Souza, Thiago Barbosa, Taís Freitas, Sinda Gomes, Frederico Sobrinho e Ana Luiza pela simpatia e apoio.

Aos meus amigos e colegas do Departamento de Ciências da Terra (DCT), André Cortesão, Helena Moura, João Tomás, Joel Carvalho, Marisa Santos, Pedro Oliveira e Vitor Oliveira. Obrigada pela amizade, paciência e companheirismo.

Aos meus amigos, Estela, Inês, João e Zé Pedro, companheiros de uma vida. Obrigada pelo vosso apoio e amizade durante todo este percurso.

À Rosinha, por toda a tua ajuda, apoio e dedicação ao longo destes cinco anos.

Ao João Pedro, por me ensinares que nenhum sonho é inalcançável.

À minha mãe, pai, Zé, Patrícia, Simão e toda a minha família, por nunca me deixarem desistir dos meus sonhos e me apoiarem em todas as minhas decisões. Sou e serei eternamente grata por tudo que vocês dedicaram e investiram em mim.

Abstract

The Early Toarcian is marked worldwide by major environmental perturbations that resulted in organic-rich black shale deposition and carbon cycle disturbances, the so-called Toarcian Oceanic Anoxic Event (T-OAE). This organic-rich sedimentation is particularly recorded in southern France, namely in the Grands Causses (GCB), Quercy (QB) and Pyrenean (PB) basins. The main objectives of this study are the characterization of the organic matter (OM) of the upper Pliensbachian – early Toarcian sedimentary successions of these basins, definition of the organic facies and depositional paleoenvironments and to assess the OM thermal maturation. With these premises, a set of 38 samples was analyzed from the Suèges (GCB), Caylus (QB) and Pont de Suert (PB) sections using organic petrology techniques, including palynofacies, and geochemistry (Total Organic Carbon - TOC, sulfur and $CaCO_3$ content).

In the GCB, sedimentation occurred, during the late Pliensbachian, in a well oxygenated water body (TOC 0.6 wt.%) proximal to the terrestrial source area with marine influence. In the lattermost Pliensbachian is observed a shallowing of the water column with a decrease of marine influence and higher separation from the terrestrial source area under an arid climate. From the Tenuicostatum to the earliest Serpentinum zones is implemented a restricted and stagnated environment (TOC 5.7 wt.%, dominated by amorphous OM >97%) with partial closure of the basin. From the middle to late Serpentinum Zone occurs the reestablishment of the oxygen levels (TOC 2.8 wt.%) and of the paleoceanographic circulation patterns, with an increase of water level.

In the QB, late Pliensbachian to the earliest Toarcian (Paltus Subzone) is characterized by low TOC (0.2 wt.%) with sedimentation occurring in a shallow oxygenated proximal water body (high percentage of amorphous zoomorphs - hydrozoans) separated from the terrestrial source area under an arid climate, with emersion episodes. From the Semicelatum Subzone to Serpentinum Zone is observed a development of dysoxic to anoxic conditions (TOC 4.2 wt.%) associated with water column stratification and a more effective non-carbonate sedimentation with the increase of water level. The lattermost Serpentinum Zone is observed a shallowing of the water body with the development of a more oxidizing environment, although still with water column stratification in terms of oxygen levels to some extent.

In the PB, from the late Pliensbachian to the base of Semicelatum Subzone, from the Elegantum to the base of the Falciferum subzones and from the top of the Falciferum to the base of the Sublevisoni subzones, sedimentation occurs in a well oxygenated proximal water body with marine influence. From the Semicelatum to the base of the Elegantum subzones and in the Falciferum Subzone, occurs a shallowing of the water column leading to a more restricted and stagnated environment under a more arid climate.

Concerning the thermal maturity assessment study it supports a very similar thermal evolution for the GCB and QB indicating that OM is in the immature to early mature stages. The PB presents entirely different thermal history with OM in late mature to post mature stages.

The studied sections present slight differences in their paleoenvironmental depositional contexts further demonstrating that, although the T-OAE has a global character, in these basins it is controlled by local mechanisms. Furthermore, it is presented first occurrence of components from the Phylum Cnidaria, Class Hydrozoa, Order Hydroida, in organopalynological preparations, in sediments from the Lower Jurassic.

Keywords: Organic matter; palynofacies; hydrozoans; thermal maturity; Toarcian oceanic anoxic event; Grands Causses Basin; Quercy Basin; Pyrenean Basin.

Resumo

O Toarciano inferior é marcado por grandes alterações ambientais a nível global que resultaram na deposição de *black shales* ricos em matéria orgânica (MO) e em perturbações do ciclo do carbono, o designado Evento Oceânico Anóxico do Toarciano (EOA-T). Esta sedimentação rica em MO está particularmente bem registada no sul de França, nomeadamente nas bacias de Grands Causses (BGC), Quercy (BQ) e Pirinéus (BP). Os objetivos principais deste estudo são a caracterização da MO presente nas sucessões sedimentares de idade Pliensbaquiano superior – Toarciano inferior destas três bacias, a definição das fácies orgânicas e dos paleoambientes deposicionais e a determinação da maturação térmica da MO. Neste contexto, foram analisadas 38 amostras pertencentes aos perfis de Suèges (BGC), Caylus (BQ) e Pont de Suert (BP) através de técnicas de petrologia orgânica, incluindo palinofácies, e geoquímica (Carbono Orgânico Total – COT, enxofre e teor em $CaCO_3$).

Na BGC, a sedimentação durante o Pliensbachiano superior ocorreu num corpo de água proximal à área fonte, com alguma influência marinha e oxigenação (COT 0,6%). No Pliensbaquiano terminal ocorre uma diminuição da coluna de água e da influência marinha, com uma separação nítida da área fonte terrestre, sob um clima árido. Da Zona Tenuicostatum à base da Zona Serpentinum, dá-se a implementação de um ambiente restrito e estagnado (COT 5,7%, com predomínio de MO amorfa >97%). Na metade superior da Zona Serpentinum observa-se o restabelecimento dos níveis de oxigénio (COT 2,8%) e dos padrões de circulação paleoceanográficos, com um aumento da coluna de água.

Na QB, o intervalo entre o Pliensbaquiano superior à base do Toarciano inferior (Subzona Paltus) é caracterizado por baixos teores de COT (0,2%) com a sedimentação a ocorrer num corpo de água raso proximal (alta percentagem de zoomorfos amorfizados – hidrozoários), separado da área fonte terrestre sob um clima árido, com emersão episódica. Da Subzona Semicelatum à Zona Serpentinum observa-se o desenvolvimento de condições disóxicas a anóxicas associadas à estratificação da coluna de água (COT 4,2%) e uma sedimentação não-carbonática mais eficiente, com o aumento do nível da água. No topo da Zona Serpentinum verifica-se uma diminuição da coluna de água aliada a um ambiente mais oxidante.

Na PB, do Pliensbachiano superior à base da Subzona Semicelatum, da Subzona Elegantum à base da Subzona Falciferum e do topo da Subzona Falciferum à base da Subzona Sublevisoni, a sedimentação ocorre num corpo de água proximal, bem oxigenado, com alguma influência marinha. Da Subzona Semicelatum à base da Subzona Elegantum e na Subzona Falciferum observa-se a diminuição da coluna de água, com a implementação de um ambiente mais restrito e estagnado, sob um clima árido.

O estudo de maturação térmica indica uma evolução térmica similar para a BGC e a BQ onde a MO se encontra imatura a matura. A BP apresenta uma história térmica diferente, com MO matura a supermatura.

As sucessões estudadas apresentam pequenas diferenças nos seus contextos paleoambientais demonstrando que, apesar do EOA-T ter um carácter global, nestas bacias os seus mecanismos de controlo são locais. Neste trabalho é ainda apresentada a primeira ocorrência de componentes pertencentes ao Filo Cnidaria, Classe Hydrozoa, Ordem Hydroida, em preparações organopalinológicas, em sedimentos de idade Jurássico Inferior.

Palavras-chave: Matéria orgânica; palinofácies; hidrozoários; maturação térmica; Evento Oceânico Anóxico do Toarciano; Bacia de Grands Causses; Bacia de Quercy; Bacia dos Pirinéus.

Table of contents

List of Figures

List of Tables

List of Acronyms

AOM: Amorphous organic matter

C: Carbon

$CaCO_3$: Calcium carbonate

CAMS: Calcaires argileux et marnes à Soaresirhynchia

CH_2Cl_2: dichloromethane

CO_2: Carbon dioxide

CO_3^{2-}: Carbonate ion

DM: Decarbonated sample weight

EOM: Extractable organic matter

FM: Fluorescence mode

Fm.: Formation

GC: Gas chromatographer

GCB: Grands Causses Basin

GC-MS: Gas chromatography coupled to mass spectrometry

H: Hydrogen

HC: Hydrocarbons

HCl: Hydrochloric acid

HCO_3^-: Bicarbonate ion

HF: Hydrofluoric acid

HR_r: Hydroid random reflectance

IR: Insoluble residue

LAFO: Palynofacies and Organic Facies Laboratory

LC: Liquid Chromatography

Mb.: Member

MCH: Marnes et calcaires à Hildoceras

Mn: Manganese

MS: Mass Spectrometer

NOB: Non-opaque biostructured

NONB: Non-opaque non-biostructured

NSO: Nitrogen, Sulfur and Oxygen

O: Oxygen

OM: Organic matter

PB: Pyrenean Basin

Q: Red/Green quotient

QB: Quercy Basin

R_{eq}: Equivalent vitrinite reflectance (Fisher et al., 1980)

R_r: Mean random vitrinite reflectance

RWL: Reflected white light

SCI: Spore Coloration Index

SO_2: Sulfur dioxide

Stdev: Standard deviation

TM: Total weight of sample before acidification

T-OAE: Toarcian oceanic anoxic event

TOC: Total organic carbon

TS: Total sulfur

TWL: Transmitted white light

UV: Ultraviolet

VR_{eq}: Equivalent vitrinite reflectance (Bertrand and Malo, 2012)

$ZnCl_2$: Zinc chloride

Chapter I - Introduction

I.1. Problem statement and objectives

The early Toarcian is marked worldwide by major environmental perturbations that resulted in organic-rich black shale deposition and carbon cycle disturbances (pronounced carbon isotope excursions) that have been described in numerous sedimentary basins (e.g. Jenkyns, 1985, 1988; Hesselbo et al., 2000, 2007; Al-Suwaidi et al., 2010; Mazzini et al., 2010; Suan et al., 2010; Caruthers et al., 2011; Gröcke et al., 2011; Izumi et al., 2012).

The widespread record of such deposits led Jenkyns (1988) to interpret the early Toarcian anoxia as a global event, the so-called Toarcian oceanic anoxic event (T-OAE). Two hypotheses are currently thought to explain this geochemical event involving, in the first one, the creation of greenhouse effect conditions (global mechanisms) (e.g. Hesselbo et al., 2000; Jenkyns, 2003) and, in the second one, the intense marine productivity associated with restricted basins (local mechanisms) (e.g. Küspert, 1982; Röhl et al., 2001; Schmid-Röhl et al., 2002; Frimmel et al., 2004; van de Schootbrugge et al., 2005; McArthur et al., 2008).

Some authors indicate the development of a global greenhouse effect associated with the tectonic activity of the fractioning of the Gondwana (southern hemisphere) and the development of the Large Igneous Province of Karoo-Ferrar as the main cause (e.g. Duncan et al., 1997; Pálfy and Smith, 2000; Jourdan et al., 2005). The high levels of CO_2 and other greenhouse gases ejected during this intense volcanic activity would therefore originate a temperature increase giving rise to a long period of global warming (e.g. Jenkyns, 2003; Rosales et al., 2004; Wignall et al., 2005; Gómez et al., 2008; Dera et al., 2009). The CO_2 would also lead to a reduction of the pH of the sea water and a saturation of carbonate. The tectonic activity and temperature rise could also promote the release, to the ocean water and atmosphere, of the methane originated from the microbiological reworking of the organic matter (OM), deposited in the seafloor as methane hydrates, that would be oxidized in the more shallow and warm water levels (e.g. Hesselbo et al., 2000; Jenkyns, 2003; Emmanuel et al., 2006; Jenkyns, 2010). The progressive evolution of the reducing conditions through the denitrification phases, ammonium anaerobic oxidation, sulfate reduction and pyrite precipitation would result in the fractioning of several isotopic systems and mobilization and incorporation of trace elements to the carbonates (Mn), sulfates and OM (e.g. Jenkyns et al., 1991; Huckriede and Meischner, 1996; Jenkyns, 2010). The CO_2 sequestration in the organic-rich black shales and by reaction with the continental silicate rocks could have resulted in a climatic balance but implying a massive chemical alteration in the oceans (Cohen et al., 2004; Jenkyns, 2010 and references therein).

Several authors such as Schouten et al. (2000), Röhl and Schmid-Röhl (2005), van de Schootbrugge et al. (2005) and McArthur et al. (2008) presented an alternative theory, based on the OM record, suggesting that this event was controlled by local mechanisms and was restricted to the northwestern European epicontinental area. This hypothesis is based on McArthur et al. (2008) restrict basin model that suggests the existence of several restricted shallow basins in the European epicontinental seaway. The temperature rise led to a faster evolution of the hydrologic cycle and consequent increase in river discharge (higher nutrient transport rate) that ultimately resulted in a water column stratification that, associated with seafloor morphology, would lead to the partial enclose of the basin (maximum restriction interval). The suboxic to anoxic conditions at the base of the photic zone would therefore favor the organic matter-rich sediments deposition (e.g. Röhl and Schmid-Röhl, 2005; van de Schootbrugge et al., 2005).

In the Western Europe, the organic-rich stratigraphic record of the T-OAE represents one of the most widespread oil source rocks. Its petrographic and geochemical characteristics have been described for the Jet Rock beds of eastern England (Morris, 1980; Jenkyns, 1985; McArthur et al., 2008), the Posidonia Shale of northern Germany (Teichmüller and Ottenjann, 1977; Littke et al., 1987, 1991), southern Germany (Müller and Blaschke, 1969; Küspert, 1982; Prauss et al., 1991; Frimmel et al., 2004) and Luxembourg (Song et al., 2014); and the Schistes Cartons of the Paris Basin (Durand et al., 1972; Tissot et al., 1974; Huc, 1977; Alpern and Cheymol, 1978; Hollander et al., 1991; Disnar et al., 1996; van Breugel et al., 2006; Lézin et al., 2013). The same studies have been performed for the Lusitanian (Portugal) and Asturian (Spain) basins (Pina, 2015; Rodrigues et al., 2015a, b, c, d).

The Lower Jurassic of southern France has been the main focus of several stratigraphic, sedimentological and geochemical studies throughout the years (e.g. Trümpy, 1983; Cubaynes, 1986; Cubaynes et al., 1989; Harazim et al., 2013; Faure, 2002). However, no emphasis has been given to the study of the OM present in the organic-rich carbonate Toarcian sediments of the basins in this region, namely, the Grands Causses, Quercy and Pyrenean basins.

With these premises, the main objectives of this study are: i) to characterize, through palynofacies and organic geochemistry, the OM of the upper Pliensbachian – lowermost middle Toarcian sedimentary successions of the Grands Causses, Quercy and Pyrenean basins; ii) to define the organic facies and the depositional paleoenvironments of the analyzed successions; (iii) to compare the paleoenvironmental settings proposed for the three basins with the models of previous studies for the European epicontinental shelf evolution; and, (iv) to assess the OM thermal maturation using petrographic techniques.

I.2. Geological Setting

The Jurassic paleogeography of southern France is characterized by a number of interconnected shallow marine epicontinental basins bordered by the Central Massif to the North and open and in connection with the Tethys Ocean, in varying degrees, towards the South. Shallow marine sedimentation occurred in each basin isolated from each other by paleo-highs (Dumont, 1988; Lemoine and de Graciansky, 1988; Thierry et al., 2000).

As previously mentioned, during the early Toarcian, the stable European epicontinental shelf witnessed a period of environmental perturbations that led to the widespread deposition of organic rich sediments (e.g. Röhl et al., 2001; Schmid- Röhl et al., 2002; Röhl and Schmid-Röhl, 2005; McArthur et al., 2008; Hermoso et al., 2013). These sediments, such as the Posidonia Shale in southern Germany, the Jet Rock Beds in the Cleveland Basin of eastern England and the Schistes Cartons in the French basins, have been interpreted as the expression of widespread marine anoxic conditions of the T-OAE (van de Schootbrugge et al., 2013). In this geological framework are included the three selected basins for this study (Figures I.1 and I.2): Grands Causses, Quercy and Pyrenean basins. From each basin was selected one reference section, namely, Suèges, Caylus and Pont de Suert sections, respectively.

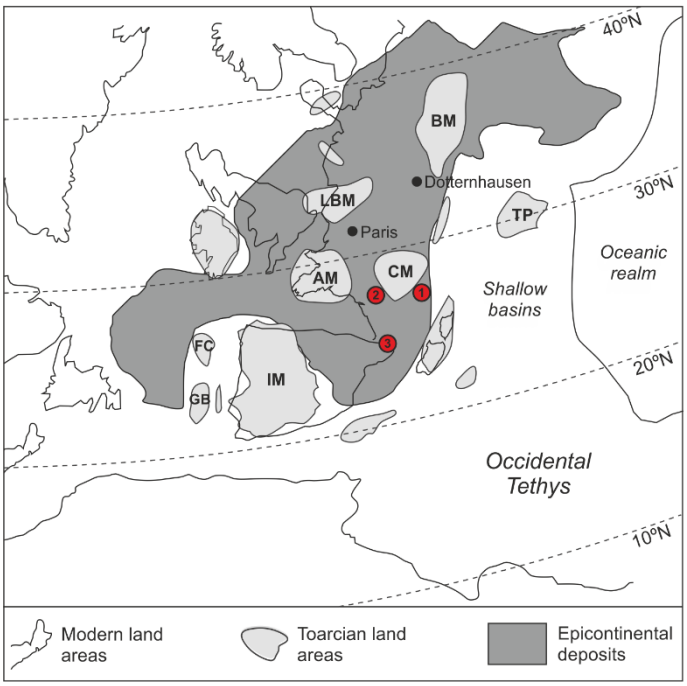

Figure I.1. Paleogeographic map of Early Jurassic with location of studied basins: 1 – Grands Causses; 2 – Quercy; 3 – Pyrenean (modified from van de Schootbrugge et al., 2005; Lézin et al., 2013). FC: Flemish Cap; GB: Galicia Bank; IM: Iberian Meseta; AM: Armorican Massif; CM: Central Massif; LBM: London-Brabant Massif; TP: Tisza Plate; BM: Bohemian Massif.

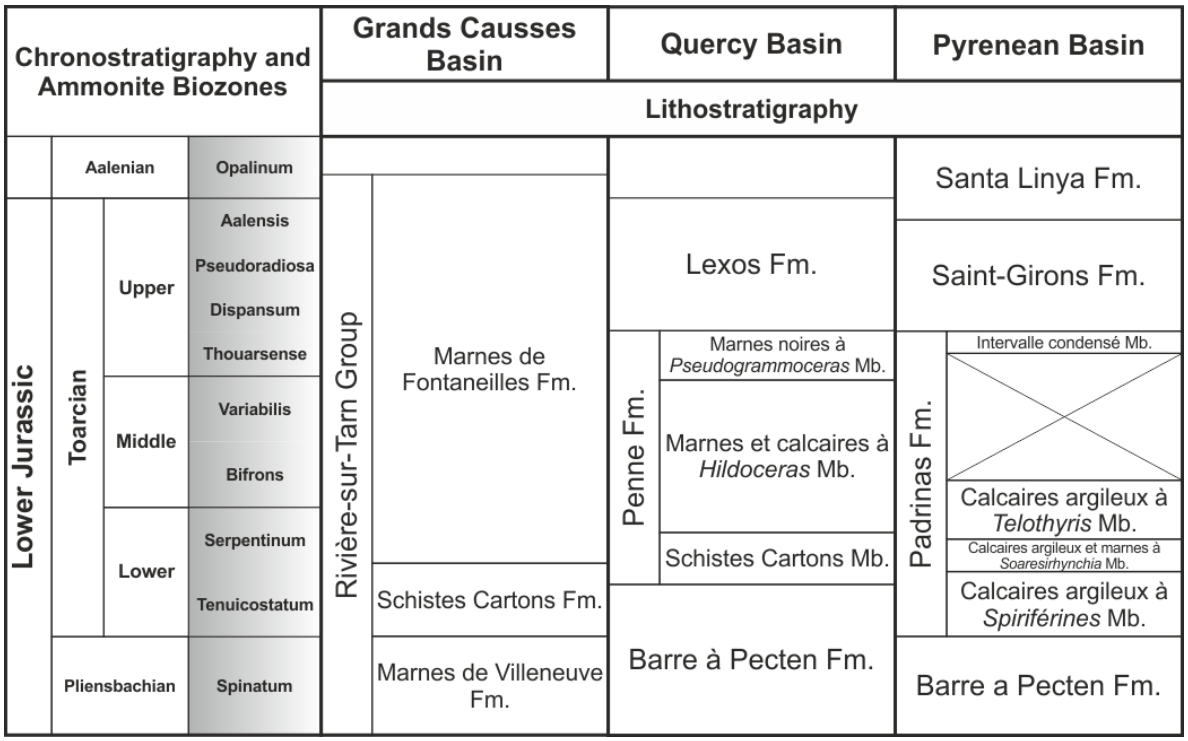

Figure I.2. Stratigraphic chart of the Grands Causses, Quercy and Pyrenean basins (compiled from Rey et al., 1995; Faure, 2002; Mailliot et al., 2009).

I.2.1. Grands Causses Basin

I.2.1.1. Definition

The Grands Causses Basin (GCB) is located in the central-South France with an extension of 30 km East-West and 70 km North-South (Figures I.1 and I.3). Jurassic sediments were deposited within an epicontinental sea associated with the Tethyan margin, at a paleolatitude comprised between 25º and 30º N (Trümpy, 1983; Disnar, 1996).

Structurally, this basin was a half-graben bounded by Hercyninan crystalline rocks belonging to different units of the French Massif Central, namely the Rouergue to the West (transition to the Quercy Basin), the Cevennes to the East and Aubrac to the North and the Montagne Noire to the south (Trümpy, 1983; Disnar, 1996) (Figure I.3).

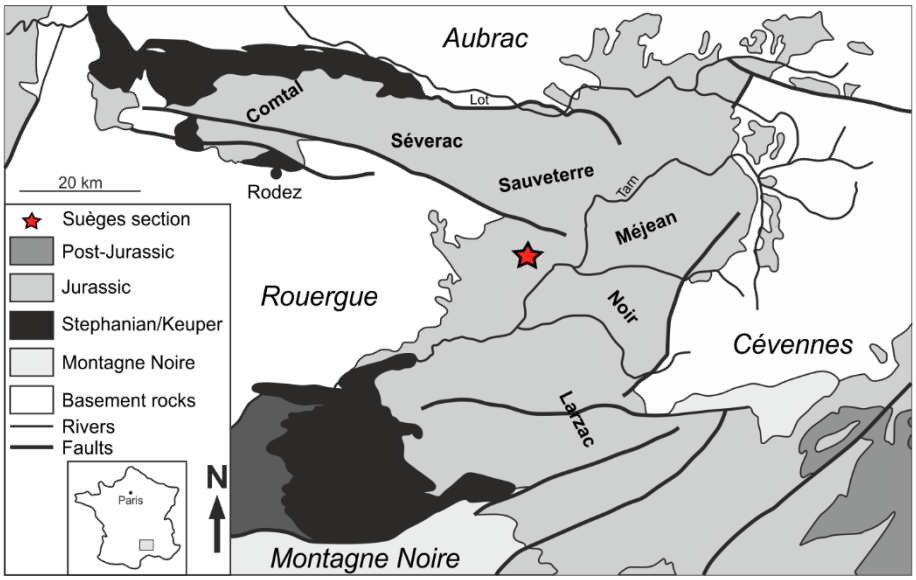

Figure I.3. Simplified geological map of the Grands Causses Basin and location of the studied Suèges section (modified from Mailliot et al., 2009).

The morphology of this small, partly enclosed, intracratonic basin was largely controlled by the late Hercynian structural evolution. The Early Jurassic is marked by an extensional tectonic phase reactivating some NNE–SSW normal faults (Arthaud and Matte, 1975). Spatial thickness variations more or less pronounced within the basin of the different lithostratigraphic units and even hiatuses suggest a clear differential subsidence (Trümpy, 1983).

Tectonics, stratigraphy and geochemistry of this basin have been studied by a number of authors, namely, Trümpy (1983), Graciansky et al. (1998), Mailliot et al. (2009), Harazim et al. (2013) and van de Schootbrugge et al. (2013).

I.2.1.2. Lower Jurassic lithostratigraphy

The thickness of the Lower Jurassic (Hettangian to Toarcian) (Figure I.2) infill strongly varies from the basin margins to the depocenter, with an average total thickness of about 400 m. Toarcian deposits vary from 15 cm to about 15 m in different localities (Morard, 2004) showing a deepening upward trend that reflects the long-term Early Jurassic first order sea level rise followed by a return to shallower conditions during the Aalenian and Bajocian. The sediments deposited on the margins of the basin are also characterized by the presence of repeated hiatuses (Trümpy, 1983).

According to Trümpy (1983), who established formally a number of lithostratigraphic units for the Lower Jurassic of the GCB, Hettangian to lower Pliensbachian sedimentation is assembled in the **Bourg Formation** (Fm). This formation is characterized by coarse grained fluvial to marginal marine sandstones overlain by

peritidal dolomicrites with subordinate claystone beds, grading upwards into oolites-and dark grey marl-limestone alternations of Sinemurian age. The lower Pliensbachian marks the onset of hemipelagic sedimentation defined by dark grey marl-limestone alternations overlain by the middle to upper Pliensbachian organic-rich marls with intercalated limestones of the **Marnes de Villeneuve Fm.** (Trümpy, 1983; Harazim et al., 2013).

The Pliensbachian/Toarcian boundary is marked by a hard-ground enriched in oxidized and phosphatized material, often in the form of nodules, corroded belemnite rostra, and fossil wood, all indications of condensation and reworking (Morard, 2004). This boundary corresponds to a depositional hiatus (Trümpy, 1983; Guex et al., 2001; Morard et al., 2003; Morard, 2004) with an estimated duration of about 200–300 kyr (Guex et al., 2001) interpreted by Mailliot et al. (2009) as an emersion surface. Although the contact between the Toarcian black shales and the underlying Pliensbachian marls is sharp, van de Schootbrudge et al. (2010) found no evidence for emergence and erosion in the Fontaneilles section advocating that submarine erosion through currents and condensation more likely explain the missing ammonite zones in basin settings.

In the early Toarcian there is an abrupt lithologic transition with the onset of organic- rich deposits of the **Schistes Carton Fm**. This unit is dominated by finely laminated organic-rich shales sometimes containing silty material interbedded with two prominent limestone beds. Rare pyritized nuclei may be found (Pinard et al., 2014). Mailliot et al. (2009) identified at the base of this formation a negative $\delta^{13}C$ anomaly that has been correlated with the well-known negative carbon isotope excursion recorded at the base of the Serpetinum Zone in numerous sections in NW Europe and elsewhere (Hesselbo et al. 2000, 2007; Caswell and Coe, 2012; Hermoso et al., 2012).

Overlaying the **Schistes Cartons Fm.** is the middle to upper Toarcian **Marnes de Fontaneilles Fm**. It consists in a monotonous grey marls succession rich in ammonites, belemnites, bivalves and gastropods. The dark marls of this unit gradually pass into limestone-marl alternations followed by sandy bioclastic carbonate platform sediments with abundant bioturbation of Aalenian to Bajocian age (*Cancellophycus* facies) (Harazim et al., 2013).

The Bourg, Marnes de Villeneuve, Schistes Carton and the Marnes de Fontaneilles Formations together form the **Rivière-sur-Tarn Group** (Harazim et al., 2013; Figure I.2).

I.2.2. Quercy Basin

I.2.2.1. Definition

The polygonal Quercy Basin (QB), located on the north-eastern edge of the Aquitaine Basin, is bordered by the Villefranche-de-Rouergue fault (east) and by the West-Quercy lineament (west) (Figure I.1 and I.4). The Lower Jurassic series crops out on the eastern border in a narrow belt of N-S general orientation (Cubaynes, 1986; Qajoun, 1994; Sissingh, 2006; Lezin et al., 2007).

The QB is subdivided into two morphostructural units: a southern unit that subsides progressively southward; and, a northern unit that subsides gradually in the direction of the Autoire area (SE). Each of these is subdivided into blocks that control the depositional pattern of the sediments (Lezin et al., 2007).

During the Early Jurassic, the morphology of this small intracratonic basin was largely controlled by an extensional tectonic phase reactivating some E-W, N-S to N20ºE and N160ºE-N170ºE faults. Spatial thickness variations more or less pronounced within the basin of the different lithostratigraphic units and even hiatuses suggest a clear differential subsidence (Cubaynes, 1986; Qajoun, 1994; Lezin et al., 2007).

The geodynamic evolution, stratigraphy, sedimentology, geochemistry and macro and micropaleontology have been studied by a number of authors, namely, Pelissié (1982), Cubaynes (1986), Rey et al. (1988), Cubaynes et al. (1989), Qajoun (1994), Andreu et al. (1995), Emmanuel et al. (2006), and references therein.

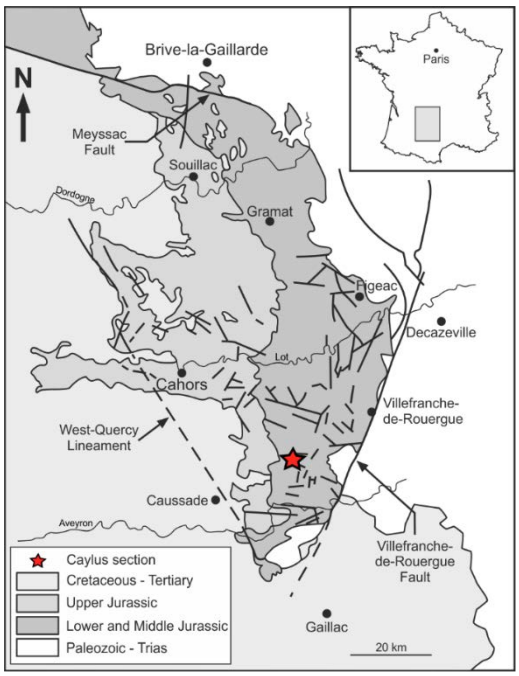

Figure I.4. Simplified geological map of the Quercy Basin and location of the studied Caylus section (modified from Emmanuel et al., 2006).

I.2.2.2. Lower Jurassic lithostratigraphy

During the Early Jurassic deposition took place south of the Lot river valley (Gresigne and Figeac-Capdenac counties) (Figure I.4). The triangular basin opens towards the north while the southern two sides of the triangle are shallow or emerged shoals. The basin deepens to the south, reaching its depocenter near the intersection of the Villefranche-de-Rouergue fault and the Western Quercy lineament (Rey et al., 1994).

According to Cubaynes et al. (1989), who established formally the lithostratigraphic units for the Lower Jurassic of the QB, Hettangian to Toarcian sedimentation is divided into ten formations (Figure I.2): **La Madeleine Fm.** (upper Trias to Hettangian), **Maillet Fm.** (Hettangian), **Capdenac Fm.** (Hettangian), **Planioles Fm.** (Sinemurian), **Cavagnac Fm.** (upper Sinemurian), **Brian-de-Vère Fm.** (lower to upper Pliensbachian), **Valeyres Fm.** (upper Pliensbachian), **Barre à Pecten Fm.** (upper Pliensbachian to lower Toarcian), **Penne Fm.** (lower to upper Toarcian) and **Lexos Fm.** (upper Toarcian)**.**

The time frame of this study comprises the **Barre à Pecten** and **Penne formations**, therefore a more detailed description of these units is performed.

The **Barre à Pecten Fm.** (10 to 20 m thick) is characterized by a set of grey or red massif decimetric layers of limestone, with irregular stratifications, disturbed at the top by a discontinuity (D7 according to Cubaynes et al., 1989) represented by a regional ferruginous karstified hard-ground. These biomicrites/biosparites, wackestone to grainstone, rich in crinoid fragments, represent infralittoral bioclastic deposits, colonized by large Pectinids, *Pseudopecten aequivalvis* or by *Pinna* (Cubaynes et al., 1989).

The **Penne Fm.** is bounded by two sedimentary discontinuities (D7 and D8; according to Cubaynes et al., 1989). It is generally characterized by marls, with thickness varying between 60 m (Grésigne) and 30 m (Capdenac). It is composed by three members: **Schistes Cartons Member** (Mb.), **Marnes et calcaires à *Hildoceras* Mb.** and **Marnes noires à *Pseudogrammoceras* Mb.** (Cubaynes et al., 1989).

The **Schistes Cartons Mb.** (7 to 9 m) is characterized by two lithological units: at the base, detrital marls with benthic microfauna of variable thickness; at the top, interbedded shales (average 6m thick). The last ones represent the Schistes cartons *s.s.* that testify to the development of anoxic conditions in the QB during the lower Toarcian and represents the only sapropelic algal facies of the Lower Jurassic in Quercy (Cubaynes et al., 1989). This member ends in a slim (10 to 15 cm) condensation level with *Harpoceratoides strangewaysi* (Cubaynes et al., 1989; Qajoun, 1994).

The **Marnes et calcaires à *Hildoceras* Mb.** corresponds to a marly dominated succession with alternation between decimetric layers of limestone and marls. The grey limestone beds (8 to 20 cm thick) are mudstone-wackestone pyritic biomicrites, with bioclasts (bivalves and crinoids) and foraminifers (*Lenticulina*, *Dentalina* and *Nodosaria*). The grey marls range between compact and laminated with fossil content rich in both macro- (brachiopods, belemnites, ammonites) and microfauna (foraminifers and ostracods) (Cubaynes et al., 1989; Qajoun, 1994).

The **Marnes noires à P*seudogrammoceras* Mb.** is characterized by pseudonodular or finely stratified black mudstones and black argillites with sandstone lenses topped by a bed of oolitic ferruginous limestone, packstone to grainstone, disrupted by the D8 discontinuity (terminology of Cubaynes et al., 1989). The sedimentary and biological properties show a moderate hydrodynamic environment possibly representing a circalittoral environment with semi-reducing conditions on the seafloor (Cubaynes et al., 1989; Qajoun, 1994).

I.2.3. Pyrenean Basin

I.2.3.1. Definition

The Pyrenees Mountains are ~400km long, and range in width from 100 to 200 km. This orogenic belt marks the former lithospheric plate boundary between Iberia and Eurasia and is limited to the west by the Bay of Biscay and to the east by the gulf of Lion (Figure I.1 and I.5) (Johnson and Hall, 1989; Faure, 2002; Vanderhaeghe and Grabkowiak, 2014).

During the Triassic to Jurassic times, in the nowadays Pyrenees, the displacement of the Pangea originated a subsiding Pyrenean Basin (PB). This basin extended between the Iberian and European plates and was controlled by Hercynian structures, such as, the North Pyrenean Frontal fault. The Pyrenean tectonics (Alpine Convergence) that occurred between the latest Cretaceous and the Oligocene, deformed, detached and fragmented the substrate resulting in diverse tectonic units (Faure, 2002; Boix and Perez, 2003). The South Pyrenean zone (Figure I.5) is one of these structural units comprising a 3000 m thick succession of Meso-Cenozoic sedimentary rocks (Sellés and Vila, 2015).

Tectonics, biostratigraphy, geochemistry and paleogeography of this basin have been studied by a number of authors, such as, Johnson and Hall (1989); Faure (2002); Boix and Perez (2003), Vanderhaeghe and Grabkowiak (2014), Bernadou (2015), Sellés and Vila (2015), and references therein.

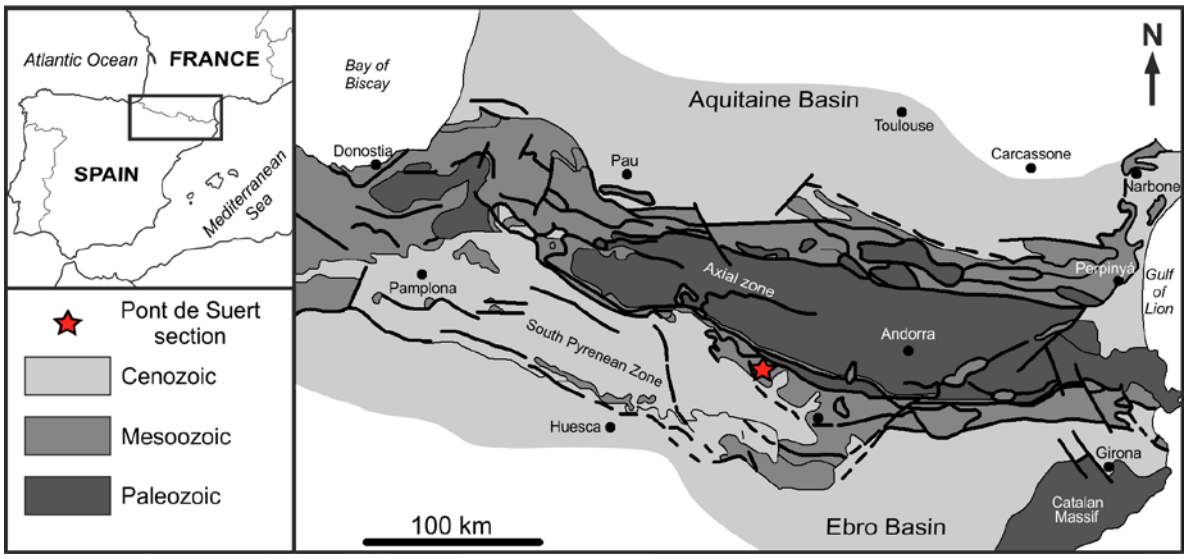

Figure I.5. Simplified geological map of the Pyrenees Mountains and location of the studied Pont de Suert section (modified from Riera et al., 2009; Sellés and Vila, 2015).

I.2.3.2. Lower Jurassic lithostratigraphy

The Lower Jurassic infill of the PB records a part of a major transgressive-regressive cycle (first order) that occurred between the Norian and upper Aalenian (Faure, 2002). Its development is done through four second order transgressive-regressive cycles: Rhaetian – lower Sinemurian, upper Sinemurian – lower Pliensbachian, upper Pliensbachian and Toarcian – Aalenian (Faure, 2002).

The studied time frame comprises the upper Pliensbachian and the Toarcian – Aalenian second order cycles. According to Faure (2002), these cycles are materialized by four units (Figure I.2): **Barre a Pecten Fm.** (upper Pliensbachian), **Padrinas Fm.** (Toarcian – Tenuicostatum to Thouarsense zones), **Saint-Girons Fm.** (Toarcian – Dispansum to Aalensis zones) and **Santa Linya Fm.** (Toarcian, Aalensis Zone, to Aalenian, Concavum Zone).

The **Barre a Pecten Fm.** (average 10 m thick) is characterized by irregular centimetric to decimetric beds of red bioclastic limestone, rich in belemnites and with clasts of Pectinidae and brachiopods. Sometimes chert beds are intercalated (Faure, 2002).

The **Padrinas Fm.** comprises a succession of carbonate and/or argillaceous- carbonate sediments, usually rich in brachiopods. The top of this unit is underlined by a condensation level. In the South Pyrenean zone, the predominantly argillaceous-carbonated succession is sub-divided into four lithostratigraphic members (Faure, 2002): **Calcaires argileux à *Spiriferines* Mb.**, **Calcaires argileux et marnes à**

***Soaresirhynchia* Mb.**, **Calcaires argileux à *Telothyris* Mb.** and **Intervalle condensé Mb.**

The **Calcaires argileux à *Spiriferines* Mb.** (2.5 to 3.5 m) is characterized by rhythmic alternations of marl and argillaceous limestone beds rich in *Liospiriferina falloti* (Tenuicostatum Zone), topped by the S1 discontinuity, post-Semicelatum. The **Calcaires argileux et marnes à *Soaresirhynchia* Mb.** (3 to 5 m) comprises argillaceous limestones intercalated with marls rich in *Soaresirhynchia bouchardi* (Serpentinum Zone, subzone Elegantum). The **Calcaires argileux à *Telothyris* Mb.** (about 10 m) consists in regular rhythmic alternations of marl and argillaceous limestone beds with ammonites and brachiopods, ranging from Falciferum to Bifrons subzones. The **Intervalle condensé Mb.** (about 2 m) corresponds to more or less lenticular condensed beds of bioclastic limestones, ferruginous, sometimes oolitic, with reworked fossils (Thouarsense Zone). All these beds are topped by ferruginous hardgrounds reflecting breaks in the sedimentation (Faure, 2002).

The **Saint-Girons Fm.** is composed by approximately 50 m of black laminated marls (Dispansum Zone to Aalensis Zone, Mactra Subzone). The **Santa Linya Fm.** comprises a marly-carbonate succession of about 15 m thick marking the transition between the Toarcian marls and the Aalenian oncolithic limestones (Faure, 2002).

Chapter II - Organic matter: Concepts and Classification

II.1. Organic Composition

Sedimentary OM corresponds to the organic material derived directly or indirectly from living organisms and usually represents a small percentage of the sedimentary content (Durand, 1980; Tissot and Welte, 1984). The OM is composed by two fractions: kerogen (fraction of the OM insoluble in organic solvents), and bitumen (fraction of the OM soluble in organic solvents). Kerogen is composed of particulate OM (organic constituent of the sedimentary rocks) and bitumen is composed by molecular OM (molecular organic compounds: saturated, aromatic and polar compounds). Its quantity and quality in sediments is the result of a dynamic process combining the influence of biomass productivity, biochemical degradation and the OM depositional processes (Tissot and Welte, 1984; Tyson, 1995; Mendonça Filho et al., 2010a).

The study of the OM in sediments and sedimentary rocks focuses on the interaction between the biosphere and geosphere which requires an understanding of the environmental controls that manage the production of OM in the biosphere; the ecological and sedimentological processes that control its deposition and distribution; the biogeochemical and geomicrobiological factors that influence the preservation; and, that geochemical and physical processes that determine the modifications occurring during the incorporation of OM in the geosphere (Tyson, 1995)

The use of the petrographic and geochemical methodologies in the characterization of the particulate OM in sediments and sedimentary rocks provide information that can be evaluated in the broader context of the general factors which control the sedimentation, distribution, and preservation of OM emphasizing the paleoenvironmental analysis (Tyson, 1995). The geochemical methodologies used in this study are: (i) total organic carbon; (ii) total sulfur; and, (iii) $CaCO_3$ content. Concerning the petrographic techniques were used transmitted and reflected white lights and incident blue light for the identification of the particulate OM (Palynofacies) and its maturation assessment (spore coloration index, spectral fluorescence analysis and vitrinite reflectance).

II.1.1. Geochemical Analysis

II.1.1.1. Total Organic Carbon (TOC)

The abundance of OM in sediments is usually expressed by the relative weight percentage of organic carbon on a dry basis. The TOC is a measure of total organic carbon in a sample (Jarvie, 1991; Bordenave et al., 1993) determined through the

combustion of the organic carbon to CO_2. This procedure determines the organic carbon content and not the total OM or kerogen. The percentage of organic carbon corresponding to bitumen is usually not more than 0.1% or 0.2% of the total (Tissot and Welte, 1984).

This quantitative evaluation of OM content constitutes the first criteria in hydrocarbon generation potential determination. It is also used for lithology, depositional environment and OM origin and preservation state interpretation (Tissot and Welte, 1984).

II.1.1.2. Total Sulfur (TS)

TS content in carbonate sediments is an important criteria to assess the depositional environment redox conditions. In fact, high TS content usually indicates a reducing depositional environment (Tyson, 1995).

II.1.1.3. Insoluble Residue (IR) versus $CaCO_3$

The IR corresponds to the fraction of sample that was not removed by acid treatment, assuming that all carbonate fraction was removed. With this premise is assumed a direct relationship between the carbonate percentage and each sample IR value represented by equation [1]:

$$CaCO_3(\%) = 100 - IR \; [1]$$

where $CaCO_3$ is the carbonate percentage of the sample and IR is the insoluble residue determined value.

II.1.2. Palynofacies

Combaz (1964) introduced the term palynofacies as the total assemblage of microscopic organic constituents present in a rock that remains after maceration in hydrochloric acid (HCl) for carbonates and by hydrofluoric acid - (HF) for silicates, concentration and mounting using normal palynological preparation procedures. Later, Tyson (1995) published a synopsis of the geochemical aspects of organic facies analysis. This work integrates the geological and biological aspects of palynofacies research introducing the modern palynofacies concept as “a body of sediment containing a distinctive assemblage of palynological OM thought to reflect a specific set of environmental conditions or to be associated with a characteristic range of hydrocarbon-generating potential”. More recently, Mendonça Filho (1999) refers to palynofacies as the study of the particulate OM present in sediments and sedimentary rocks using the OM isolation methods for sample preparation (kerogen concentration)

and applying microscopy techniques as the main tool for acquiring data and statistical methods for its interpretation.

II.1.2.1. Kerogen groups

Several classifications systems have been proposed for the classification of dispersed kerogen (e.g., Traverse, 1988; Tyson, 1995; Vincent, 1995; Mendonça Filho et al., 2010a). They are based primarily on the appearance and preservation state of the particulate OM and their biological origin using transmitted white light (TWL) with additional observation employing fluorescence modes (FM) (blue or UV). According to Tyson (1995) there are several criteria that should be used in the kerogen classification, such as: origin; structure; morphology; measurable optical properties; geochemical composition; and, preservation state. It is important to use a classification system that provides as much information as possible to achieve the objectives of the OM study.

Tables II.1 to II.4 show the detailed classification system of the individual palynological components based on Tyson (1995), Vincent (1995) and Mendonça Filho et al. (2010a; 2011c; 2012; 2014c; 2016, *Ineditus in efficiendis*), indicating the appropriate use of the nomenclature for the observation of kerogen under TWL. According to this classification three main morphological kerogen groups can be recognized within a kerogen assemblage: i) Phytoclast (fragments of tissues derived from higher plants or fungi); ii) Amorphous (structureless material derived from non-fossilizing algae, or advanced tissue biodegradation, phytoplankton or bacterially derived amorphous OM (AOM), higher plants resins and amorphous products of the diagenesis of macrophyte tissues); and, iii) Palynomorph (organic walled constituents that remain after maceration using HCl and HF acids); However, the classification system is still not standardized between studies.

II.1.2.1.1 Phytoclast Group

The term phytoclast was introduced by Bostick (1971) to describe all particles with clay or fine-sand size derived from highly lignified mechanical support tissue of higher plants, i.e. wood (xylem), or fungi, with autofluorescence depending on the derived tissue. The Phytoclast group (Table II.1) is divided in opaque (dark), non-opaque (translucent, including cuticular tissues and fungal hyphae) (Figure II.1) and sclereids.

Table II.1. Detailed classification system of the individual palynological components from Phytoclast Group (based on Tyson, 1995; Vincent, 1995; Mendonça Filho et al., 2010a; 2011c; 2012; 2014c).

	GROUPS & SUBGROUPS		DESCRIPTION	
PHYTOCLAST	Fragments of Tissues Derived from Higher Plants or Fungi	Opaque: **Equidimensional (Equant)** lenght: width ratio < 2	Black or opaque in colour even at grain boundary. Sharp outline; mostly no internal structure.	
		Opaque: **Lath** lenght: width ratio > 2	Black or opaque in colour even at grain boundary. Sharp outline; it may shows pits.	
		Opaque: **Corroded**	Black in colour. More diffuse outline; irregular.	
		Non-Opaque (Translucent): ***Undegraded*** Sharp outline (may be slightly irregular). May be splintered. or ***Degraded*** Irregular and diffuse outline or ***Pseudoamorphous/ "Amorphous"*** Diffuse outline, it may light brown, brown and dark brown in colour. Starting to show some features of AOM, but homogenous in apperance, not pyrite specked, no inclusions. It may exhibits fluorescence. or ***In decomposition (gelified) "Highly preserved"*** Irregular outline in transmitted white light, it exhibits coloration of fluorescence. The characteristics indicate a highly degree of chemistry preservation due to specific conditions.	**Fungal Hyphae**	Fragments of hyphae. Brown in colour. Individual filaments of the mycelium of the vegetative phase of eumycote (higher) fungi.
			Non-biostructured	No botanical structure. Translucent, generally brown in colour. Lath or equant in shape.
			Cuticle	Epidermal tissue of higher plants. Pale yellow-green, yellow, reddish-yellow in colour particle. Regular cell outlines; sheet-like, in some cases with visible stomata. It may occurs thick translucent phytoclasts that under fluorescence, present a yellow fluorescing cuticle overlaying ("coating") on these phytoclasts. This particular feature (cuticular layer fragments associated with innermost part of epiderms) could be indicating that the land plants fragments derived from leaves.
			Membrane	Pale yellow in colour; thin; sheet-like; irregular. They often fluorescent; highly translucent. Lack of diagnostic internal structure.
			Biostructured	Generally brown in colour; lath to equant in shape; clearly visible internal structure. Striate: shown thin (regular fibrous lineation). Striped: Irregular or unequal stripes (may be thicknings). Banded: Regular and equal parallel sided thickenings. Pitted: Bordered or scalariform pits.
		Sclereids	Generally opaque, but may be translucent (dark brown). Sclerenchymatic tissue cells, with thickened secondary wall and impregnated with lignin. Found in different parts of the plant (root, stem and leaf) with the sustentation function and mechanical resistance.	

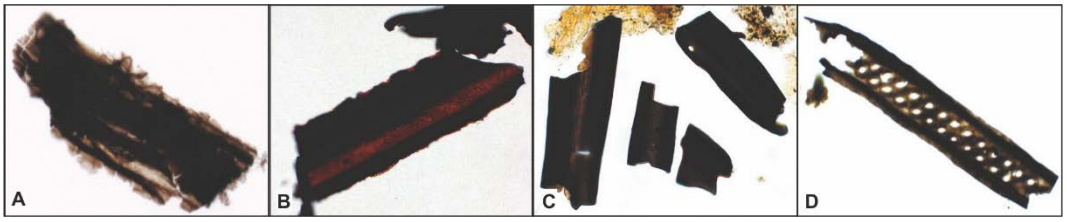

Figure II.1. Examples of non-opaque biostructrured Phytoclasts. **A** - Striate (TWL); **B** - Striped (TWL); **C** - Banded (TWL); **D** - Pitted (TWL) (in Mendonça Filho et al., 2014c).

Phytoclast particles commonly become less abundant, smaller and more oxidized with the increase of the distance to the terrestrial source. High percentage of these components in the assemblage is associated with several aspects, such as: high supply; preferential preservation; selective sedimentation due to hydrodynamic equivalence of the particles; and/or, preferential sedimentation (Tyson, 1995).

II.1.2.1.2 Amorphous Group

The Amorphous Group (Table II.2) consists of all particulate organic components that appear structureless at the scale of the optical microscopy; including phytoplankton derived AOM, bacterially derived AOM, higher plant resins and amorphous products of the diagenesis of macrophyte tissues (Tyson, 1995; Mendonça et al., 2011b).

Table II.2. Detailed classification system of the individual palynological components from Amorphous Group (based on Tyson, 1995; Vincent, 1995; Mendonça Filho et al., 2010a; 2011c; 2012; 2014c).

GROUP	SUBGROUP	DESCRIPTION
AMORPHOUS GROUP	**"AOM"** AOM derived from microbiological reworking of phytoplankton.	Structureless material with no morphology or form; color: yellow-orange-red; orange-brown or grey; often has palynomorphs and pyrite inclusions, may sometimes exhibit fluorescence.
	Products of macrophyte tissues (*Pseudoamorphous/ "Amorphous"*) AOM derived from microbiological reworking of macrophyte tissues (higher plants).	Diffuse outline, light brown, brown and dark brown in colour. Starting to show some features of AOM, but homogenous in appearance (*flat fluorescence*), not pyrite specked, no inclusions. It may exhibit fluorescence.
	Microbial mats AOM derived from primary productivity of bacterias (phtotosynthesis).	They consist predominantly of the maceral lamalginite when examined in reflected white light. They form rather uniformly and strongly fluorescent cohesive particles which show relatively sharp and distinct (sometimes quite angular) outlines after maceration.
	Products from bacteria Bacterial Extracellular Polymeric Substance (EPS).	Mucilagenous sheet. Diffuse outline, thin, pale yellow, yellow, orange, grey in colour. Not pyrite specked, no inclusions. Exhibits intense fluorescence.
	Resin Mostly produced by terrestrial higher plants in tropical climates.	Structureless particle (glassy shards), hyaline, usually round, homogeneous, strongly fluorescent.

The dominance of AOM (Figure II.2) in total assemblage of kerogen can correspond to reducing environments (at least temporarily dysoxic to anoxic) or distal depositional environments (inexistent sedimentation from active sources of terrestrial OM) (Tyson, 1995). The preservation state of the AOM is important in the characterization of the depositional conditions, namely the redox conditions, being expressed by the fluorescent intensity of the components. In dysoxic-anoxic conditions the hydrogen-rich components of the AOM are easily preserved (Tyson, 1995).

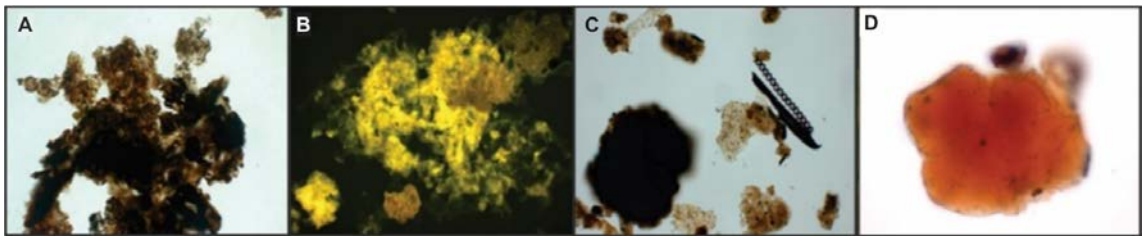

Figure II.2. Examples of Amorphous Group. **A** - AOM (TWL); **B**- Bacterial AOM (FM); **C** - Plant Tissues AOM (TWL); **D** - Resin (TWL) (in Mendonça Filho et al., 2014c).

II.1.2.1.3 Palynomorph Group

Tschudy (1961) introduced the term palynomorph to describe all the organic-walled microfossils (resistant to HCl and HF) that may be present in palynological preparations (Table II.3). They are discrete, coherent, individual or colonial entities that can be subdivided into terrestrial (sporomorphs) and aquatic (marine and freshwater) subgroups (Tyson, 1995).

Table II.3. Detailed classification system of the individual palynological components from Palynomorph Group (based on Tyson, 1995; Vincent, 1995; Mendonça Filho et al., 2010a; 2011c; 2012; 2014c).

GROUP	SUBGROUPS				DESCRIPTION
PALYNOMORPH	Sporomorph	**Spores**	Terrestrial Palynomorph produced by Pteridophyte, Briophyte and Fungi.		Triangular or circular form palynomorph, trilete mark ("Y") or monolete (scar). They can occur as massulae of the freshwater fern (Azolla), agglomerates and tetrad. "First spores" (Cambrian): Cryptospores (spore-like bodies) and Embryophyte Spores: Upper Ordovician-Recent.
		Pollen Grain	Terrestrial Palynomorph produced by Gymnosperms and Angiosperms		Palynomorph with varied ornamentation, most with circular or oval outline; could present opening or not. They can occur as agglomerates or tetrads. Devonian-Recent.
	Freshwater Microplanckon	***Botryococcus***	Green Algae	Chlorophyta (Chlorococcales)	Irregular globular colonies; size 30 to 2000 µm, sometimes with several lobes (like miniature cauliflower); Ordovician-Recent.
		Pediastrum			Colonial green algae (coenobia). Rounded colonies with 30-200 µm diameter. In polygonal form the cells have a concentric arrangement; cells present two horns in the side external. Jurassic (?) - Recent.
		Scenedesmus			*Scenedesmus* genus of colonial (coenobia) green algae with 4, 8, or 16 cells arranged in a row and non-motile. Different forms of coenobia are found including linear, costulatoid, irregular, alternating, or dactylococcoid patterns.
		Zignemataceae		Chlorophyta (Zignematales)	They are hydro-terrestrial, filamentous or unicellular, uniseriate (unbranched) green algae which produce acid-resistant spores. The filaments are septated and they present diversely shaped chloroplasts, such as stellate in Zygnema, helical in Spirogyra, and flat in Mougeotia. Only the filamentous algae spores are preserved. The majority of species have spores of constant form, only a very few are polymorphic. The forms are of four primary types (globose, obovoid, ellipsoid and quadrangular) of which a number of variation are known (Grenfell, 1995).
		Gloeocapsomorpha	Green Algae (?)	Chlorophyta	*Gloeocapsomorpha* is a colonial organism. In colonies the cell voids are completely ensheathed by thick, multilayered walls and do not open to the surface of the colonies. The outer layer of the cell walls of the colony is smooth. Ordovician *G. prisca* is considered occur in marine systems
			Blue-Green Algae (?)	Cyanophyta	
	Marine Microplankton	**Dinoflagellate Cysts**	Cell produced during the sexual phase of the dinoflagellate life cycle		The fossil record of dinocysts is almost entirely confined to forms that have a meroplanktonic life cycle. Major dinocyst morphotypes: Proximate, Cavate and Chorate. Triassic-Recent. According to their nutritional behavior they can be autotrophic, heterotrophic or mixotrophic.
		Prasinophyte	Fossilized structure produced by small quadri-flagellate motile phase.		Majority, like *Tasmanites*, are spherical; diameter 50 to 2000 µm. Modern species include freshwater. Precambrian-Recent.
		Acritarchs	Unicellular fossilized cysts with organic cell walls. They have no formal taxonomic status.		The acritarchs are a polyphyletic group of palynomorphs whose name means "of uncertain origin". Acritarcha (*akritos* = uncertain, mixed and *arche* = origin). Small dimension organism (5 a 150 µm). Simmetrically shaped withvaried ornamentation. They first appeared in the late Precambrian, attained their acme during the Ordovician-Devonian.
	Zoomorph	**Foraminiferal Test-Linings**	They are tectinous linings derived from certain marine benthic foraminifera.		The linings are typically dark brown colour, although their outer chambers are often more thin-walled and translucent. Good indicator of marine conditions.
		Scolecodonts	Elements of the jaw of benthic polychaete annelid worms.		They are the part-calcified and scleroprotenaceous ("chitinous") mouth parts ("pharyngeal jaws") of benthic polychaete annelid worms. Ordovician - Recent.
		Chitinozoa	Vesicles in format of flasks or small hollow bottles (30 to 2000 µm). Uncertain affinity.		They constitute an extinct group of organic-walled microfossils found in Palaeozoic marine sediments. Early Ordovician - Late Devonian.
Others	Zooclasts (Graptolite, Crustacean eggs); *Spongiophyton;* Salviniaceae; Solid Bitumen.				

The sporomorph subgroup (Figure II.3) corresponds to all palynomorph produced by land plants. It is composed by two components: spores and pollen grains;

with variable fluorescence properties (Tyson, 1995). Spores are produced by Bryophyte, Pteridophyte plants and their primitive ancestors. Pollen Grains are produced by the seed-producing plants, such as Gymnosperms (e.g. Conifers), observed from Carboniferous to Present; Angiosperms (flowering plants), Early Cretaceous-Present (dominate global flora from Late Cretaceous onwards). They are produced in dyads, tetrads and polyads and their presence is a good indicator of proximity of a source area (Mendonça Filho et al., 2014c).

The aquatic components (Figure II.3) are divided into: Freshwater Microplankton (*Botryococcus*, *Pediastrum*, *Scenedesmus*, *Gloeocapsomorpha* genus and zygospores of Zygnemataceae family); Marine Microplankton (Dinoflagellate Cysts, Prasinophyte algae and Acritarchs); and, Zoomorph (Foraminiferal Test-Linings, Scolecodonts and Chitinozoa).

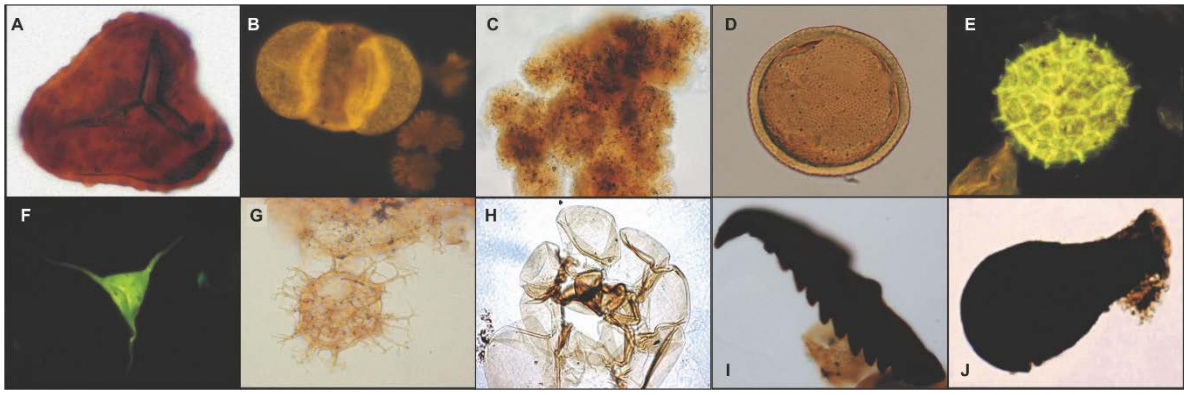

Figure II.3. Examples of Palynomorph Group. **A** – Spore (TWL); **B** – Bisaccate pollen grain (FM); **C** – *Botryococcus* (TWL); **D** – *Tasmanites* (TWL); **E** – *Cymatiosphaera* (FM); **F** – Acritarch (FM); **G** – Dinocyst (TWL); **H** - Foraminiferal Test linings (TWL); **I** – Scolecodont (TWL); **J** – Chitinozoa (TWL) (in Mendonça Filho et al., 2014c).

Other categories of palynomorphs include organic particles which cannot be confidently assigned to any subgroup due to their state of preservation or lack of diagnostic features (undifferentiated Palynomorphs), or organic particles which cannot be classified as a result of lack of analyst knowledge to recognize diagnostic features to identify the organic particles (uncertain Palynomorphs) (Mendonça Filho et al., 2014c).

The Zoomorph subgroup (Figure II.3; Table II.4) is composed by discrete unitary animal-derived particles, whether whole or damaged, encompassing foraminiferal test-linings, chitinozoans, and scolecodonts (Tyson, 1995; Vincent, 1995; Mendonça Filho et al., 2010a; 2011 a, b, c; 2012; 2014 a, b, c; Suárez-Ruiz et al., 2012). Recently, Mendonça Filho et al. (2016, *Ineditus in efficiendis*) also included in this Subgroup the presence of cuticles of ostracods and, most importantly, hydrozoans.

The Zooclast Group and Zoomorph Subgroup are reported in most scientific papers as minor components. Gonçalves et al. (2014) described the absolute predominance of zooclasts and zoomorphs in the Middle Jurassic carbonate Candeeiros formation of the Lusitanian Basin, Portugal, emphasizing the importance of these organic components in paleoenvironmental reconstruction.

Table II.4. Detailed classification system of the individual palynological components from Zoomorph Subgroup and Zooclast Group (based on Tyson, 1995; Vincent, 1995; Mendonça Filho et al., 2010a; 2011c; 2012; 2014c; 2016, *Ineditus in efficiendis*).

SUBGROUP	ORIGIN	DESCRIPTION	
Zoomorph	**Foraminiferal Test-Linings**	Tectinous linings derived from certain marine benthic foraminifera.	The linings are typically yellow to dark brown color in transmitted white light, although their outer chambers are often more thin-walled and translucent. They can present fluorescence yellow to dark orange.
	Cuticle of Ostracods	Chitinous cuticle coating the ostracod shells.	Organic composition wall; varied coloration in transmitted white light; they can present fluorescence.
	Scolecodonts	Elements of the jaw of benthic polychaete annelid worms.	They are the part-calcified and scleroprotenaceous ("chitinous") mouth parts of benthic polychaete annelid worms. Ordovician – Recent.
	Chitinozoans	Vesicles in format of flasks or small hollow bottles (30 to 2000 µm), uncertain affinity.	They constitute na extinct group of organic-walled microfossils found in Paleozoic marine sediments. Early Ordovician – Late Devonian.
	Hydrozoans	Polypoid forms of cnidarians (Phylum Cnidaria, Class Hydrozoa, Order Hydroida).	Sessile polyps of organic exoskeleton (chitin). Marine and freshwater.
		Colonial forms of hydroids (Phylum Cnidaria, Class Hydrozoa, Order Hydroida).	Colonial polyps of organic exoskeleton (chitin). Marine and freshwater.
		Medusoid forms of cnidarians (Phylum Cnidaria, Class Hydrozoa, Order Hydroida or Class Scyphozoa).	Medusoid forms (medusae). Marine and freshwater.
Zooclast Group	Zooclasts are unknown organic particle, structured, fragmentary particle (clast), angular broken outline, obviously not a whole discrete entity (spines, slits, hairs, joints, etc.) and those particles identifiable as fragmented zoomorph palynomorphs are not classified as zooclasts. The most common varieties of zooclasts include arthropod exoskeletal debris, organic linings from some bivalve shells and ostracod		

Mendonça Filho et al. (2016, *Ineditus in efficiendis*) identified for the first time in organopalynological preparations the occurrence of Cnidarians (Phylum Cnidaria), Class Hydrozoa (Hydrozoans), and Hydroida Order (Hydroids). In literature, the fossil record of these organisms is mostly restricted to the forms with carbonate skeleton. Nevertheless, Eisenack (1932, 1934, 1935) defined 4 genus of Hydrozoa polypoid forms with chitin skeleton (2 from the Ordovician, 1 Silurian and 1 Jurassic). Kozlowski (1959) describes 15 genus and 22 species of polypoid forms of Ordovician Hydroids with chitin skeleton and doubts Eisenack (1932, 1934, 1935) conclusions due to sample fragmentation. Bertrand (1987), based on Kozlowski (1959) descriptions, presents the first reflectance measurements in Hydroids.

Due to the scarce record of the occurrence of these components in isolated OM in the literature, it is vital to make a brief description of the Phylum Cnidaria.

II.1.2.1.3.1. Hydrozoans

Mendonça Filho et al. (2016, *Ineditus in efficiendis*) described discrete unit particles or damaged debris derived from Cnidarians (Phylum Cnidaria), Class Hydrozoa (Hydrozoans), and Hydroida Order (Hydroids) displaying typical polymorphism, specific of this group of organisms. Individual (simple) sessile polypoid forms (hydroid polyps), disarticulated colonial fragments (hydroid colony), and medusoid forms (free-swimming) at all stages of the life cycle, from embryonic stage to mature forms (adult), were identified.

Phylum Cnidaria

Phylum Cnidaria covers carnivorous aquatic fauna, mainly marine forms, although a small number of species are found in rivers and freshwater lakes. It is estimated that there are between 7000-11000 described species, including corals, hydroids and medusae. Cnidarians are classified into four main groups: non-moving (sessile) Anthozoa, which includes true corals, anemones, and sea pens; Cubozoa (box jellies with complex eyes and potent toxins); swimming Scyphozoa (the true jellyfish); and Hydrozoa, a broad group that includes all the freshwater cnidarians as well as many marine forms. Only the Class Hydrozoa features freshwater organisms, represented by some hydroids and medusa (Oliver Jr. and Coates, 1987; Bouillon et al., 2006; Jankowski et al., 2008).

Polymorphism is a general feature of Cnidarians, i.e. different body shapes can occur within the same species, sequentially at different stages of the life cycle, or simultaneously within a colony (Figure II.4). There are two major body forms among the Cnidaria - the polyp and the medusae. Polyps have a tube-like body with an opening on top that is surrounded by outward- and upward-facing tentacles. Medusae are usually bell-shaped animals with a concave oral surface, or mouth, and tentacles that dangle downward from the rim of an umbrella-like body. Cnidarians are abundant in many aquatic environments, although fossils are known only in marine sedimentary rocks. The geological record of Cnidaria extends from the end of the Proterozoic (Ediacara Fauna) to the Holocene (Oliver Jr. and Coates, 1987; Bouillon et al., 2006; Jankowski et al., 2008).

Class Hydrozoa (Hydrozoans)

The Hydrozoa is a diverse subgroup of cnidarians containing approximately 3700 species (predominantly marine but freshwater also occurs) with a multiplicity of life cycles, growth forms, and specialized structures. Hydrozoans have both polyp (often dominant but can be absent) and medusa stages in their life cycle which begins with the growth of medusae from buds or from metamorphosis. Most hydrozoans form

colonies of asexual polyps (polyp stage often dominates) and free-swimming sexual medusae. Colonies are usually benthic with specialized colonial polyps (function of defense, feeding, or reproduction) (Oliver Jr. and Coates, 1987; Brusca and Brusca, 2003; Bouillon et al., 2006; Grohmann, 2008; Jankowski et al., 2008; Portella et al., 2009; Gutierre, 2012).

The Hydrozoans comprise a particularly large range of polypoid and medusoid animals distributed into six orders: Hydroida, Trachylinida, Siphonophorida, Spongiomorphida, Milleporina and Stylasterina (Oliver Jr. and Coates, 1987; Brusca and Brusca, 2003; Bouillon et al., 2006; Grohmann, 2008; Jankowski et al., 2008; Portella et al., 2009; Gutierre, 2012). They are found in nearly all marine habitats but are most abundant and diverse in warm shallow waters, probably a reflection of food availability. The small number of freshwater species occur in both lotic and lentic habitats, and are more abundant in eutrophic and mesotrophic waters (Bouillon et al., 2006; Jankowski et al., 2008).

Hydrozoans have a complex life cycle, usually with two or three morphologically different stages (Figure II.4). The classic cycle starts with fertilized eggs developing into small, free swimming larvae (planula), which may be able to enter a dormant resting state to resist unsuitable environmental conditions. Planula transform into sessile polyps, usually attached to substrate, but free-floating in some groups. Polyps duplicate themselves asexually by budding, often producing colonies of hundreds or thousands of polymorphic individual polyps. These polyps then produce "adult", solitary, free-swimming and sexually-reproducing medusae by budding. They release sperm and eggs into the water, where fertilization occurs. In nearly half of species (e.g. Hydra) the medusa stage is entirely suppressed but in other taxa the polyp stage can be absent. Numerous taxa have suppressed the planula stage as well (Brusca and Brusca, 2003; Bouillon et al. 2006).

The body of an individual hydrozoan comprises a stomach (coelenteron) and a mouth surrounded by tentacles. The number, shape and size of tentacles vary greatly, but there are usually between 8 and 50 on a single polyp. Polyps are radially symmetric, and may be urn-shaped, conical, cylindrical, or club-shaped, usually only a few millimeters tall. At their base, hydrozoan polyps have basal disks or elongate processes for attaching to substrate (Brusca and Brusca, 2003; Mills, 2009).

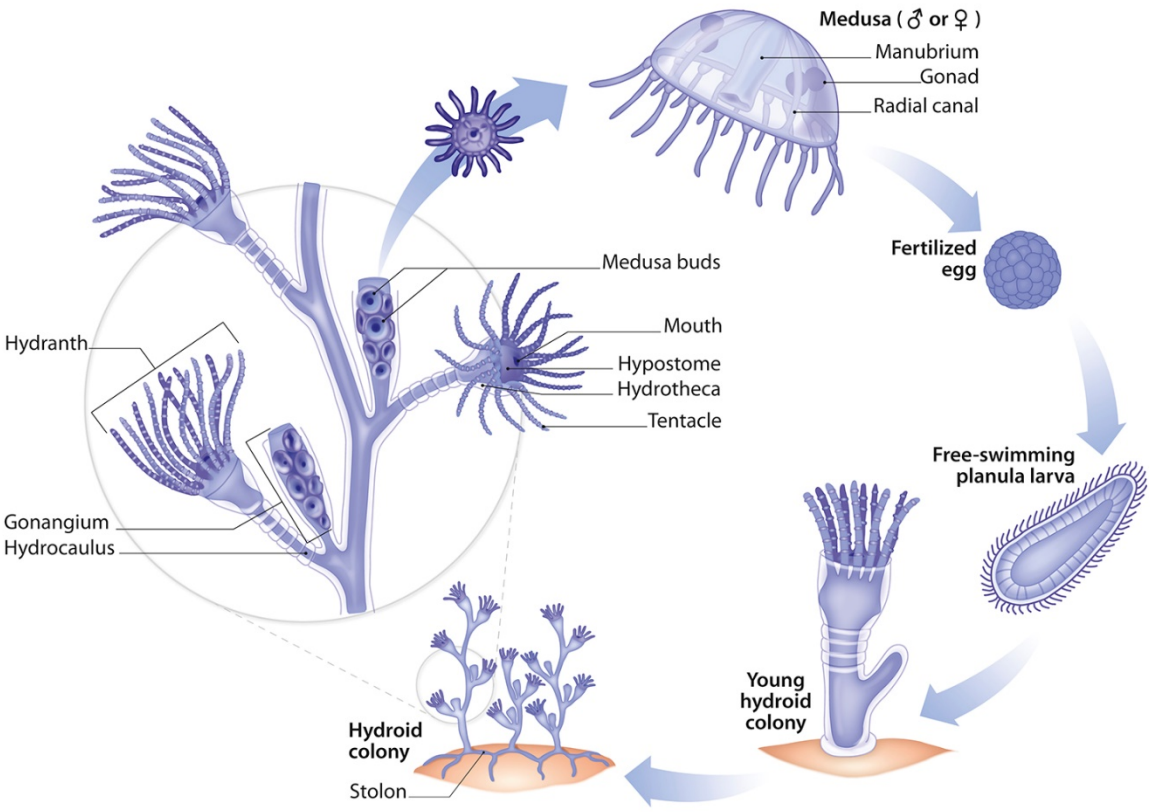

Figure II.4. Hydrozoans life cycle (modified from Rupert and Barnes, 1994).

Most hydrozoan species are colonial. A founding polyp produces new polyps by budding, growing a network of interconnected hollow tubes (stolons) formed of living tissue, collectively called the coenosarc. Colony growth forms vary between species, some may form a single layer of polyps spreading across the substrate, and others grow as erect stems, with polyps growing off the stems. Polyps and the coenosarc may secrete chitinous sheaths or stems, or calcareous coatings. In many colonies, polyps are polymorphic, with different structures reflecting different functions. Some have no mouth but are armed with large spines or cnidae-equipped tentacles for defense, some have tentacles and functional mouths for feeding, and other, with neither mouth nor tentacles, are strictly reproductive producing medusae or gametes (Brusca and Brusca, 2003; Bouillon et al., 2006).

Hydrozoans combine sessile or sedentary polyp stages and free-swimming solitary stages in their life cycles. Polyps, solitary or colonial, can move by crawling but most are sessile, with variable feeding habits. Many trap small zooplankton with their tentacles, some filter suspended particles (such as fish eggs and fecal pellets) from the water column and others consume phytoplankton. A few groups contain symbiotic algae, and may get most of their nutritional needs from their symbionts (Purcell, 1997; Brusca and Brusca, 2003; Bouillon et al., 2006; Dunn, 2009; Mills, 2009).

The medusa is the sexually reproducing stage in most hydrozoans. They are often formed by budding from polyps, and are usually solitary free-swimming organisms. They are similar in structure to an inverted polyp, radially symmetric, and often have four-fold symmetry. Their main body part is the umbrella, a bell or cone shaped gelatin-filled structure. Medusa are usually small, usually 1-50 mm in diameter, though a few are larger. A hydromedusa has an umbrella-shaped bell housing the stomach. Unlike most cnidarians, the medusae of hydrozoans may not always occur as free-living jellyfish. In many colonial species, they exist as buds on the surface of the colony for sexual reproduction purposes (Figure II.4) (Oliver Jr. and Coates, 1987; Brusca and Brusca, 2003; Bouillon et al., 2006; Grohmann, 2008; Portella et al., 2009; Gutierre, 2012).

Order Hydroida (Hydroids)

Hydroida are a taxonomic order of very small predatory animals, solitary or colonial, living in both marine and freshwater systems. The hydroid form is usually colonial, with multiple polyps connected by tubelike hydrocauli. The colonies are generally small, no more than a few centimeters across, but in some species can reach larger sizes. The hydrocaulus form a horizontal root-like stolon along the substrate that anchors the colony to the bottom. The individuals making up the colony are called zooids or polyps (Oliver Jr. and Coates, 1987; Brusca and Brusca, 2003; Bouillon et al. 2006; Grohmann, 2008; Mills, 2009).

The typical pattern is sympodial growth for the vertical shoots with each branch terminating in a hydranth and giving rise to another branch. The sympodial structure means that rather than a single growing axis, the main axis is made up of several units added on top of one-another. Many plants also grow in a sympodial manner (Oliver Jr. and Coates, 1987; Brusca and Brusca, 2003; Bouillon et al., 2006; Grohmann, 2008; Mills, 2009).

The reproductive polyps (gonangia or blastostyles) generally grow from axis or angles in the colony, typically in the angle between a hydranth and its parent stalk. Tentacled feeding zooids or hydranths (feeding polyps), and terminal (apical) buds (developing hydranths) are also present. The tentacled feeding polyps are called hydranths and the perisarc enclosing them forms a supporting cup called a hydrotheca. Each hydranth terminates in a cone (hypostome) bearing the mouth and surrounded by a ring of tentacles. The tentacles and the hypostome are the only parts of the colony that generally bear nematocysts (stinging structures located in cells called

nematoblasts, nematocytes, cnidoblasts or cnidocytes) (Oliver Jr. and Coates, 1987; Brusca and Brusca, 2003; Bouillon et al., 2006; Grohmann, 2008; Mills, 2009).

Of all the orders belonging to the Class Hydrozoa, the Order Hydroida is the only one able to secrete a chitin exoskeleton (others produce mineral skeleton). Thus, components belonging to Order Hydroida are the only ones able to remain after the use of acid maceration process (HCl and HF acids) needed to the OM isolation procedure (Mendonça Filho et al., 2016 *Ineditus in efficiendis*).

II.1.3. Maturation (Thermal Maturity)

During the geological history of sedimentary basins the OM goes through a physiochemical transformation that is controlled firstly by biological activity followed by thermodynamic factors (temperature and pressure) (Tissot and Welte, 1984). This continuous series of processes is denominated as maturation and it is divided in four consecutive stages of evolution: diagenesis, catagenesis, metagenesis, and metamorphism. These progressive and almost continuous changes in the chemical and physical properties of the sedimentary OM reflect and are an indicator of the thermal and burial history of the basins (Tissot and Welte, 1984). For this study were selected three maturation parameters, more specifically: Spore coloration index (SCI), Spectral fluorescence, and Organic matter reflectance.

Pollen and spores are the organic-walled microfossils most commonly used to estimate burial paleotemperature. With increase in thermal maturation of OM a gradual change in color (from pale yellow to black) is observed in TWL. These palynomorphic coloration changes produced as increasing burial and rise in temperature also cause chemical changes in organic components and can be used to evaluate the state of thermal maturation (Tissot and Welte, 1984; Mendonça Filho et al., 2014b).

Fluorescence is also an important method in determining the level of maturity of kerogen by estimating the intensity and color of fluorescence (qualitative) or by quantitative measurement of the fluorescence spectrum. However, the color spectrum (quantitative fluorescence) is progressively changed, the wavelength range of the fluorescence light moves from yellow towards red with increasing catagenesis (Tissot and Welte, 1984; Mendonça Filho et al., 2014b).

Determination of organic matter reflectance is an established mean of accessing the level of maturation of sedimentary OM. Reflectance is fundamentally dependent upon the refractive and absorption indices that increase with the degree of aromatization, and are dependent upon the concentration of delocalized electrons (Taylor et al., 1998).

Figure II.5 shows the approximate correlation of various maturation parameters for OM in coal and kerogen (Mukhopadhyay, 1994).

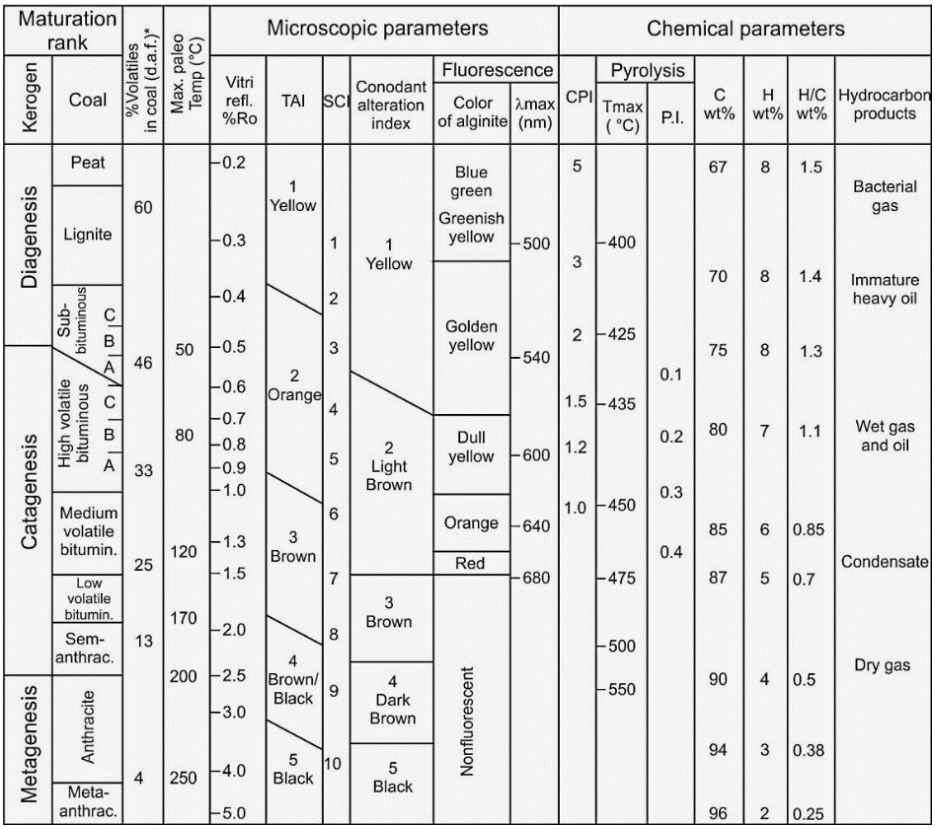

Figure II.5. Correlation of indicators for OM in coal and kerogen and their relation to the organic maturation stages and the hydrocarbons generated (Staplin, 1969; Teichmüller, 1974; Mukhopadhyay, 1994; Hunt, 1995; Pearson, 1990). R_o= reflectance; TAI= Transmission Alteration Index; SCI= Spore Coloration Index; CPI= carbon preference index; PI= production index. *Dry ash free basis.

Chapter III - Materials and Methodologies

III.1. Materials

For the development of this research, sample collection was performed with the purpose of evidencing the organofaciologic and organogeochemistry variations during the T-OAE in the studied basins. With that premise, sampling comprised the interval between the upper Pliensbachian to lowermost middle Toarcian (base of Bifrons Zone) of three reference sections of GCB (Suèges), QB (Caylus) and PB (Pont de Suert) (Cubaynes, 1986; Faure, 2002; Mailliot et al., 2009) (Figures I.1 and III.1). Ammonite biostratigraphy of the three sections was carried out by Dr. Philippe Fauré.

The samples were collected by Professor Carine Lézin from Paul Sabatier University – Toulouse III and received at the Department of Earth Sciences of University of Coimbra where an inventory of all samples and their accommodation in labeled transparent plastic bags was performed. The samples were at a later time sent to the Laboratory of Palynofacies and Organic Facies of the Federal University of Rio de Janeiro (LAFO-UFRJ). At LAFO-UFRJ was executed all the sample preparation for application of geochemistry (TOC, TS, IR and biomarker) and petrographic (palynofacies and organic petrology) techniques for the identification and characterization of the organic facies. Before storage a hand specimen description of each sample was performed according to Mendonça Filho et al. (2014b) recording grain size, color, sediment fabric, macrofossil content and the presence or absence of macroscopic details, such as, occurrence of iron oxides.

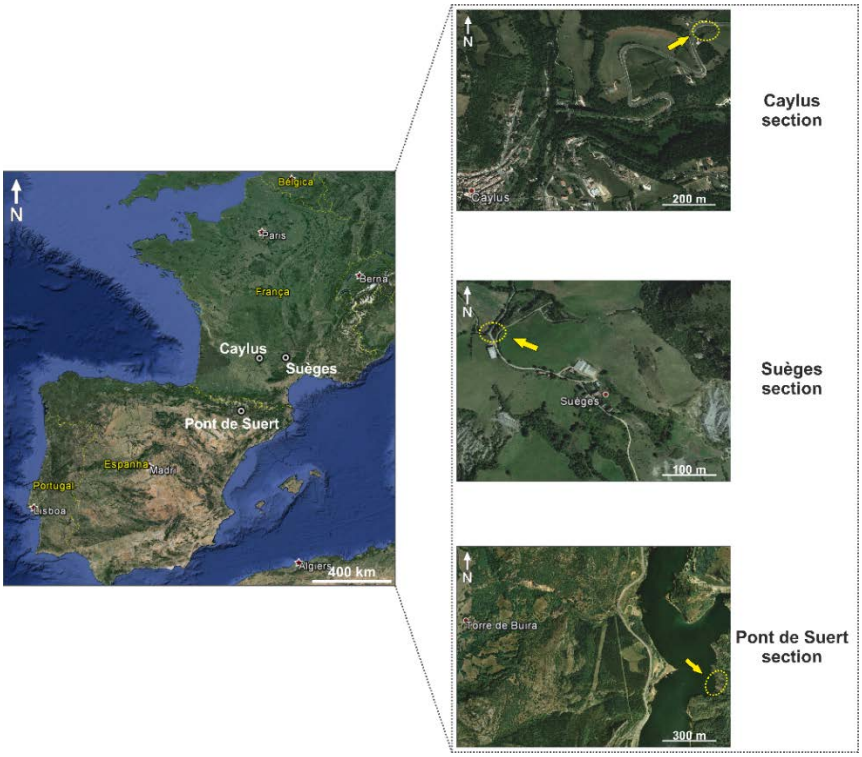

Figure III.1. Sampling location and geographical setting (adapted from Google Earth, 2016).

III.1.1. Grands Causses Basin – Suèges Section

In the GCB, the Suèges section (coordinates: 44°12'34.51''N; 3°6'16.18''E) was selected for sample collection, based on the stratigraphic log by Lézin and Fauré (unpublished) (Figure III.2).

From this section were collected 13 samples (S10 to S69, Figure III.2) belonging to the **Rivière-sur-Tarn Group**: three from late Pliensbachian **Marnes de Villeneuve Fm.** (S10, S11 and S12), seven from Toarcian (Tenuicostatum and Serpentinum zones) **Schistes Cartons Fm.** (S15, S17, S19, S22, S50, S52 and S55) and three from Toarcian (top of Serpentinum Zone) **Marnes de Fontaneilles Fm.** (S61, S62 and S69).

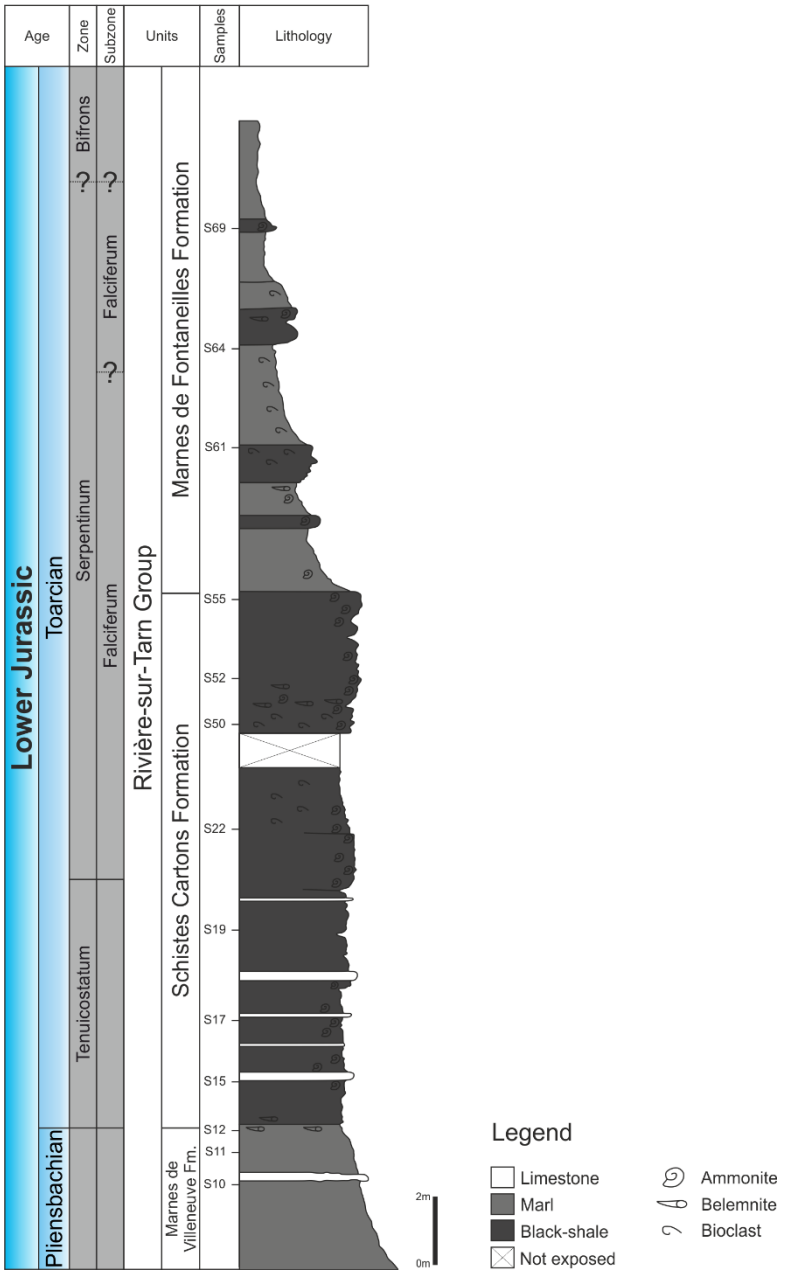

Figure III.2. Suèges section stratigraphic log (modified from Lézin and Fauré, unpublished) with sample location.

III.1.2. Quercy Basin – Caylus Section

In the QB, the Caylus section (coordinates: 44°14'35.75''N; 1°47'5.75''E) was selected for sample collection, based on the stratigraphic log by Lézin and Fauré (unpublished) (Figure III.3).

From this section were collected 11 samples (Cay 1 to Cay 28, Figure III.3): four from upper Pliensbachian to lowermost Toarcian (Tenuicostatum Zone) **Barre à Pecten Fm.** (Cay1, Cay3, Cay6 and Cay7), six from Toarcian (Tenuicostatum to Serpentinum zones) **Schistes Cartons Mb.** of the **Penne Fm.** (Cay10, Cay13, Cay18, Cay20, Cay23 and Cay26) and one from the Toarcian (Serpentinum Zone) **Marnes et calcaires à *Hildoceras* Mb.** of the **Penne Fm.** (Cay28).

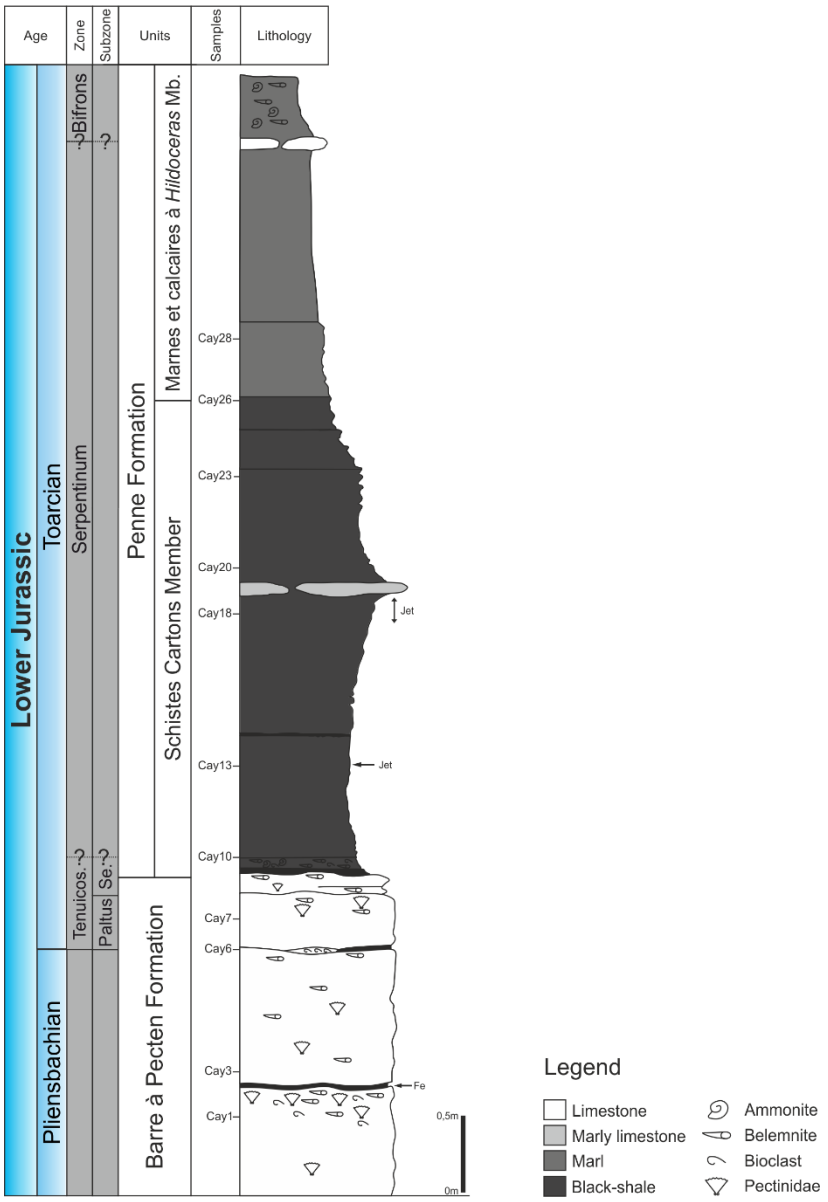

Figure III.3. Caylus section stratigraphic log (modified from Lézin and Fauré, unpublished) with sample location. Tenuicos.=Tenuicostatum; Se.=Semicelatum.

III.1.3. Pyrenean Basin – Pont de Suert Section

In the PB, the Pont de Suert section (coordinates: 42°23'0.25''N; 0°44'49.73''E) was selected for sample collection, based on the stratigraphic profile by Lézin and Fauré (unpublished) (Figure III.4).

From this section were collected a total of 14 samples (20PS to 255PS, Figure III.4): one from upper Pliensbachian **Barre a Pecten Fm.** (20PS), five from the Toarcian (Tenuicostatum Zone) **Calcaires argileux à *Spirifèrines* Mb.** of the **Padrinas Fm.** (45PS, 65-7PS, 75PS, 100PS and 115PS), three from the Toarcian (Serpentinum Zone) **Calcaires argileux et marnes à *Soaresirhynchia* Mb.** of the **Padrinas Fm.** (300PS, 330PS and 355PS) and five from the Toarcien (Serpentinum to Bifrons zones**) Calcaires argileux à *Telothyris* Mb.** of the **Padrinas Fm.** (380PS, 420PS, 470PS, 255PS and 265PS).

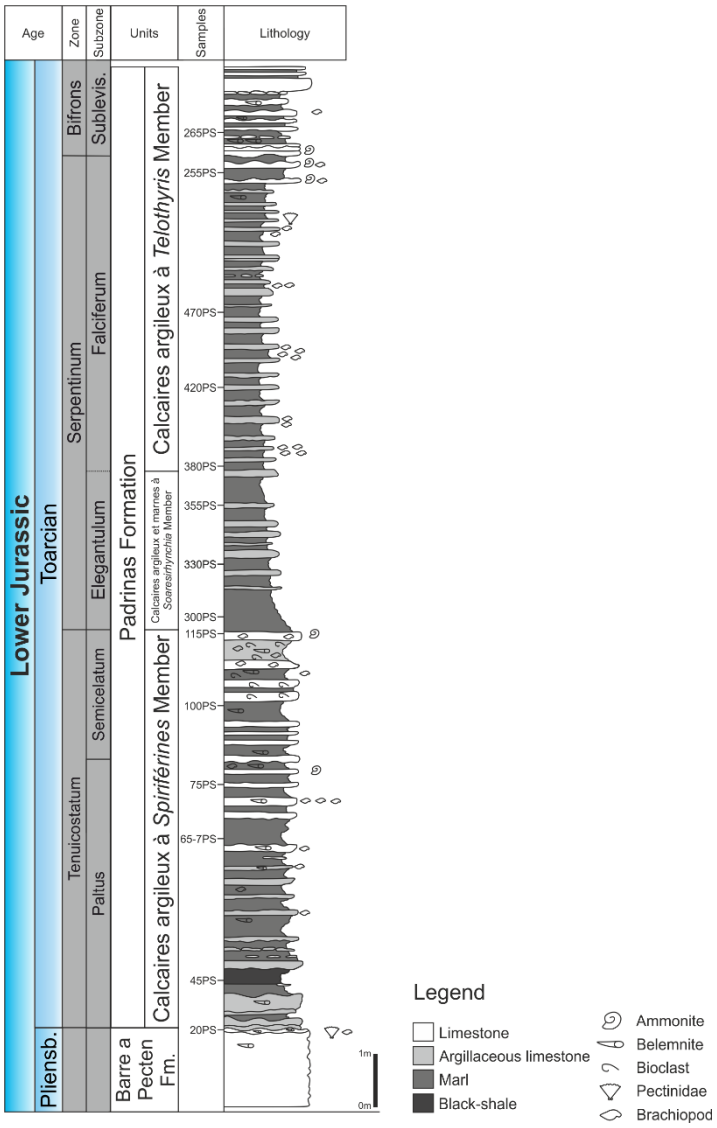

Figure III.4. Pont de Suert section stratigraphic log (modified from Lézin and Fauré, unpublished) with sample location. Pliensb.=Pliensbachian; Sublevis.=Sublevisoni.

III.2. Methodologies

This section comprises a detailed description of the sample preparation and methodologies employed in this study. The selected techniques allow the petrographic characterization and classification of the kerogen (palynofacies and organic petrology) and geochemical representation of the samples (Figure III.5).

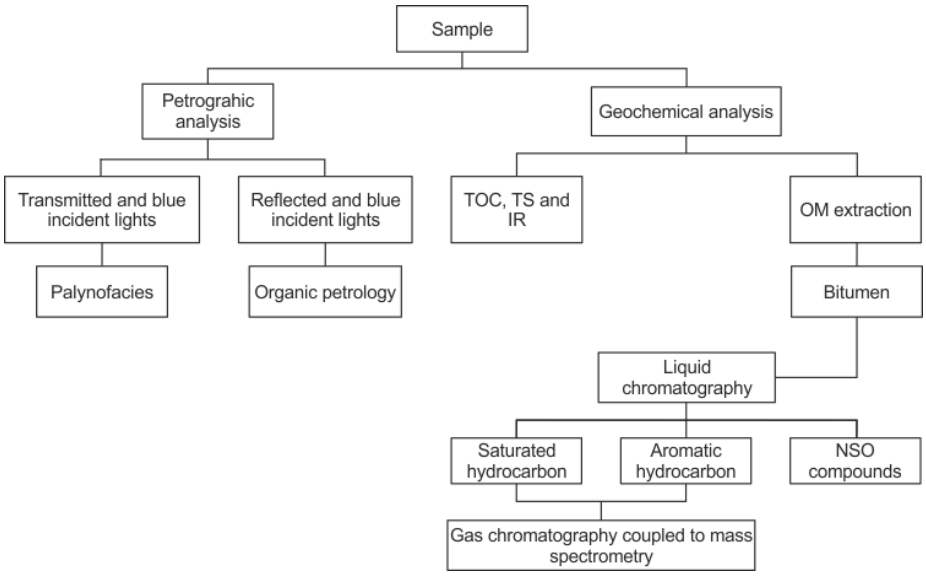

Figure III.5. Flowchart of the analytic techniques implemented in this study for the characterization of the kerogen and bitumen. TOC=Total organic carbon; TS=Total Sulfur; IR=Insoluble residue; OM=Organic matter; NSO=Polar compounds.

III.2.1. Petrographic analysis

III.2.1.1. Palynofacies

The pattern of sample collection and sample processing technique strongly affects the value of kerogen analysis data. The reliability of the interpretation of organic constituents' assemblage can be strongly influenced by the quality of the samples and their preparation. These interpretations are, therefore, conditioned by the know-how of the sample technician and processor. Control over these factors can have major impact on the utility and application of kerogen analysis data.

A handful of protocols are available for kerogen analysis sample preparation. These techniques generally involve methods of freeing organic-walled microfossils from sediment and concentrating them for ease of examination (Mendonça Filho et al., 2010a; 2011a; 2014a).

III.2.1.1.1. Sample Preparation

Kerogen isolation from the rock matrix was performed using standard non-oxidative procedures according to Tyson (1995) and Mendonça Filho et al. (2010a; 2011a; 2014a) (Figure III.6). Each rock sample was fragmented to a size of 2 mm to 5 mm with posterior elimination of contaminations. For cleaning, mechanical (washing with water, detergent or alcohol) and chemical (extraction method using organic solvents, etc.) techniques can be used depending of the type or condition of the samples.

A total of 20 g of sediment underwent acid treatment for removal of the mineral matrix. Acidification comprises the sequential addition of: (i) HCl (37%) for 18 hours for removal of the carbonates; (ii) HF (40%) for 24 hours for removal of the silicates; and, (iii) (37%) for 3 hours to remove possible neoformed fluorides. Between each step the pH material was neutralized with distilled water and the sample was then sieved using polyester net (10 μm to 20 μm) keeping only the retained material. The organic and non-organic material was separated by flotation using a heavy liquid, in this case $ZnCl_2$ (density=1.9 to 2 g/cm^3), for a period of 24 hours. The sample was homogenized and centrifuged to obtain the separation in two fractions – organic fraction was recovered and the heavy liquid was eliminated using drops of HCl (10%) followed by a wash with distilled water.

The isolated kerogen was sieved at 10 μm and a portion of the retained material was used to prepare palynofacies microscope slides using one glass slide (24x76mm) and two cover slips (24x24mm). In one of the slips is deposited the non-sieved material and in the other the kerogen previously sieved at 10 μm. In both is added 2 drops of acacia gum and a few drops of distilled water to homogenize. This procedure is prepared in a hot plate (50^{o}C). When dry, they are fixed with a xylene based resin (Entellan-Merck) to a glass slide properly labeled.

The same material was used to prepare plugs of concentrated kerogen that are prepared using a Teflon mold and mounted with a mixture of epoxy resin and hardener. The plug is then labeled and polished for posterior microscopic analysis.

The isolated kerogen of some samples underwent panning following the methodology described by Oliveira et al. (2004) to increase palynomorph recovery and microscope slides were prepared with the 5-60 μm and >60 μm OM fractions.

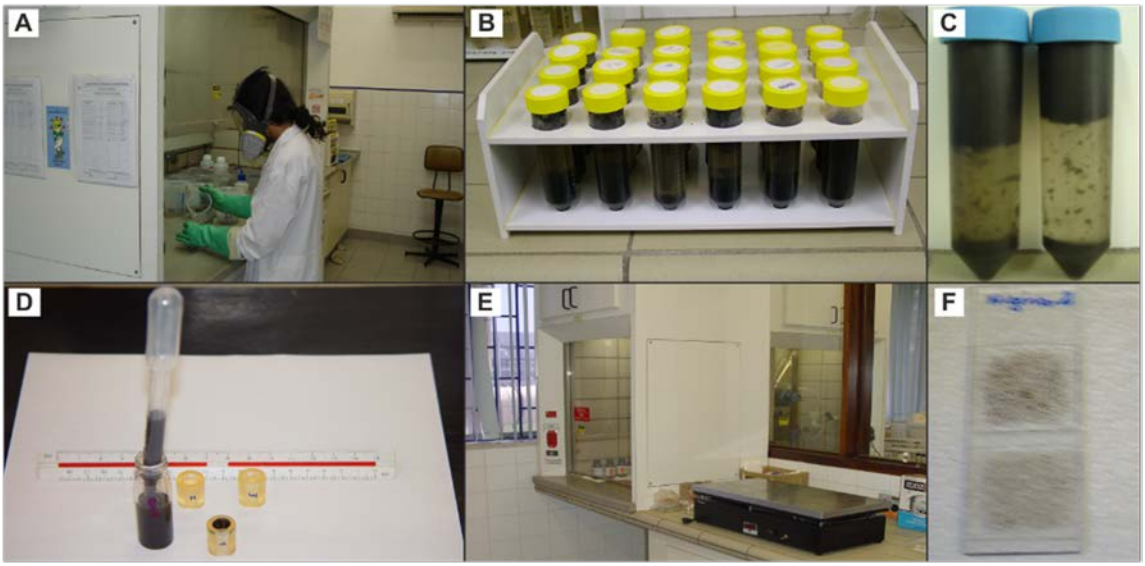

Figure III.6. Sample preparation laboratory procedures. **A** - Acid maceration, washing, and neutralization; **B** - Density flotation ($ZnCl_2$); **C** - Organic residue - supernatant; **D** - Isolated kerogen and plug assembling; **E** - Slide assembling (hot plate); **F** – Palynofacies slide.

III.2.1.1.2. Microscopic analysis

For isolated kerogen examination was performed a microscopic analysis of the slides, using transmitted white and incident blue lights, and the plugs of concentrated kerogen, using reflected white and incident blue lights. In some cases, reflected white light (RWL) was used in the palynofacies slides to distinguish specific components (phytoclasts and zooclasts). The combined use of these lights allows the identification of the different particles that constitute the palynological OM assemblage by their morphology and optical properties (qualitative fluorescence, translucency and texture) (Tyson, 1995; Mendonça Filho et al., 2010a, b; 2011 a, b, c; 2012; 2014a, b, c; Suárez-Ruiz et al., 2012).

For obtaining the palynofacies data a qualitative (identification of the particles) and quantitative (counting) analysis of the kerogen components were performed. The counting of the organic particles was based on the models proposed by Tyson (1995) and Mendonça Filho et al. (2010a, 2011a, b, c, 2012, 2014a, b, c) which state that 300 to 500 particles are necessary to estimate the amount of OM present in a sample (300 particles are sufficient for particulate OM).

Organic particles classification followed the system of groups and subgroups of OM proposed by Tyson (1995); Vincent (1995); Mendonça Filho et al. (2010a, 2011c, 2012, 2014c, 2016, *Ineditus in efficiendis*). This counting was executed using a Carl Zeiss Axio Imager A1 microscope equipped with an ocular with 10x and objective with 20x magnification and the data was obtained by performing a series of non-overlapping transverses lines across the slide using a vertical or horizontal cross graduated reticule

(scale) and registering only the particles that pass directly under the cross-wires, omitting any remaining particles. All particles under the field of view of the cross lines of the reticule are counted except those with size smaller than 10μm (except palynomorphs) and any contaminants (identified by color, relief or form), unrecognizable fragments of palynomorphs which had less than half of the original form are ignored. The slide must also be methodically scanned for any rare palaeoecological indicators that were not documented during the counting process (Mendonça Filho et al., 2010a; 2011a, b, c; 2012; 2014a, b, c; Suárez-Ruiz et al., 2012).

III.2.1.1.3. Statistical treatment

Following the organic particulate component count a basic statistical treatment of the data was performed recalculating and normalizing absolute values for percentages. Binary and ternary plots were produced for a better visualization of the results. This data was also submitted to the multivariate statistical analyses (cluster analysis), among kerogen groups and subgroups (correlation coefficient Pearson/R-Mode) and for the similarities between samples (Q-Mode), using the StatSoft® STATISTICA software version 7.0 (Valentin, 2000).

III.2.1.2. Organic petrologic analysis

III.2.1.2.1. Sample Preparation

Optical petrography was performed on whole rock polished blocks prepared according to standard procedures (ISO 7404-2, 2009) and plugs of concentrated kerogen and palynofacies slides prepared according to sample preparation protocol described in point III.2.1.1.1. of this chapter.

III.2.1.2.2. Microscopic analysis

Spore coloration index (SCI)

SCI determination was based on the standard slides of LAFO-UFRJ with a scale of 1 to 10 with intervals of 0.5 (Figure III.7). With the increase in thermal maturity of OM is observed a gradual change in color of the spores in TWL, from yellow (immature samples) through orange, brown and black, finishing with opaque organic particles. SCI was performed in slides with presence of sporomorphs (based on previous palynofacies analysis). It was carried out in a Carl Zeiss Axio Imager A1 microscope with 20x magnification through the optical comparison of sporomorphs coloration in TWL.

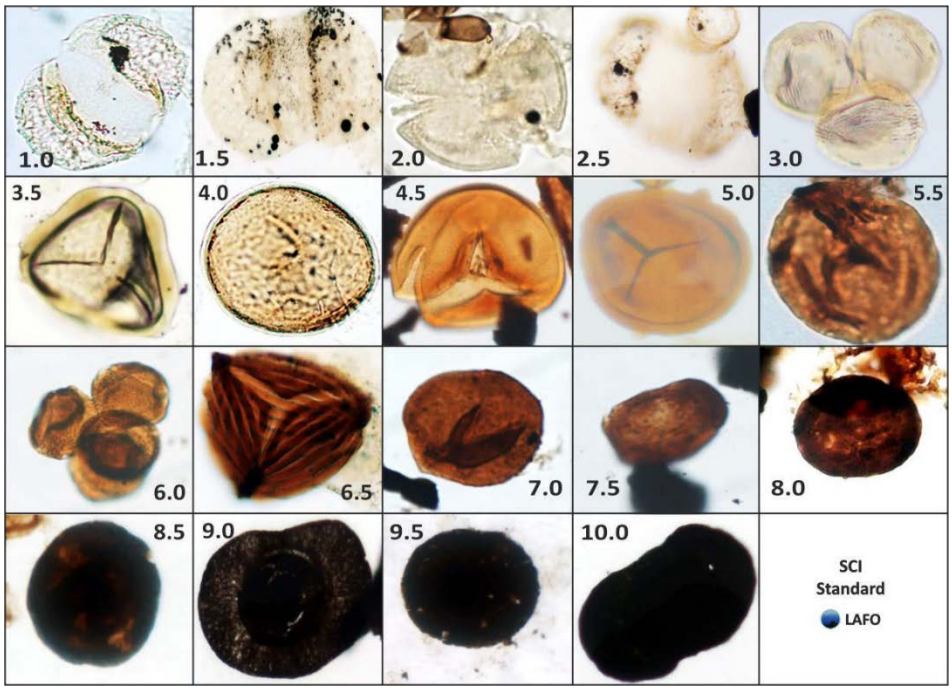

Figure III.7. SCI scale proposed by Fischer et al. (1980). Standard from LAFO/UFRJ (Mendonça Filho et al., 2014b).

Spectral fluorescence analysis

Spectral fluorescence analysis is based on the measure of spectral intensity between 400 to 700 nm (Ottenjahn et al., 1974, 1981; Ottenjahn, 1975, 1980). Spectral fluorescence measurements were executed with a Zeiss Axioskop 2-plus microscope, with 50X magnification in immersion oil (η_e=1.518 to 23 °C), and (Zeiss) ultraviolet G 365, FT 395 and LP 420 filters. The correction factor was obtained based on the calibration of a lamp (Baranger et al., 1991). Spectral fluorescence analysis was performed on selected macerals from the liptinite group (Taylor et al., 1998) (*Tasmanites* - Prasinophyte algae) using calibration procedures described by Araujo et al. (2002, 2003).

Organic matter reflectance

Reflectance measurements were performed in plugs of concentrated kerogen with a Zeiss Axioskop 2-plus microscope, equipped with spectrophotometer J&M (MSP 200), with 50x magnification in immersion oil (η_e=1.518 to 23 °C), according to ASTM D7708, 2014 procedure. The microscope was calibrated with a YAG standard (0.905% R_f). The OM reflectance was measured in Hydroid fragments and the reflectance values were converted to equivalent vitrinite reflectance using the equation [1] proposed by Bertrand and Malo (2012) and Hartkopf-Fröder et al. (2015):

$$VR_{eq} = 0.6493 * HR_r + 0.2126 \ [1]$$

where VR_{eq} is the equivalent vitrinite reflectance and HR_r is the measured hydroid random fragment reflectance.

These zooclasts have been used for vitrinite reflectance assessment in previous OM maturation studies of Paleozoic basins in Ordovician and Silurian sediments (Bertrand, 1987, 1990, 1993; Héroux and Chagnon, 1994; Héroux et al., 1996, 2000; Bertrand et al., 2003; Bertrand and Malo, 2005, 2012).

III.2.2. Geochemical analysis

III.2.2.1. Total Organic Carbon (TOC), Total Sulfur content (TS), Insoluble Residue (IR)

The TOC determination provides a simple measure of OM content in sediments and sedimentary rocks usually expressed as the relative weight percentage of organic carbon on a dry basis (Jarvie, 1991; Bordenave et al., 1993), including both the insoluble (kerogen) and soluble (bitumen) OM.

TOC is determined through the combustion of the organic carbon to CO_2 in an oxygenated atmosphere using the decarbonated residue of the powered sample (after acid treatment) following the ASTM D 4239, 2008 and NCEA-C-1282, 2002.

About 0.5 g of sample was pulverized using an agate mortar from which, a portion of 0.26 g was weighed in sample holder porcelain filter (of known weight) and added HCl (50%) for the removal of the carbonate fraction with an acid treatment with the duration of 24 hours. For the elimination of the chloride fraction was added distilled hot water (100ºC) for 1 hour. The water was neutralized at temperature room (checking with universal paper), followed by the rejection of the excess water and the sample was dried in an oven at 65ºC for about 3 hours followed by weighing. TOC and TS were determined simultaneously by a SC 144DR – LECO® analyzer, composed by an oven with an oxygen atmosphere (super dry) at the temperature 1350ºC, which leads to the entire combustion of the components by the oxidation-reduction process, and by an infrared analyzer (Figure III.8).

The data of the carbon and sulfur gases (CO_2 and SO_2) concentrations are expressed in percentage over the relative weight of the sample.

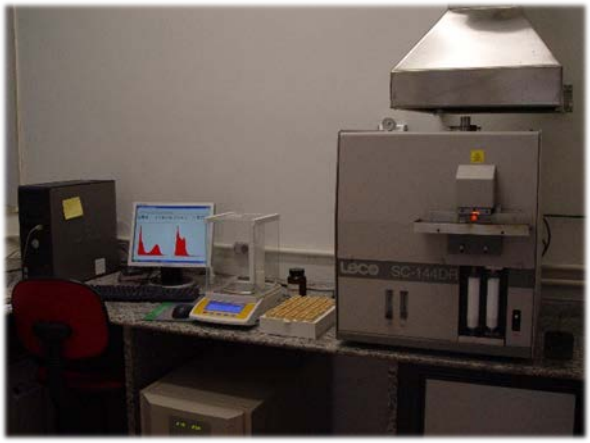

Figure III.8. SC 144DR – LECO® analyzer (LAFO-UFRJ).

The IR was calculated at the end of the sample preparation process utilizing equation [2]:

$$IR(\%) = \frac{DM}{TM} \times 100 \text{ [2]}$$

where DM is the decarbonated sample weight and TM is the total weight of the sample before acidification. The results are expressed in weight percentage.

III.2.2.2. Molecular compounds

III.2.2.2.1. Bitumen Extraction

The bitumen was obtained by extraction in a Dionex® ASE 350 equipment using dichloromethane as solvent (Figure II.9). Extraction begins with the previously grinded and weighed sample in the extraction cell. The cell is loaded in the system and is added ultrapure dichloromethane (CH_2Cl_2) followed by the increasing of the temperature (60ºC) and pressure (from 700psi to 1700psi). Extraction occurred in a static mode (without solvent flux through the cell), in a total of five cycles (5 minutes each). This procedure is repeated according to each sample needs. The extract is then transferred to a recovery tube containing activated copper filings for capture of free sulfur. The samples with the most amount of sulfur are subjected to an activated copper column to confirm the capture of whole free sulfur.

The recovery tubes are placed in a rotating evaporator for solvent/extract separation. The extractable organic matter (EOM) is then transferred to a new recipient and weighed.

Figure III.9. Dionex® ASE 350 extraction equipment.

III.2.2.2.2. Liquid Chromatography (LC)

The EOM was separated into saturated hydrocarbons (HC), aromatic HC and NSO (Nitrogen, Sulfur and Oxygen containing non-hydrocarbons) compounds by an open-column chromatography with activated silica gel. A 25 mm i.d. column is packed with pre-activated silica gel (28-200 mesh). The bitumen sample is poured on to the column and fractions are collected by successive elution of solvents with increasing polarity of a particular molecule. The solvents *n*-hexane, *n*-hexane/dichloromethane (8:2, v/v) and dichloromethane/methanol (1:1, v/v) were used to elute saturated, aromatic and polar NSO fractions, respectively.

III.2.2.2.3. Gas Chromatography coupled to Mass Spectrometry (GC-MS)

The saturated and aromatic fractions were analyzed in an Agilent® 7890 gas chromatographer (GC) equipped with an Agilent® 7683 autosampler coupled to a triple quadrupole mass spectrometer (MS) (Figure III.10).

Figure III.10. Agilent® 7890 gas chromatographer (LAFO – UFRJ).

The GC operated with a capillary column DB-5 Agilent (5% phenyl, 95% methylsiloxane, 30 m x 0.25 mm i.d., thickness 0.25 μm), at an initial temperature of 70ºC (1 min) raising up to 170ºC at 20ºC/min and 310ºC at 2ºC/min (10 min). The inert carrier gas used was helium at a constant flow mode of 1.2 ml/min. The injector run at a constant temperature (280ºC) and was injected 1 μm with split or splitless, according to each sample. Transfer line temperature was 300ºC. MS run with an ion source temperature 280ºC, interface temperature 300ºC, quadrupole temperature 150ºC and ionization voltage 70 eV.

Each injected sample is vaporized and mixed with the helium moving along the capillary column. This movement induces the separation of the different compounds that are repeatedly retained by a stationary phase. The compounds are then released into the mobile phase depending on their volatility and affinity for each phase (retention time) inducing a separation according to molecular weight and volatility. The separated compounds enter the MS ion chamber where they are bombarded with a high-energy electron beam ionizing the molecules by knocking off one electron. The molecule and fragment ions produced differ in mass, but most bear a +1 charge. These differences in mass/charge (m/z) caused by differences in mass allow the particles to be separated by a magnetic field or quadrupole mass filters. The separated ions move then to the detector where the relative abundances of each mass are recorded.

The analyses were performed using **selected ion monitoring** of the ions (m/z) 85, 191, 217 and 218 for the saturated HC fraction and a full **scan** was performed for the aromatic HC fraction. The data was reviewed in the Agilent® MassHunter software for mass chromatogram identification and pick area determination of each compound by retention time and mass spectrum comparison with known molecular compounds.

Chapter IV - Results

In this chapter are presented the results of sample macroscopic characterization, palynofacies study, geochemistry and organic petrology techniques for the three studied sections: Suèges (GCB), Caylus (QB) and Pont de Suert (PB). For the photographic characterization of the OM of each succession was assembled, in the item Appendix B, a petrographic atlas with the microscopic aspects observed on the palynofacies slides and plugs of concentrated kerogen. In this chapter are only displayed some photomicrographs of the new components described by the most recent OM classification system (hydrozoans).

IV.1. Suèges section – Grands Causses Basin

IV.1.1. Macroscopic characterization

According to the macroscopic analysis performed, following the standard methodology for organic petrology analyses, the studied samples from the Suèges section (GCB) represent a succession of light to dark grey organic-rich marls with levels of black shales, namely in the Schistes Cartons Fm.. Lamination of different intensities is present throughout the profile and was possible to recognize belemnite fragments in sample S55 (Table IV.1).

Table IV.1. General macroscopic characterization, geochemistry and palynofacies data of samples from the Suèges section.

Age	Biostratigraphy		Units		Sample	General Characterization			Geochemistry			Palynofacies			
						Lithology	Color	Other Characteristics	TOC (wt.%)	TS (wt.%)	IR (wt.%)	Phytoclast (%)	Amorphous (%)	Palynomorph (%)	Zooclast (%)
Toarcian	Serpentinum	Falciferum	Rivière-sur-Tarn Group	Marnes de Fontanelles Fm.	S69	Marl	Dark grey	Lamination	2.60	0.95	64	0.97	51.94	6.77	40.32
					S64	Marl	Dark grey	Intense lamination	1.28	0.98	50	6.33	44.62	21.20	27.85
					S61	Marl	Dark grey	Lamination	4.31	0.50	56	0.00	79.33	0.67	20.00
		Exaratum		Schistes Cartons Formation	S55	Marl	Dark grey	Belemnites, Lamination	3.12	0.61	59	0.00	67.44	1.00	31.56
					S52	Black Shale	Dark grey	Lamination	4.56	0.29	56	1.33	97.67	0.66	0.33
					S50	Black Shale	Dark grey	Mild lamination	5.97	1.17	50	0.33	99.34	0.33	0.00
					S22	Black Shale	Dark grey	Lamination	6.53	1.75	49	0.65	98.39	0.32	0.65
	Tenuicostatum	Semicelatum			S19	Black Shale	Dark grey	Lamination	4.40	0.86	42	1.31	96.72	0.66	1.31
					S17	Black Shale	Dark grey	Lamination	6.13	0.45	62	1.30	95.44	0.65	2.61
					S15	Black Shale	Dark grey	Intense lamination	6.79	1.30	84	0.31	97.17	0.63	1.89
Pliensbachian				Marnes de Villeneuve Fm.	S12	Marl	Grey	Lamination	0.91	0.78	71	10.19	35.99	19.43	34.39
					S11	Marl	Light grey	Lamination	0.70	0.87	63	19.87	14.57	31.13	34.44
					S10	Marl	Light grey	Mild lamination	0.50	0.87	64	23.92	17.28	25.91	32.89

IV.1.2. Geochemistry

The TOC, TS and IR data obtained for samples from the Suèges section are summarized in Table IV.1.

The geochemical study of this section revealed TOC values ranging between 0.50 wt.% (S10) and 6.79 wt.% (S15). The highest values are associated to the black

shales of the Schistes Cartons Fm. (average of 5.36 wt.%) and the lowest values are recorded in the Marnes de Villeneuve Fm. (average of 0.70 wt.%). The Marnes de Fontaneilles Fm. shows the mean values for the section with an average 2.73 wt.%.

TS data varies from 0.29 wt.% (S52) to 1.75 wt.% (S22), both values recorded in the Schistes Cartons Fm.. Despite the disparity of the results observed, this unit presents the highest average of the section (0.92 wt.%). The Marnes de Villeneuve Fm. and Marnes de Fontaneilles Fm. show similar averages, 0.84 wt.% and 0.81 wt.%, respectively.

IR values range from 42 wt.% (S19) to 84 wt.% (S15).The lowest registered average (57 wt.%) corresponds to both Schistes Cartons and Marnes de Villeneuve formations and the highest is observed in the Marnes de Villeneuve Fm. (66 wt.%).

IV.1.3. Palynofacies

The palynofacies analysis performed in samples from the Suèges section revealed the presence of particulate organic compounds from all the OM groups (Phytoclast, Amorphous, Palynomorph and Zooclast groups) with a predominance of the Amorphous group in the majority of the samples, except samples S10 and S11, where the Zooclast group predominates (Appendix A.1; Table IV.1).

The **Phytoclast group** is present in most samples of the succession, ranging between 0% (S55 and S61) and 23.92% (S10) (Appendix A.1; Table IV.1). Its highest abundance is recorded in the Marnes de Villeneuve Fm. (average 17.99%) and the lowest values are observed in the Schistes Cartons Fm. and Marnes de Fontaneilles Fm. (average 0.75% and 2.43%, respectively) (Appendix A.1; Table IV.1). This group is mainly composed of **non-opaque non-biostructured phytoclasts (NONB)** (63.7% of total phytoclast) with dark brown color under TWL and, usually, without fluorescence (Appendix A.1). These phytoclasts present irregular outlines and are, in most cases, degraded. The other subgroup of phytoclast present in the samples is the **non-opaque biostructured phytoclast (NOB)** (Appendix A.1). This subgroup is represented by stripped, banded and pitted **NOB** phytoclasts with brown to dark brown color under TWL and usually without fluorescence (Appendix B.1.1). In these samples no opaque phytoclasts or membranes were identified in the palynological assemblage. Some cuticle layer fragments associated with innermost part of epidermis were identified (but not accounted), which could indicate that the land fragments derived from leaves (Appendix B.1.1).

The **Amorphous group** dominates most of the succession, with its values ranging between 14.57% (S11) and 99.34% (S50) (Appendix A.1; Table IV.1). The Schistes Cartons Fm. is particularly rich in these components showing the highest values of the section

(average 93.17%). The lowest average percentage of this constituents is recorded in the Marnes de Villeneuve Fm. (average 22.61%). This group is dominated by **AOM** related with microbiological reworking processes of components from the **Zoomorph subgroup** (possibly Hydrozoan polyps, medusae, tentacles, unarticulated colonies elements, etc.) (Appendix A.1, B.2.1 and B.5; Figure IV.1). The AOM shows a heterogeneous characteristic, sometimes with inclusions (hydrozoan medusae and zooclasts). Different amorphization stages were identified ranging from subangular particles with neat boundaries to particles with diffuse limits or even completely unstructured. The AOM shows a brown to dark brown color under TWL and a dark orange fluorescence. Some resin particles were identified in some samples (S10, S11, S12, S17 and S69) (Appendix A.1 and B.2.1).

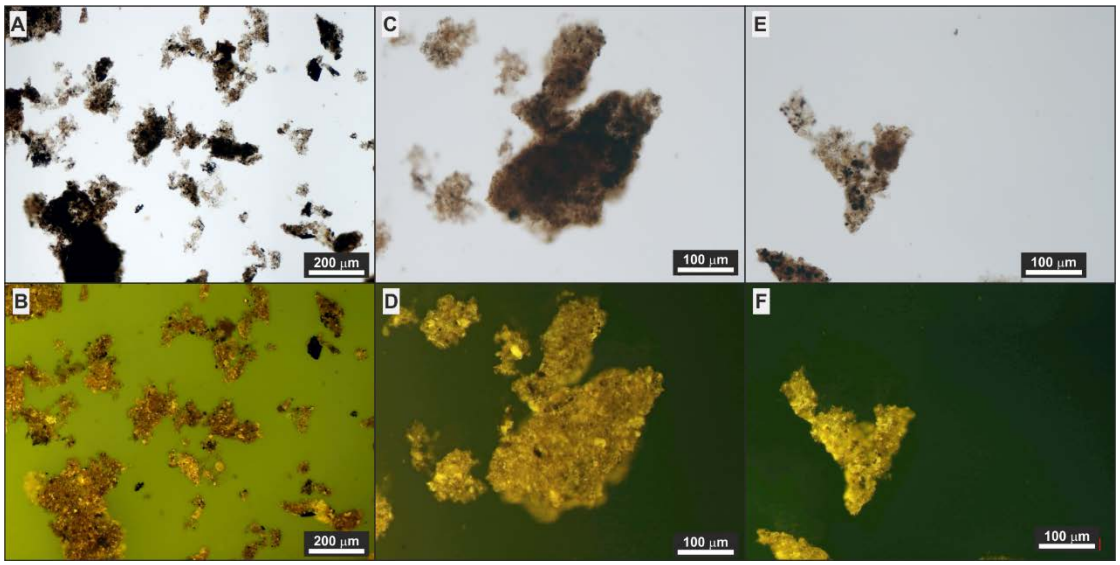

Figure IV.1. General aspects of Hydrozoan derived AOM. **A** (S50), **C** (S17), **E** (S15) - TWL; **B**, **D**, **F** - FM.

The **Palynomorph group** exhibits very low values for the majority of the samples varying from 0.32% (S22) to 31.13% (S11) (Appendix A.1; Table IV.1). In this section were identified components from all palynomorph subgroups (sporomorph, freshwater microplankton, marine microplankton and zoomorph). Terrestrial components from the **sporomorph subgroup** were observed mainly in samples from the Marnes de Villeneuve Fm. and Marnes de Fontaneilles Fm., showing very low to null percentages in the Schistes Cartons Fm. (Appendix A.1). This subgroup is represented by spores and pollen grains. The **spores** display different sizes, shapes (from oval to triangular) and ornamentations, with some of them exhibiting the trilete mark on the surface. They present an orange to light brown coloration under TWL and orange fluorescence (Appendix B.3.1.1). **Pollen grains** exhibit various form, sizes and ornamentations, an orange to dark orange coloration under TWL and orange fluorescence (Appendix B.3.1.1). In some samples was possible to observe agglomerates (dyads, tetrads and polyads) and bisaccate pollen

grains, especially in samples S12, S64 and S69 (Appendix A.1 and B.3.1.1). In samples S10, S11 and S 12 was possible to identify pollen grains and dyads from the genus *Classopollis*, with important paleoenvironmental significance (Appendix B.3.1.1).

Freshwater microplankton is represented by **Gloeocapsomorpha** specimens, being one of the main constituents of the palynological assemblage of sample S64 (12.03%), but they are also present in samples S12, S19, S55 and S69. These components usually exhibit a light brown outline with a dark opaque center under TWL due to sulfide inclusions and a dark orange fluorescence (Appendix A.1, B.3.1.2 and B.5).

The **marine microplankton** components were identified as Dinoflagellate Cysts, Acritarchs and Prasinophyte algae (*Tasmanites*). The **Dinoflagellate Cysts** were identified in all samples from the Marnes de Villeneuve Fm. (S10, S11 and S12) and one sample from the Marnes de Fontaneilles Fm. (S64). They display a very light brown coloration under TWL and an intense yellow fluorescence (Appendix A.1 and B.3.1.3). **Acritarchs** were observed in samples S10, S11 and S12 (Marnes de Villeneuve Fm.), S15 (Schistes Cartons Fm.) and S64 (Marnes de Fontaneilles Fm.). They are small sized and exhibit a very light brown color under TWL and a yellow fluorescence (Appendix A.1 and B.3.1.3). **Prasinophyte algae** (*Tasmanites*) were mainly observed in samples from the Schistes Cartons Fm. (S19, S22, 50 and S52), but were also found in samples S11 (Marnes de Villeneuve Fm.) and S69 (Marnes de Fontaneilles Fm.). *Tasmanites* are spherical, smooth and thick-walled, displaying a brown coloration under TWL and a yellow fluorescence (Appendix A.1 and B.3.1.3).

The **zoomorph subgroup** is represented by Foraminiferal Test-Linings (S10 and S11) (Appendix B.3.1.4) and **Hydrozoan medusae** (S10, S11, S12, S61, S64 and S69) (Appendix A.1). **Hydroids in an embryonic stage** (medusae in initial stages of development – Figure IV.2; and, medusae eggs - Figure IV.3) were also identified in the 5-60μm and >60μm OM fractions of samples S10 and S11.

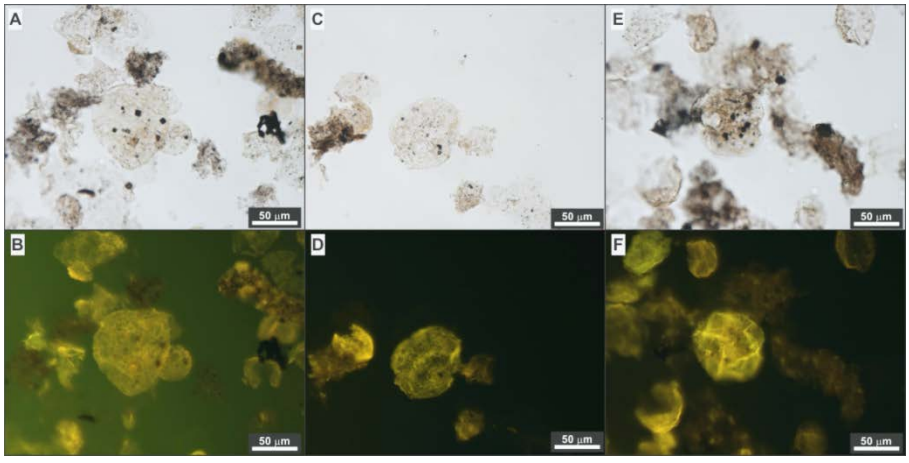

Figure IV.2. Embryo stage of Hydrozoans in initial stages of development (S12). **A**, **C**, **E** - TWL; **B**, **D**, **F** – FM.

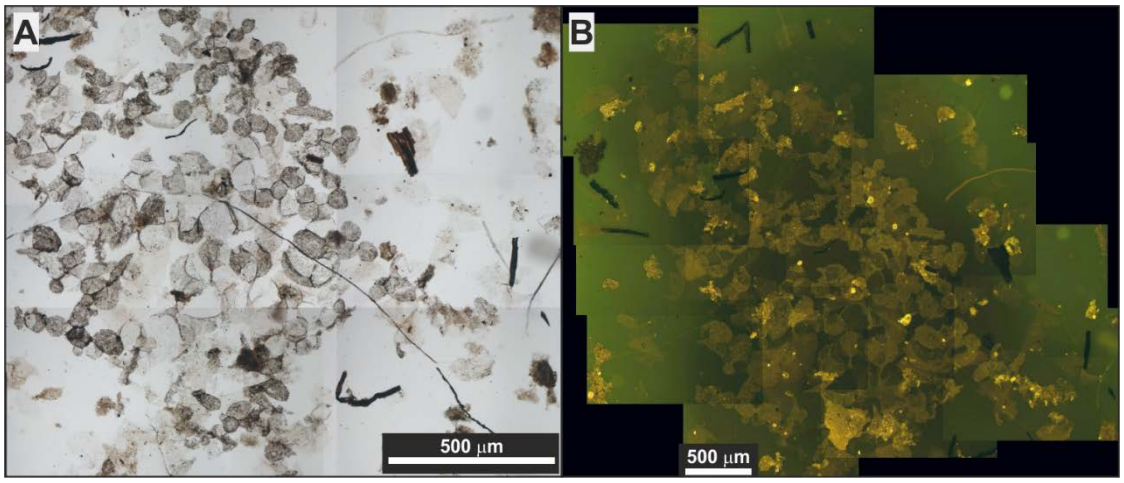

Figure IV.3. Hydrozoan medusae eggs (S12). **A** - TWL; **B** - FM.

The **Zooclast group** (zoomorph fragments) is characterized by **possible hydrozoan polypoid forms fragments** (Appendix B.4.1; Figure IV.4). Some of the particles present morphological characteristics that allow their probable association with hydrozoans. Typically these fragments present no fluorescence but in some cases can display a fluorescence coloration ranging from dark orange to dark brown. Their abundance varies from 0% (S50) to 40.32% (S69) with the highest mean value being recorded in samples from Marnes de Villeneuve Fm. (33.91%) and their lowest mean value in samples from the Schistes Cartons Fm. (5.48%) (Appendix A.1; Table IV.1).

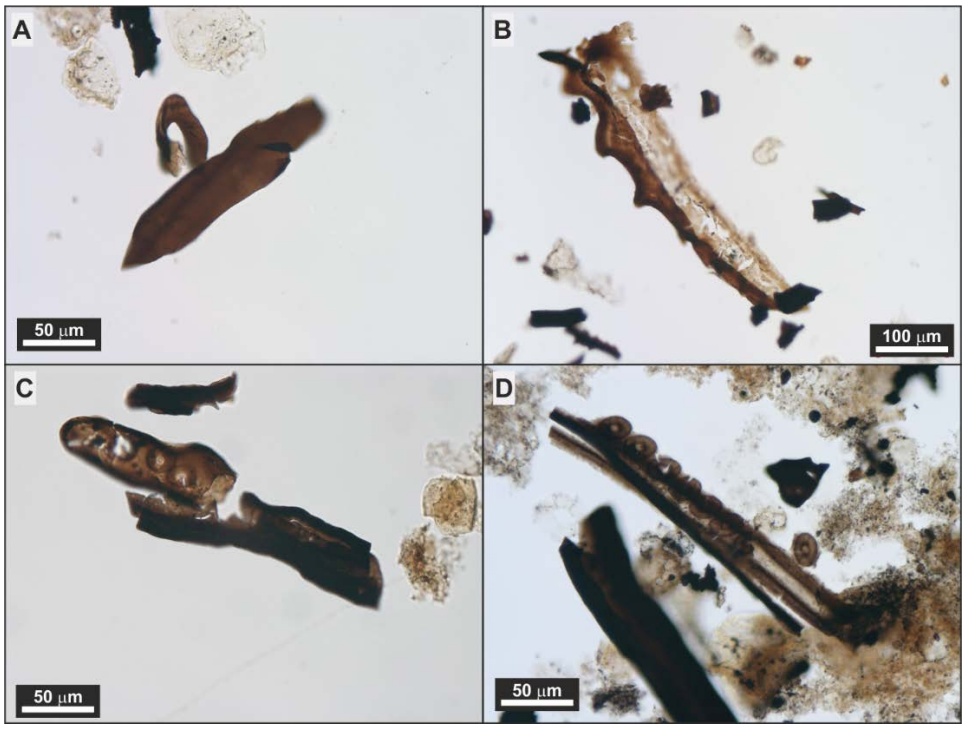

Figure IV.4. Possible hydrozoan polypoid form fragments. **A** - Fragment of polyp showing lateral budding (S10, TWL); **B** - Detail of the epidermis showing the column-like epithelial cells packed side-by-side (S10, TWL); **C** – Feature of tentacle form of hydrozoan polyp showing cells of cnidocytes (S11, TWL); **D** - Detail of hydroid colonial stalk showing the cnidocyte cells preserved (S64, TWL).

IV.2. Caylus section – Quercy Basin

IV.2.1. Macroscopic characterization

A general macroscopic characterization was performed in all samples from the Caylus section (QB), according to standard methodology for organic petrology analyses (Table IV.2). The section displays a more carbonated base with the Barre à Pecten Fm. being composed by light grey to grey limestones with the occurrence of iron oxides (Cay3, Cay6 and Cay7) and fractures with calcite recrystallization (Cay6 and Cay7). The top of the succession is composed by brown marls from the Penne Fm. with the presence of laminated marls in the Schistes Cartons Mb..

Table IV.2. General macroscopic characterization, geochemistry and palynofacies data of samples from the Caylus section. MCH Mb.=Marnes et calcaires à *Hildoceras* Member; Se.=Semicelatum.

Age	Biostratigraphy	Units		Sample	General Characterization			Geochemistry			Palynofacies			
					Lithology	Color	Other Characteristics	TOC (wt.%)	TS (wt.%)	IR (wt.%)	Phytoclast (%)	Amorphous (%)	Palynomorph (%)	Zooclast (%)
Toarcian	Serpentinum	Penne Formation	MCH Mb.	Cay 28	Marl	Brownish yellow	-	0.32	0.026	59	0.95	84.18	3.48	11.39
			Schistes Cartons Member	Cay 26	Marl	Dark Brown	Intense Lamination	8.80	0.40	71	0.00	0.00	99.35	0.65
				Cay 23	Marl	Dark Brown	Intense Lamination	7.94	0.39	78	0.00	0.00	100.00	0.00
				Cay 20	Marl	Dark Brown	Lamination	3.35	0.16	82	0.00	0.00	100.00	0.00
				Cay 18	Marl	Brown	Mild Lamination	3.24	0.15	82	0.00	0.00	99.37	0.63
				Cay 13	Marl	Brown	Lamination	1.71	0.37	66	0.00	0.00	98.43	1.57
	Tenuicostatum		Se.	Cay 10	Marl	Brown	-	0.38	2.90	54	6.31	0.00	81.40	12.29
		Barre à Pecten Formation	Paltus	Cay 7	Limestone	Grey	Fracture Calcite Recrystallizations, Iron Oxides	0.12	6.15	17	0.65	0.00	88.27	11.07
				Cay 6	Limestone	Grey		0.12	4.59	15	Low Recovery			
Pliensbachian				Cay 3	Limestone	Light Grey	Iron Oxides	0.16	0.01	18				
				Cay 1	Limestone	Light Grey	-	0.18	0.08	15	2.78	0.00	87.65	9.57

IV.2.2. Geochemistry

The geochemical data (TOC, TS and IR) of samples from the Caylus section is summarized on Table IV.2.

The TOC values vary from 0.12 wt.% (Cay6 and Cay7) to 8.80 wt.% (Cay26). The marls of the Schistes Cartons Mb. of the Penne Fm. present the highest values recorded (average 4.24 wt.%) and the lowest values are observed in the Barre à Pecten Fm. and Marnes et calcaires à *Hildoceras* Mb. of the Penne Fm. (average 0.14 wt. % and 0.32 wt.%, respectively).

TS values range between 0.01 wt.% (Cay3) and 6.15 wt.% (Cay7), both values recorded in the Barre à Pecten Fm.. The Schistes Cartons Mb. and Marnes et calcaires à *Hildoceras* Mb. of the Penne Fm. present average 0.73 wt.% and 0.03 wt.%, respectively.

IR values vary between 15 wt.% (Cay1 and Cay6) and 82 wt.% (Cay18 and Cay20) The Barre à Pecten Fm. presents the highest $CaCO_3$ content of the section with an average IR of 16.25 wt.%. The highest IR values are observed in the Schistes Cartons Mb. of the Penne Fm. (average 72 wt.%).

IV.2.3. Palynofacies

The palynofacies analysis was performed in the majority of the samples from the Caylus section being identified particulate organic compounds from all the OM groups (Phytoclast, Amorphous, Palynomorph and Zooclast groups) (Appendix A.2; Table IV.2). Samples Cay3 and Cay6 displayed low OM recovery and palynofacies data was not accounted for interpretation due to bias, nevertheless an analysis of the components and their preservation state was performed.

The **Phytoclast group** is absent in the majority of the samples of the succession but components from this group were identified in samples Cay1, Cay7, Cay10 and Cay28 (Appendix A.2; Table IV.2). Their relative percentage ranges between 0% (Cay13, Cay18, Cay20, Cay23 and Cay26) and 6.31% (Cay10) (Appendix A.2; Table IV.2). Its highest mean abundance is recorded in the Barre à Pecten Fm. (average 1.71%) and the lowest mean abundance in the Marnes et calcaires à *Hildoceras* Mb. of the Penne Fm. (average 0.95%) (Appendix A.2; Table IV.2). This group is mainly represented by **NONB phytoclasts** (63.0% of total phytoclast) with irregular outlines and, in most cases, with some degree of degradation (Appendix A.2). They display dark brown color under TWL and no fluorescence under blue incident light (Appendix B.1.2). In some samples were also identified particles from the **NOB** phytoclast subgroup, namely pitted and stripped **NOB** phytoclasts and some membranes (Appendix A.2). The **NOB** phytoclasts exhibit brown to dark brown color under TWL and usually no fluorescence. The **membranes** have a light brown color under TWL and a dark yellow to dark orange fluorescence (Appendix B.1.2). In these samples no opaque phytoclasts were observed in the palynological assemblage. Some cuticle layer fragments were identified but not accounted during the palynofacies analysis (Appendix B.1.2).

The **Amorphous group** is not present in the majority of the succession, being only identified in sample Cay28 from the Marnes et calcaires à *Hildoceras* Mb. of the Penne Fm. (84.18%) (Appendix A.2; Table IV.2). This group consists in **AOM** related with microbiological reworking processes of components from the **Zoomorph Subgroup** (possibly Hydrozoan polyps, medusae, tentacles, unarticulated colonies elements, etc.) and

bacterial AOM (Appendix A.2 and B.2.2; Figure IV.5). The AOM identified in sample Cay28 results from a mixture of these two types of AOM exhibiting two different fluorescence colorations, ranging between yellow and dark orange and a brown to dark brown color under TWL. The particles displayed diffuse limits or were completely unstructured.

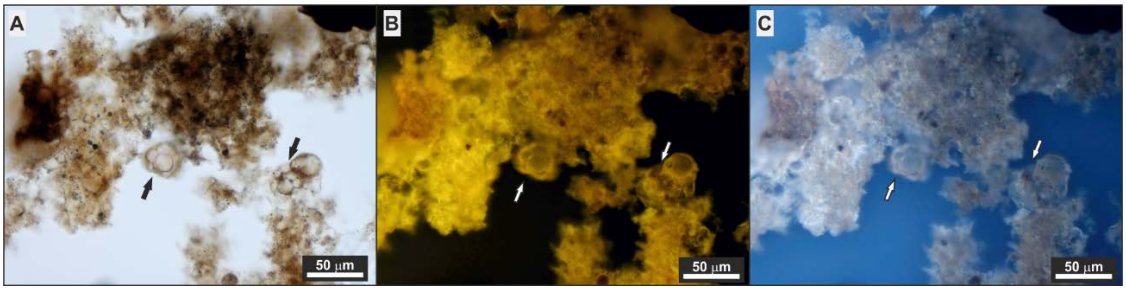

Figure IV.5. Bacterial AOM, zoomorph derived AOM and Gloeocapsomorpha detail (arrow) (Cay28). **A** – TWL; **B** – FM, UV light; **C** – FM, blue light.

The **Palynomorph group** dominates the majority of the samples varying from 3.48% (Cay28) to 100% (Cay20 and Cay23) (Appendix A.2; Table IV.2). In these samples were identified components from all palynomorph subgroups (sporomorph, freshwater microplankton, marine microplankton and zoomorph). Terrestrial components from the **sporomorph subgroup** were observed mainly in samples from the Barre à Pecten Fm., showing very low to null percentages in the Schistes Cartons Mb. and Marnes et calcaires à *Hildoceras* Mb. of the Penne Fm. (Appendix A.2). This subgroup is represented by **spores** of different sizes, shapes (from oval to triangular) and ornamentations, with some of them exhibiting the trilete mark on the surface. They present an orange to light brown coloration under TWL and orange fluorescence (Appendix B.3.2.1). **Pollen grains** exhibit various form, sizes and ornamentations, an orange to dark orange coloration under TWL and orange fluorescence (Appendix B.3.2.1). In some samples was possible to observe agglomerates (dyads, tetrads and polyads) and bisaccate pollen grains, especially in samples Cay7 and Cay20 (Appendix A.2 and B.3.2.1). In samples Cay1, Cay6 and Cay10 was possible to identify pollen grains and tetrads from the genus *Classopollis* (Appendix B.3.2.1).

Freshwater microplankton is represented by **Gloeocapsomorpha** particles that exhibit a light brown color under TWL and a dark yellow to orange fluorescence (Appendix A.2 and B.3.2.2; Figure IV.5).

Marine microplankton components were identified as Dinoflagellate Cysts, Acritarchs and Prasinophyte algae (*Tasmanites* and *Cymatiosphaera*). The **dinoflagellate cysts** and **acritarchs** were observed in samples Cay1 and Cay7 from the Barre à Pecten Fm. and in sample Cay10 from the Schistes Cartons Mb. of the Penne Fm (Appendix A.2).

The **dinoflagellate cysts** display a very light brown coloration under TWL and an intense yellow fluorescence. They can sometimes exhibit a dark opaque particles in their interior under TWL due to sulfide inclusions (as observed in sample Cay7) (Appendix B.3.2.3). **Acritarchs** are small sized and show a very light brown color, almost transparent, under TWL and a yellow fluorescence (Appendix B.3.2.3). **Prasinophyte algae** were observed in samples from the Schistes Cartons Mb. (Cay10, Cay18, Cay20, Cay23 and Cay26) and from the Marnes et calcaires à *Hildoceras* Mb. (Cay28) of the Penne Fm. (Appendix A.2). ***Tasmanites*** are spherical, smooth and thick-walled, displaying a brown coloration under TWL and a yellow fluorescence and were the main Prasinophyte algae identified. In samples Cay23, Cay26 and Cay28 ***Cymatiosphaera*** specimens were also recognized (Appendix B.3.2.3). The ***Cymatiosphaera*** have a spherical form and a surface divided into polygonal fields and exhibit a light brown coloration in TWL and a yellow fluorescence under blue incident light (Appendix B.3.2.3).

The **zoomorph subgroup** is the major component of the palynological assemblage in most of the samples (except sample Cay28) (Appendix A.2). This group is dominated by **Amorphous Zoomorphs** that were identified as possible **amorphous Hydrozoan** polyps, medusae, tentacles, unarticulated colonies elements, etc. (Appendix A.2 and B.3.2.4; Figure IV.6). These components exhibit AOM characteristics but with still recognizable specific and distinctive morphological traits of animal origin (zoomorphs). They still present sharp and neat outlines, typical shapes with a heterogeneous texture, a brown coloration under TWL and a weak yellow to orange fluorescence. Foraminiferal Test-Linings (Cay1, Cay7, Cay10 and Cay28) (Appendix B.3.2.4) and **Hydrozoan medusae** (Appendix B.5; Figure IV.7) (Cay1, Cay7, Cay13, Cay20, Cay23 and Cay28) were also identified (Appendix A.2).

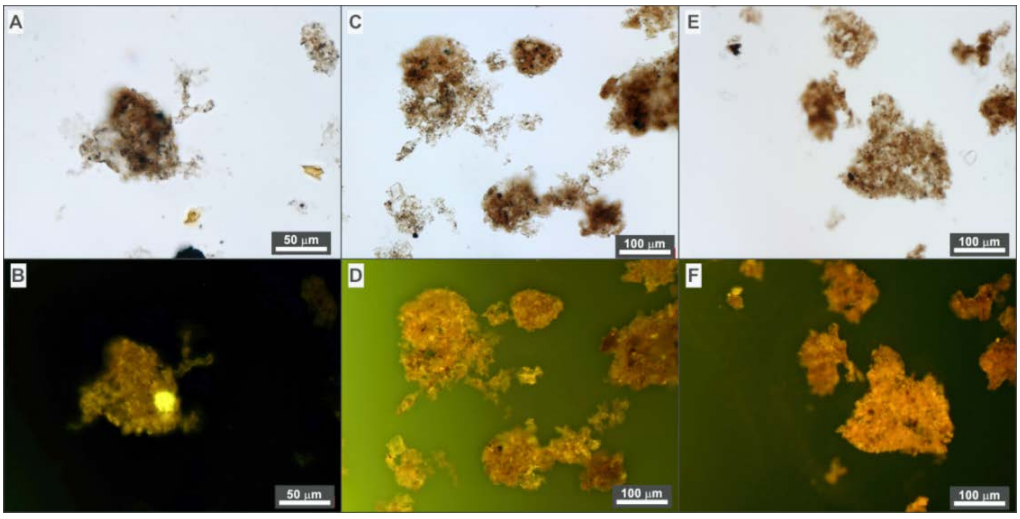

Figure IV.6. General aspects of amorphous Hydrozoan. **A** (Cay10), **C** (Cay18), **E** (Cay23) - TWL; **B**, **D**, **F** - FM.

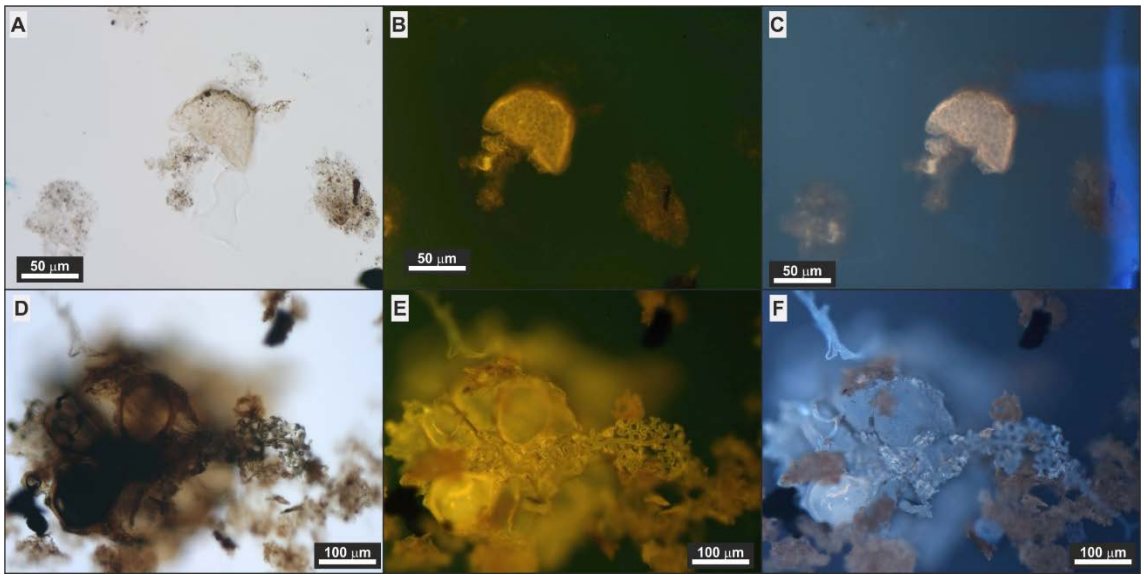

Figure IV.7. Hydrozoan Medusae. **A** (Cay1), **D** (Cay28) - TWL; **B**, **E** - FM, UV light; **C**, **F** - FM, blue light.

Other organic components from the Palynomorph group were identified as **undifferentiated palynomorphs** (Appendix A.2). This category includes organic particles, which cannot be confidently assigned to any subgroup from palynomorph assemblage (e.g. sporomorphs or organic-walled microplankton) because of their state of preservation or lack of diagnostic features.

The **Zooclast group** is characterized by **possible hydrozoan polypoid forms** fragments (Appendix B.4.2; Figure IV.8). Typically these elements present no fluorescence but in some cases can exhibit a fluorescence varying from dark orange to dark brown. Their abundance varies from 0% (Cay20 and Cay23) to 12.29% (Cay10) with the highest mean value being recorded in samples from the Barre à Pecten Fm. (10.32%) and Marnes et calcaires à *Hildoceras* Mb. of the Penne Fm. (11.39%) and their lowest mean value in samples from the Schistes Cartons Mb. of the Penne Fm. (2.52%) (Appendix A.2; Table IV.2).

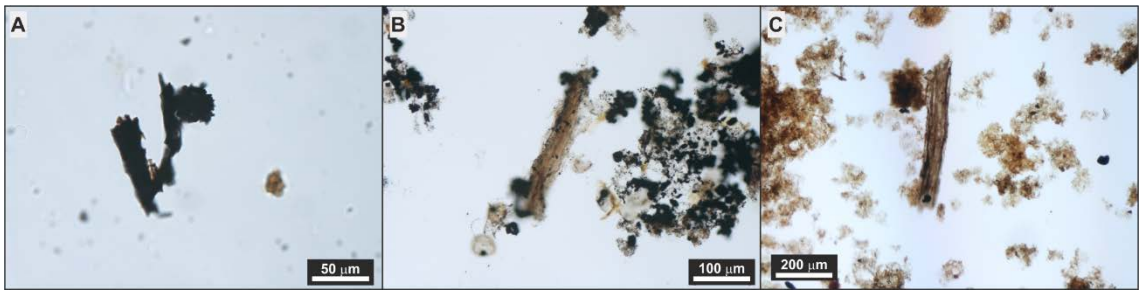

Figure IV.8. Possible Hydrozoan polypoid forms showing lateral budding. **A** (Cay6), **B** (Cay7), **C** (Cay18) –TWL.

Although samples Cay3 and Cay6 were considered sterile for particulate OM, were identified components from the four OM groups. The **Phytoclast group** is mainly represented by **NONB** phytoclasts, in most cases, with some degree of degradation and **NOB** phytoclasts, namely pitted and stripped **NOB** phytoclasts. The **Palynomorph group**

is characterized by **marine microplankton** (Dinoflagellate cysts and Acritarchs), terrestrial components (pollen grains and spores), **zoomorphs** (foraminiferal test-linings, hydrozoan medusae and amorphous zoomorphs that were identified as possible amorphous Hydrozoan polyps, medusae, tentacles, unarticulated colonies elements, etc.) and **undifferentiated palynomorphs**. The **Zooclast group** is characterized by possible hydrozoan polypoid forms fragments. Some of the particles present morphological characteristics that allow their probable association with hydrozoans. These samples are also characterized by features of oxidized OM and is clear an abundance of sulfide particles.

IV.3. Pont de Suert section –Pyrenean Basin

IV.3.1. Macroscopic characterization

The general macroscopic aspects of the samples from the Pont de Suert section (PB) were characterized according to the standard methodology for organic petrology analyses. The samples represent a limestone-marl alternation succession (Table IV.3). The base of the section is represented by the Barre à Pecten Fm. with dark grey limestones with the presence of belemnites and fractures with calcite recrystallizations (20PS). To the top the succession consists of limestone-marly limestone-marl alternations of the Padrinas Fm. The majority of the samples exhibit a dark grey color and, sometimes, intense lamination. Some iron oxides were identified in sample 300PS from the Calcaires argileux et marnes à *Soaresirhynchia* Mb. of the Padrinas Fm.

Table IV.3. General macroscopic characterization, geochemistry and palynofacies data of samples from the Pont de Suert section. Pliensb.=Pliensbachian; Sublev.=Sublevisoni.

Age	Biostratigraphy	Units	Sample	General Characterization			Geochemistry			Palynofacies			
				Lithology	Color	Other Characteristics	TOC (wt.%)	TS (wt.%)	IR (wt.%)	Phytoclast (%)	Amorphous (%)	Palynomorph (%)	Zooclast (%)
Toarcian	Bifrons Sublev.	Padrinas Formation – Calcaires argileux à *Telothyris* Mb.	265PS	Calcareous Marl	Dark Grey	Lamination	0.25	0.02	40	0.65	0.00	2.28	97.07
	Serpentinum Falciferum		255PS	Marl	Dark Grey	Lamination	0.33	0.02	67	2.31	0.00	4.32	93.37
			470PS	Marl	Dark Grey	Lamination, Iron Oxides	0.25	0.21	51	1.27	0.00	52.87	45.86
			420PS	Marly limestone	Dark Grey	-	0.14	0.12	21	0.00	0.00	89.35	10.65
			380PS	Marl	Dark Grey	Lamination	0.30	0.09	60	1.29	0.00	28.06	70.65
	Elegantulum	Calcaires argileux et marnes à *Soaresirhynchia* Mb.	355PS	Marly limestone	Dark Grey	-	0.16	0.15	27	0.00	0.00	32.69	67.31
			330PS	Marl	Dark Grey	Lamination	0.31	0.24	58	1.62	0.00	34.42	63.96
			300PS	Calcareous Marl	Dark Grey	Lamination, Iron Oxides	0.25	0.31	39	2.31	0.00	54.46	43.23
	Tenuicostatum Semicelatum	Calcaires argileux à *Spiriférines* Mb.	115PS	Marly Limestone	Dark Grey	Lamination	0.35	0.77	51	0.00	0.00	79.03	20.97
			100PS	Marl	Dark Grey	Lamination	0.31	0.49	53	0.96	0.00	59.87	39.17
	Paltus		75PS	Limestone	Dark Grey	-	0.21	0.20	24	0.99	0.00	18.21	80.79
			65-7PS	Marl	Grey	Intense Lamination	0.40	0.56	58	2.56	0.00	15.75	81.68
			45PS	Marl	Dark Grey	Lamination	0.40	0.72	61	3.65	0.00	10.30	86.05
Pliensb.		Barre a Pecten Fm	20PS	Limestone	Dark Grey	Fracture Calcite Recrystallizations, Belemnites	0.24	0.43	13	3.64	0.00	26.16	70.20

IV.3.2. Geochemistry

The results of the geochemical analyses (TOC, TS and IR) performed in samples from the Pont de Suert section is summarized on Table IV.3.

The geochemical study of this section revealed TOC values ranging between 0.14 wt.% (420PS) and 0.40 wt.% (45PS and 65-7PS). The highest values recorded correspond to the Calcaires argileux à *Spiriférines* Mb. of the Padrinas Fm. (average 0.34 wt.%) and the lowest to the Barre a Pecten Fm. and the Calcaires argileux et marnes à *Soaresirhynchia* Mb. of the Padrinas Fm.(average 0.24 wt.%). The Calcaires argileux à *Telothyris* Mb. of the Padrinas Fm. shows the mean values for the section with an average 0.25 wt%.

TS values vary from 0.02 wt.% (255PS and 265PS) to 0.77 wt.% (115PS). The Calcaires argileux à *Spiriférines* Mb. of the Padrinas Fm. presents the highest mean value of the section (0.55 wt.%) and the Calcaires argileux à *Telothyris* Mb. of the Padrinas Fm. the lowest (average 0.09 wt.%).

IR values range from 13 wt.% (20PS) to 67 wt.% (255PS). The lowest recorded average (13 wt.%) corresponds to the Barre a Pecten Fm.. The three members of the Padrinas Fm., Calcaires argileux à *Spiriférines* Mb., Calcaires argileux et marnes à *Soaresirhynchia* Mb. and Calcaires argileux à *Telothyris* Mb., exhibit very similar mean values (49 wt.%, 41 wt.% and 48 wt.%, respectively).

IV.3.3. Palynofacies

Palynofacies analysis of samples from the Pont de Suert section revealed the presence of particulate organic compounds from some of the OM groups (Phytoclast, Palynomorph and Zooclast groups) (Appendix A.3; Table IV.3).

The **Phytoclast group** is present in very low percentages, sometimes absent, in most of the samples of the succession. Their relative percentage ranges between 0% (115PS, 355PS and 420PS) and 3.65% (45PS) (Appendix A.3; Table IV.3). This group highest mean abundance is recorded in the Barre a Pecten Fm. (average 3.64%) and the lowest mean abundance in the Calcaires argileux à *Telothyris* Mb. of the Padrinas Fm. (average 1.10%) (Appendix A.3; Table IV.3). This group is mainly represented by **NONB** phytoclasts (56.9% of total phytoclast) with irregular outlines and with some degree of degradation (Appendix A.3). They display dark brown to black color under TWL and no fluorescence under blue incident light (Appendix B.1.3). In some samples were also identified particles from the **NOB** phytoclast subgroup, namely pitted and stripped **NOB** phytoclasts and some particles of lath **opaque phytoclasts** (**OP**) and **cuticles**

(Appendix A.3 and B.1.3). The **NONB** exhibit dark brown to black color under TWL and no fluorescence. The lath **OP** display black color under TWL and no fluorescence. The cuticles exhibit a brown color under TWL and no fluorescence.

The **Palynomorph group** presents relative percentages ranging between 2.28% (265PS) and 89.35% (420PS) (Appendix A.3; Table IV.3). In these samples were identified components from palynomorph subgroups, namely sporomorph, marine microplankton and zoomorph subgroups. Components from the **sporomorph subgroup** were observed in all samples but were not accounted in samples 300PS, 330PS, 420PS, 255PS and 265PS (Appendix A.3). This subgroup is represented by **spores** of different sizes and triangular shapes, with some of them exhibiting the trilete mark on the surface. They presented a dark brown coloration under TWL and no fluorescence (Appendix B.3.3.1). **Pollen grains** exhibited various form and sizes, a dark brown coloration under TWL and no fluorescence. In some samples was possible to observe agglomerates (dyads, tetrads and polyads) and bisaccate pollen grains, especially in samples 75PS, 100PS, 115PS, 380PS and 470PS (Appendix A.3 and B.3.3.1). In sample 380PS was possible to identify pollen grains and tetrads from the genus *Classopollis.*

From the **marine microplankton** subgroup were identified Dinoflagellate Cysts, Acritarchs and Prasinophyte algae (*Tasmanites*). The **dinoflagellate cysts** were identified in samples 65-7PS and 115PS from Calcaires argileux à *Spiriférines* of the Padrinas Fm. displaying a brown coloration under TWL and no fluorescence (Appendix A.3 and B.3.3.2). **Acritarchs** were observed in the majority of samples (except 255PS and 265PS) exhibiting a small size, brown color under TWL and no fluorescence (Appendix A.3 and B.3.3.2). **Prasinophyte algae** were observed only in sample 330PS from the Calcaires argileux et marnes à *Soaresirhynchia* Mb. of the Padrinas Fm (Appendix A.3). In these samples ***Tasmanites*** are spherical and thick-walled, displaying a dark brown coloration under TWL and no fluorescence (Appendix B.3.3.2).

The **zoomorph subgroup** is dominated by **Amorphous Zoomorphs** that were identified as **amorphous Hydrozoan medusae** (Appendix A.3; Figure IV.9). These components exhibit AOM characteristics but with still recognizable specific and distinctive morphological traits of animal origin (zoomorphs). They still present sharp and neat outlines, typical medusoid shapes with a heterogeneous texture, a dark brown to black coloration under TWL and no fluorescence. Foraminiferal Test-Linings (75PS, 115PS, 300PS, 355PS and 380PS) (Appendix B.3.3.3) and some **Hydrozoan medusae** were also identified (Appendix A.3; Figure IV.10).

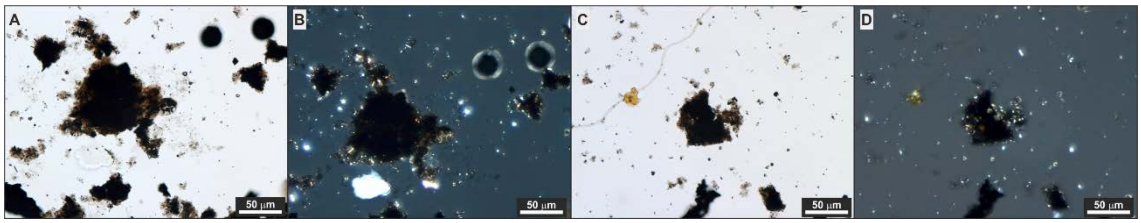

Figure IV.9. General aspects of amorphous Hydrozoan medusae (115PS). **A**, **C** - TWL; **B**, **D** - Dark field.

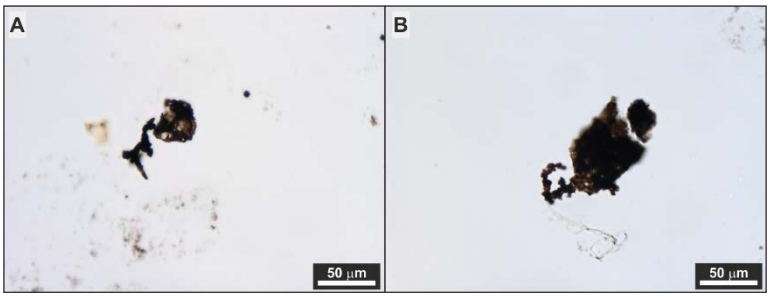

Figure IV.10. Hydrozoan medusoid forms. **A** (20PS), **B** (75PS) - TWL.

Other organic components from the Palynomorph group were identified as **undifferentiated palynomorphs** (organic particles which cannot be confidently assigned to any subgroup due to their state of preservation or lack of diagnostic features) (Appendix A.3).

The **Zooclast group** is characterized by **possible hydrozoan polypoid forms** fragments (Figure IV.11). These components present a dark brown to black coloration under TWL and no fluorescence. Their abundance ranges between 10.65% (420PS) and 97.07% (265PS) with the highest mean value being recorded in samples from the Barre a Pecten Fm. (70.20%) and lowest mean value in samples from the Calcaires argileux et marnes à *Soaresirhynchia* Mb. of the Padrinas Fm. (58.17%) (Appendix B.3; Table IV.3).

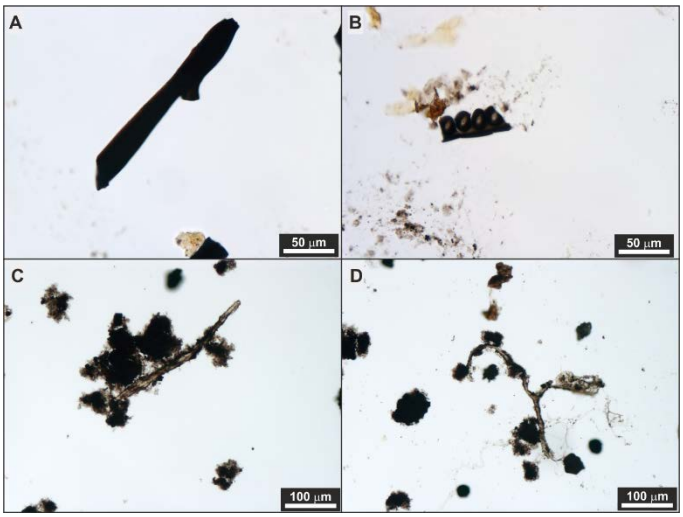

Figure IV.11. Possible Hydrozoan polypoid forms. **A** – Portion of polypoid form showing lateral budding (20PS, TWL); **B** - Fragment of hydroid colonial stalk showing the cnidocyte cells preserved (20PS, TWL); **C**, **D** - Disarticulated fragment of hydroid colony (multiple polyps connected by tubelike hydrocauli) (300PS, 330PS, TWL).

IV.4. Biomarkers

The petrographic studies developed in the samples from the three studied sections lead to the conclusion that the majority of the OM present in these samples belongs to new constituents of the zoomorph group (Hydrozoans) whose knowledge is currently under development. Only after the microscopic identification of these zoomorphs was possible to assess that the biomarker data obtained from the saturated and aromatic HC fractions of these samples' bitumen characterizes only a small and non-representative portion of the OM assembly. The chemical composition of these components is still unknown due to their animal provenance and therefore no information about the biological biomarkers is available in the literature.

Moreover, the majority of the data obtained from these samples is inconsistent with the palynofacies data and, therefore will not be presented in this dissertation.

IV.5. Thermal maturity

A thermal maturity study was performed for all samples of the three studied sections (Suèges, Caylus and Pont de Suert) using three different techniques (SCI, spectral fluorescence and OM reflectance) according to each sample characteristics (presence of spores, macerals from the liptinite group and zoomorphs).

IV.5.1. Suèges section – Grands Causses Basin

For samples from Suèges section (Table IV.4) the **SCI** presented value of 3.5-4.0 which corresponds to an Equivalent Vitrinite Reflectance (R_{eq}) of 0.45% according to the $\%R_r$, SCI, temperature, and age correlation chart proposed by Fisher et al. (1980). Due to the lack of vitrinite macerals in sample S10, and according to Bertrand and Malo (2012), it was measured the reflectance of hydroids and then converted in the **equivalent vitrinite reflectance (VR_{eq})**. The hydroid average reflectance is 0.43% corresponding to 0.49 $\%VR_{eq}$. **Spectral fluorescence** analysis was performed in *Tasmanites* of eleven samples of the section (Figure IV.12). The lambda maximum (λ_{max}) is 560 nm for the majority of samples with the exception of sample S12 that presented λ_{max} of 510 nm. Red/green quotient (Q) values ranged between 0.53 (S12) and 0.77 (S17).

Table IV.4. Thermal maturity data from the Suèges section samples. SCI=Spore Coloration Index; $\%HR_r$=measured hydroid random reflectance; $\%VR_{eq}$=equivalent vitrinite reflectance; λ_{max}=lambda maximum; Q=Red/green quotient; Stdev=Standard deviation.

Age	Biostratigraphy		Units		Sample	SCI	Organic Matter Reflectance			Spectral Fluorescence	
							% HR_r	% VR_{eq}	Stdev	λ_{max}	Q
Toarcian	Serpentinum	Falciferum	Rivière-sur-Tarn Group	Marnes de Fontanilles Fm.	S69	3.5-4.0	-	-	-	560	0.67
					S64	3.5-4.0	-	-	-	560	0.71
					S61	3.5-4.0	-	-	-	560	0.64
		Exaratum		Schistes Cartons Formation	S55	3.5-4.0	-	-	-	560	0.68
					S52	3.5-4.0	-	-	-	560	0.74
					S50	3.5-4.0	-	-	-	560	0.63
					S22	3.5-4.0	-	-	-	560	0.60
	Tenuicostatum	Semicelatum			S19	3.5-4.0	-	-	-	560	0.64
					S17	3.5-4.0	-	-	-	560	0.77
					S15	3.5-4.0	-	-	-	-	-
Pliensbachian				Marnes de Villeneuve Fm.	S12	3.5-4.0	-	-	-	510	0.53
					S11	3.5-4.0	-	-	-	560	0.78
					S10	3.5-4.0	0.43	0.49	0.06	-	-

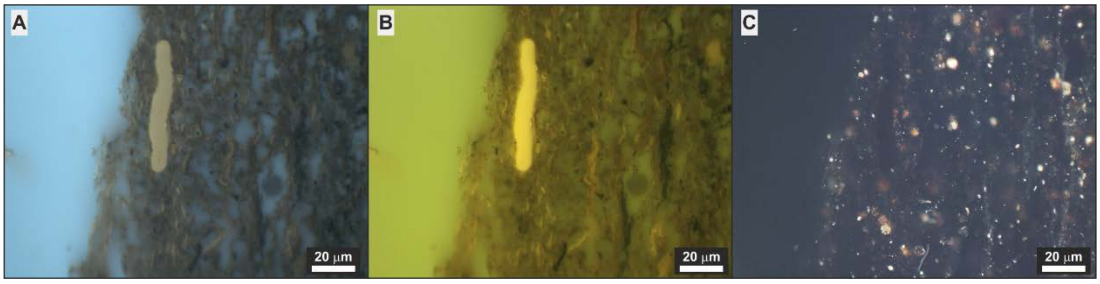

Figure IV.12. Example of liptinite maceral (telalginite - *Tasmanites*) from sample S17 used for spectral fluorescence measurements (**A** - blue FM; **B** – UV FM; **C** – RWL).

IV.5.2. Caylus section – Quercy Basin

The Caylus section samples (Table IV.5) exhibited **SCI** values of 3.5-4.0 (Figure IV.13) which corresponds to a R_{eq} value of 0.45% according to the $\%R_r$, SCI, temperature, and age correlation chart proposed by Fisher et al. (1980). **Spectral fluorescence** analysis was performed in two samples of the section with the liptinite (telalginite - *Tasmanites*) exhibiting λ_{max} of 560 nm for both samples and Q ratio ranging between 0.59 (Cay28) and 0.60 (Cay26). **OM reflectance** was not determined in these samples due to the absence of measurable particles.

Table IV.5. Thermal maturity data from the Caylus section samples. SCI=Spore Coloration Index; λ_{max}=lambda maximum; Q=Red/green quotient; MCH Mb.=Marnes et calcaires à *Hildoceras* Member; Pliensb.=Pliensbachian; Se.=Semicelatum.

Age	Biostratigraphy		Units		Sample	SCI	Spectral Fluorescence	
							λ_{max}	Q
Toarcian	Serpentinum		Penne Formation	MCH Mb.	Cay 28	3.5-4.0	560	0.59
				Schistes Cartons Member	Cay 26	3.5-4.0	560	0.60
					Cay 23	3.5-4.0	-	-
					Cay 20	3.5-4.0	-	-
					Cay 18	3.5-4.0	-	-
					Cay 13	3.5-4.0	-	-
	Tenuicostatum	Se.			Cay 10	3.5-4.0	-	-
		Paltus	Barre à Pecten Formation		Cay 7	3.5-4.0	-	-
					Cay 6	3.5-4.0	-	-
Pliensb.					Cay 3	3.5-4.0	-	-
					Cay 1	3.5-4.0	-	-

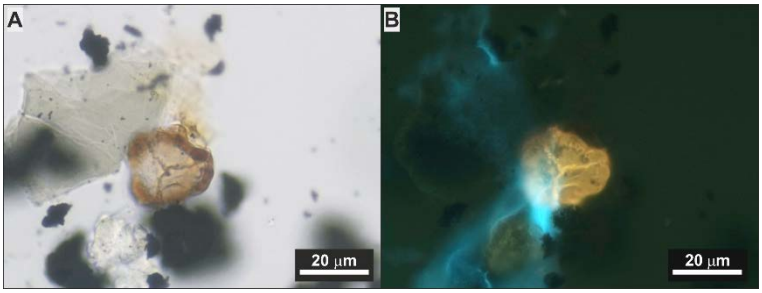

Figure IV.13. Example of spore from sample Cay6 used to determine SCI (**A** – TWL; **B** – FM).

IV.5.3. Pont de Suert section – Pyrenean Basin

For samples from Pont de Suert section (Table IV.6) the **SCI** presented values ranging between 8.0-8.5 and 8.5-9.0 which corresponds to a R_{eq} value of 0.90%-1.20% (Fisher et al., 1980). Due to the lack of vitrinite macerals in all samples, it was measured the reflectance of hydroids and then converted into VR_{eq} according to Bertrand and Malo (2012). The hydroid reflectance varies between 0.87% and 1.28% equivalent to **Vitrinite reflectance** of 0.78% to 1.04 %VR_{eq} (Figure IV.14). **Spectral fluorescence** analysis was not performed due to the high maturation of these samples.

Table IV.6. Thermal maturity data from the Pont de Suert section samples. SCI=Spore Coloration Index; $\%HR_r$=measured hydroid random reflectance; $\%VR_{eq}$=equivalent vitrinite reflectance; Stdev=Standard deviation; Plien.=Pliensbachian; Bif.=Bifrons; Se.=Semicelatum; Subl.=Sublevisoni.

Age	Biostratigraphy		Units		Sample	SCI	Organic Matter Reflectance		
							% HR_r	% VR_{eq}	Stdev
Toarcian	Bif.	Subl.	Padrinas Formation	Calcaires argileux à *Telothyris* Mb.	265PS	8.0-8.5/8.5-9.0	-	-	-
	Serpentinum	Falciferum			255PS	8.0-8.5/8.5-9.0	0.88	0.78	0.07
					470PS	8.0-8.5/8.5-9.0	0.87	0.78	0.07
					420PS	8.0-8.5/8.5-9.0	-	-	-
					380PS	8.0-8.5/8.5-9.0	0.92	0.81	0.06
		Elegantulum		Calcaires argileux et marnes à *Soaresirhynchia* Mb.	355PS	8.0-8.5/8.5-9.0	1.09	0.92	0.02
					330PS	8.0-8.5/8.5-9.0	1.07	0.91	0.08
					300PS	8.0-8.5/8.5-9.0	1.09	0.92	0.10
	Tenuicostatum	Se.		Calcaires argileux à *Spiriferines* Mb.	115PS	8.0-8.5/8.5-9.0	1.12	0.94	0.07
					100PS	8.0-8.5/8.5-9.0	1.08	0.91	0.12
		Paltus			75PS	8.0-8.5/8.5-9.0	-	-	-
					65-7PS	8.0-8.5/8.5-9.0	1.28	1.04	0.11
					45PS	8.0-8.5/8.5-9.0	1.14	0.95	0.15
Plien.			Barre a Pecten Fm		20PS	8.0-8.5/8.5-9.0	1.18	0.98	0.11

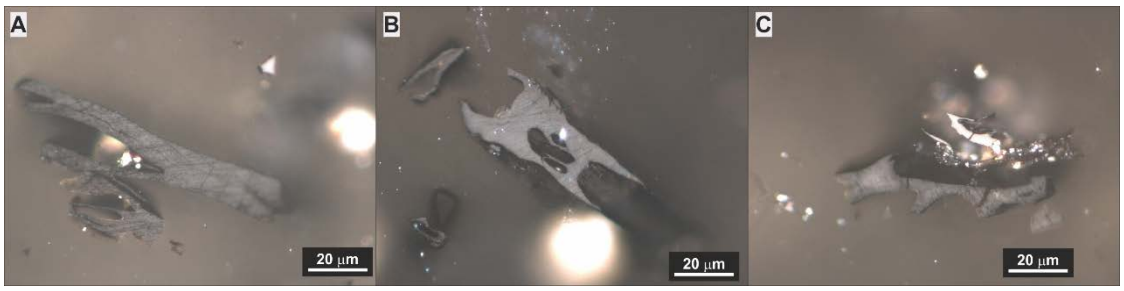

Figure IV.14. Examples of reflectance measured Hydroid particles. **A** - sample 45PS; **B** - sample 65-7PS; **C** - sample 380PS (photomicrographs taken in RWL).

Chapter V - Discussion

In this chapter will be discussed, based on a multivariate statistical analysis, the results presented previously in order to define the organic facies and the depositional paleoenvironments of the studied sections. For the definition of the organic facies were determined the palynofacies associations according to the OM abundance of groups and the degree of similarity between individual organic components and then determined the intervals for paleoenvironmental interpretation based on their vertical variation. This definition took into account the organofaciologic characteristics (palynofacies and geochemistry) of the samples resulting in a possible interpretation of sea level variation, from bottom to top of the succession. The paleoenvironmental contexts proposed were then compared with evolution models for the Toarcian European epicontinental shelf suggested by other authors. Considering that this study was developed in three different basins, a discussion of the thermal maturity data and the definition of the maturity stage of these basins was also performed.

V.1. Paleoenvironmental interpretation

V.1.1. Suèges section – Grands Causses Basin

V.1.1.1. Cluster Analysis

Using **R-Mode cluster analysis** the samples were organized in four groups (A to D) according to the degree of similarity of the OM components in relation to origin criterion (Table V.1): **Group A** contains exclusively marine components (Prasinophyte algae); **Group B** includes only AOM; **Group C** is composed solely by freshwater microplankton (Gloeocapsomorpha); **Group D** is composed by marine components (Foraminiferal Test-Linings, Dinocysts and Acritarchs), aquatic continental constituents (Hydrozoan medusae), zooclasts (possible Hydrozoan polyp fragments), terrestrial palynomorphs (Sporomorph subgroup) and higher plants derived components (Phytoclast group and Resin).

Table V.1. Suèges section R-Mode cluster analysis description.

Group	Description
A	Prasinophyte algae
B	AOM
C	Gloeocapsomorpha
D	Foraminiferal test-linings + dinocysts + acritarchs + terrestrial palynomorph + phytoclast + resin + Hydrozoan medusae + zooclasts

Q-Mode cluster analysis subdivided the samples into three palynofacies associations, according to the OM abundance of the groups and subgroups (Figure V.1):

(i) **Palynofacies Association I**, with a predominance of zooclasts; (ii) **Palynofacies Association II**, with a prevalence of zoomorph derived AOM and zooclasts; and, (iii) **Palynofacies Association III**, with a dominance of zoomorph derived AOM.

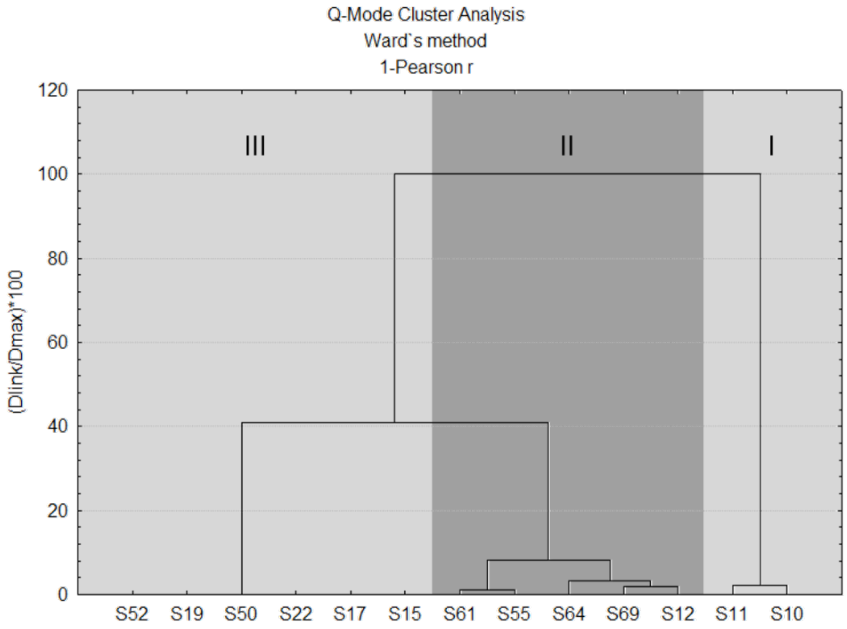

Figure V.1. Q-Mode cluster analysis for samples from the Suèges section.

Palynofacies Association I

The palynofacies is dominated by **zooclasts** (zoomorph fragments), characterized as possible hydrozoan polypoid form fragments, with an average percentage of 33.64%. Some of the particles present morphological characteristics that allow their probable association with hydrozoans. TOC ranges between 0.50 wt.% and 0.70 wt.%. All samples present IR values >60 wt.%.

The Phytoclast group presents high percentages (average 21.90%), indicating a significant input of terrestrial higher (vascular) plants (continental contribution). The Amorphous group is dominated by AOM with an average percentage of 15.93% which is related with microbiological reworking processes of components from the Zoomorph subgroup (possibly Hydrozoan polyps, medusae, tentacles, unarticulated colonies elements, etc.). The Palynomorph group presents high percentages (average 28.52%). The Zoomorph subgroup is the most representative with an average percentage of 11.61%. It is characterized by Foraminiferal Test-Linings and Hydrozoan Medusae. Hydroids in an embryonic stage (medusae eggs and medusae in initial stages of development) were also identified in the 5-60μm and >60μm fractions. In all samples were identified marine components (average 9.95%) and terrestrial components with an

average percentage of 6.97%, some in the form of agglomerates (dyads, tetrads and polyads) and bisaccate pollen grains. Some dyads, tetrads and grains were from the genus *Classopollis*, one type of extinct coniferous. These plants were adapted to arid climates (hot and dry) and also to a wide range of salinity conditions (Srivastava, 1976; Tyson, 1995; Mendonça Filho et al., 2010a, 2011c, 2014c). According to Mendonça Filho et al. (2016 *Ineditus in efficiendis*) this OM association is related to a Kerogen Type III. Hydrozoans are predominantly constituted by chitin, a polysaccharide with a similar structure to vegetable cellulose, and protein. They present a lower carbon and higher oxygen contents than the predominantly lipid-rich organisms (e.g. phytoplankton). Furthermore, the mesoglea of the medusoid forms (main constituent of the gelatinous body of these forms) is predominantly constituted by water with low lipid content (Rupert and Barnes, 1994; Bouillon et al., 2006). Taking into consideration the chemical composition (C, H and O) these particulate organic components (zoomorphs) could be associated with a Kerogen Type III (OM mostly derived from lignified mechanical support tissue of higher plants rich in cellulose, a high molecular weight polysaccharide, and lignin, a high molecular weight polyphenol) (Mendonça Filho et al., 2016 *Ineditus in efficiendis*).

Palynofacies Association II

The palynofacies is dominated by **AOM** probably derived from microbiological attack of components from the **Zoomorph subgroup** (same components as palynofacies association I) and **zooclasts** (probably hydrozoan polypoid form fragments) with an average percentage of 55.61% and 30.82%, respectively. Some of the zooclast particles present morphological characteristics that allow their possible association with hydrozoans. TOC values are higher than the ones associated with palynofacies association I, ranging between 0.91 wt.% and 4.31 wt.%. IR values fluctuate between 50 wt.% and 71 wt.%, with the majority of the samples with values <60 wt.%, indicating a higher carbonate content than palynofacies association I.

The Phytoclast group presents very low percentages (average 3.50%), indicating a very low influence of terrestrial higher (vascular) plants components (continental contribution), lower than on palynofacies association I. The Amorphous group is dominated by AOM with the percentages previously described. The Palynomorph group exhibits very low values, where marine and terrestrial components are present in low percentages (average 2.23% and 2.75%, respectively). Some of the sporomorphs occur in the form of agglomerates (dyads, tetrads and polyads) and bisaccate pollen grains. Some dyads and grains were from the genus *Classopollis*. Both the marine and terrestrial

components present a lower relative abundance than in the palynofacies association I. The Zoomorph subgroup is represented by Hydrozoan Medusae specimens with very low percentages (average 2.04%). According to Mendonça Filho et al. (2016 *Ineditus in efficiendis*) this OM association is related to a Kerogen Type III.

Palynofacies Association III

The palynofacies is dominated by **AOM** probably derived from microbiological attack of components from the **Zoomorph subgroup** (same components as palynofacies associations I and II). TOC values are higher than the ones associated with palynofacies associations I and II, ranging between 4.40 wt.% and 6.79 wt.%. IR values range between 42 wt.% and 84 wt.%, with the majority of the samples with values <60 wt.%, showing higher carbonate content than palynofacies associations I and II.

The Phytoclast group displays very low percentages (average 0.87%). These values indicate the lowest influence of terrestrial higher (vascular) plants components (continental input) in the succession, lower than palynofacies associations I and II. The Amorphous group is dominated by AOM. The Palynomorph group exhibits very low values. The marine components are present in very low percentages (average 0.38%). Terrestrial components are mostly absent. The marine and terrestrial palynomorphs demonstrate lower relative abundance than in palynofacies associations I and II. The Zoomorph subgroup is absent. Low percentages of zooclasts are present. According to Mendonça Filho et al. (2010a, 2011a, 2014a, 2016 *Ineditus in efficiendis*) this OM association is related to a Kerogen Type II.

V.1.1.2. Paleoenvironmental characterization and evolution

The Suèges sedimentary succession was subdivided into four intervals based on the palynofacies associations established for this section (Figure V.2).

Interval 1 (samples S10 and S11) corresponds to the **Palynofacies Association I** and includes samples from the **Marnes de Villeneuve Fm.** (Figure V.3A). The low TOC values associated with low percentages of AOM and high percentages of phytoclasts and terrestrial palynomorphs indicate an oxidizing environment. In terms of a microbial biofacies, it represents an aerobic system that would allow the development of a high primary organic productivity (phytoplanktonic), as the food chain base, that supports the primary consumers and ultimately the secondary consumers, Hydrozoan fauna (simple and sessile colonial polypoid and free-swimming medusoid forms) (Mendonça Filho et al., 2016 *Ineditus in efficiendis*). The presence of *Classopollis* ssp. indicates an arid climate (hot and dry) promoting evaporation that could lead to an increase in salinity

(Srivastava, 1976; Tyson, 1995; Mendonça Filho et al., 2010a, 2011c, 2014c). The high percentage of phytoclasts and terrestrial palynomorphs together with the high percentage of marine components indicate a water body proximal to the terrestrial source area with marine influence (Tyson, 1995).

Interval 2 (sample S12) relates to the **Palynofacies Association II** and corresponds to a sample from the **Marnes de Villeneuve Fm.** (Figure V.3B). In relation to the previous interval there is a decrease of the marine influence in the system and also a separation from the terrestrial source area, possibly due to aridity conditions and high evaporation rates (presence of *Classopollis* ssp.) (Tyson, 1995). This ultimately results in shallowing of the water column. There is also a decrease of the $CaCO_3$ content demonstrating a more effective non-carbonate (siliciclastic) sedimentation in the system.

Interval 3 (samples S15, S17, S19, S22, S50 and S52) corresponds to the **Palynofacies Association III** and includes samples from the **Schistes Cartons Fm.** (Figure V.3C). The high occurrence of amorphous material coupled to high TOC contents (average 5.43 wt.%) indicate a restricted, stagnated environment. The environment presented dysoxic to anoxic conditions which, in terms of a microbial biofacies, represents a dysaerobic to anaerobic system. It is possible to infer a stratification in terms of oxygen levels of the water column. The upper part would be more oxygenated allowing the development of a high primary organic productivity (phytoplanktonic), as the food chain base, that would support the primary consumers and ultimately the secondary consumers, Hydrozoan fauna, as the top of the low energy food chain (Mendonça Filho et al., 2016 *Ineditus in efficiendis*). The lower layer of the water column would present an oxygen deficiency (dysoxic to anoxic), allowing more effective amorphization processes by microbiological reworking (anaerobic), reflected in higher AOM relative proportions, and consequently in an increase of the chemical preservation of the particulate organic components (Tyson, 1995) which lead to higher TOC contents than previous intervals. The presence of Prasinophyte algae with high preservation state (low amorphization) indicates possibly some communication with the Tethys Ocean. The water stratification conditions can be related to an increase in salinity of the system possibly due to high evaporation rate (arid climate) that would lead to a decrease of the water level. The increase of the $CaCO_3$ content of the succession reflects a higher alkalinity of the system. This fact can be corroborated by the high concentration of CO_3^{2-} and HCO_3^- ions that could be associated with the OM decomposition processes due to high dissolution of CO_2 originated from bacterial reworking (Tyson, 1995; Mendonça Filho et al., 2016 *Ineditus in efficiendis*). All of these facts lead to interpret this part of the succession as the highest restriction interval of the whole section.

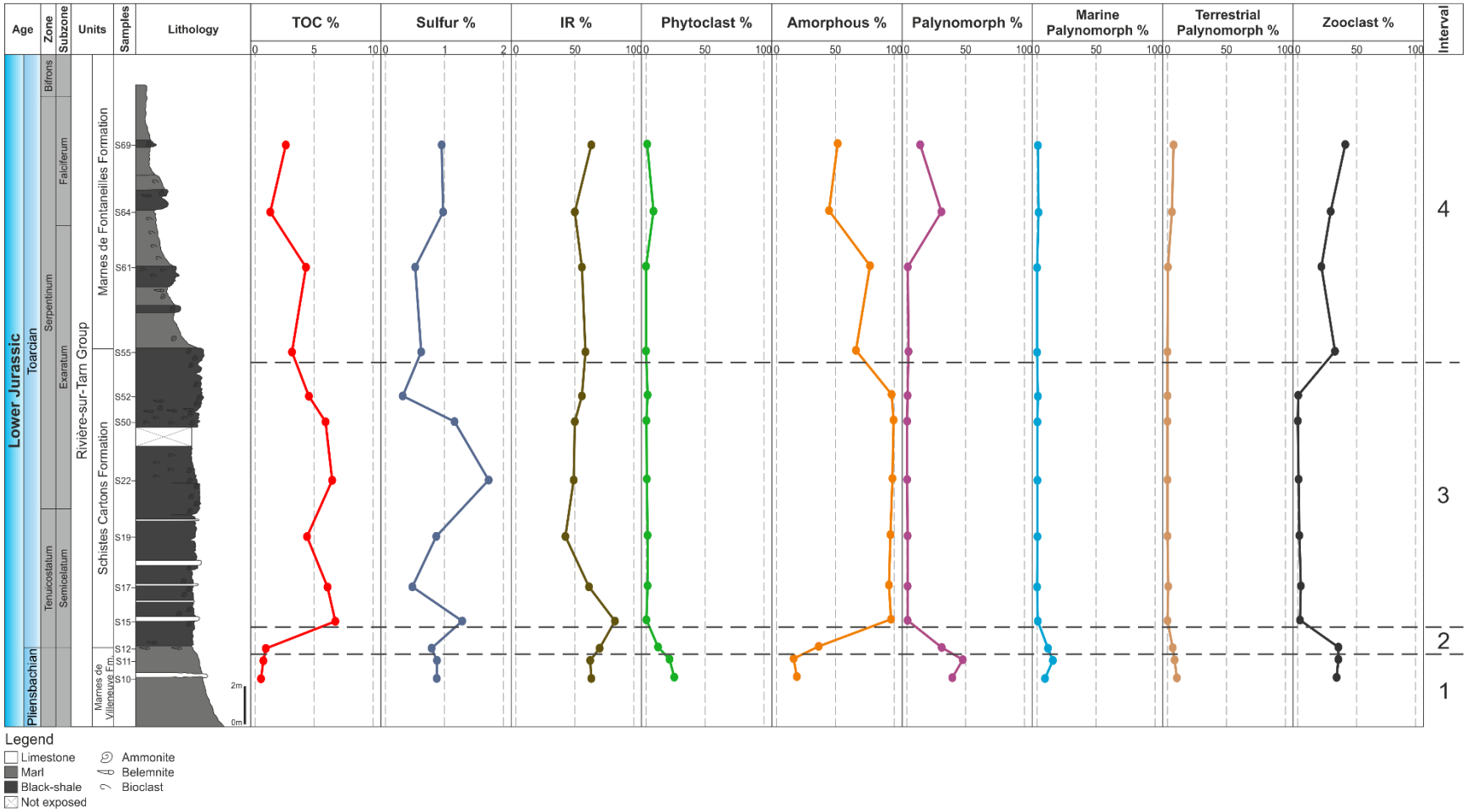

Figure V.2. Palynofacies and geochemical data stratigraphic variation across the Suèges section.

Interval 4 (samples S55, S61, S64 and S69) represents **Palynofacies Association II** including samples from the **Schistes Cartons** and **Marnes de Fontaneilles formations** (Figure V.3D). The decrease in TOC content (average 2.83 wt.%) and AOM relative percentage indicates the beginning of the reestablishment of the oxygen levels and of the paleoceanographic circulation patterns, with a decline of the restriction conditions of the water body. There is an increase in the water column and the entrance of marine water represented by a proliferation of marine palynomorphs and, to the top of the succession, a decrease of the aridity conditions with the input of phytoclasts and terrestrial palynomorphs into the system (proximity to the terrestrial source area) (Tyson, 1995).

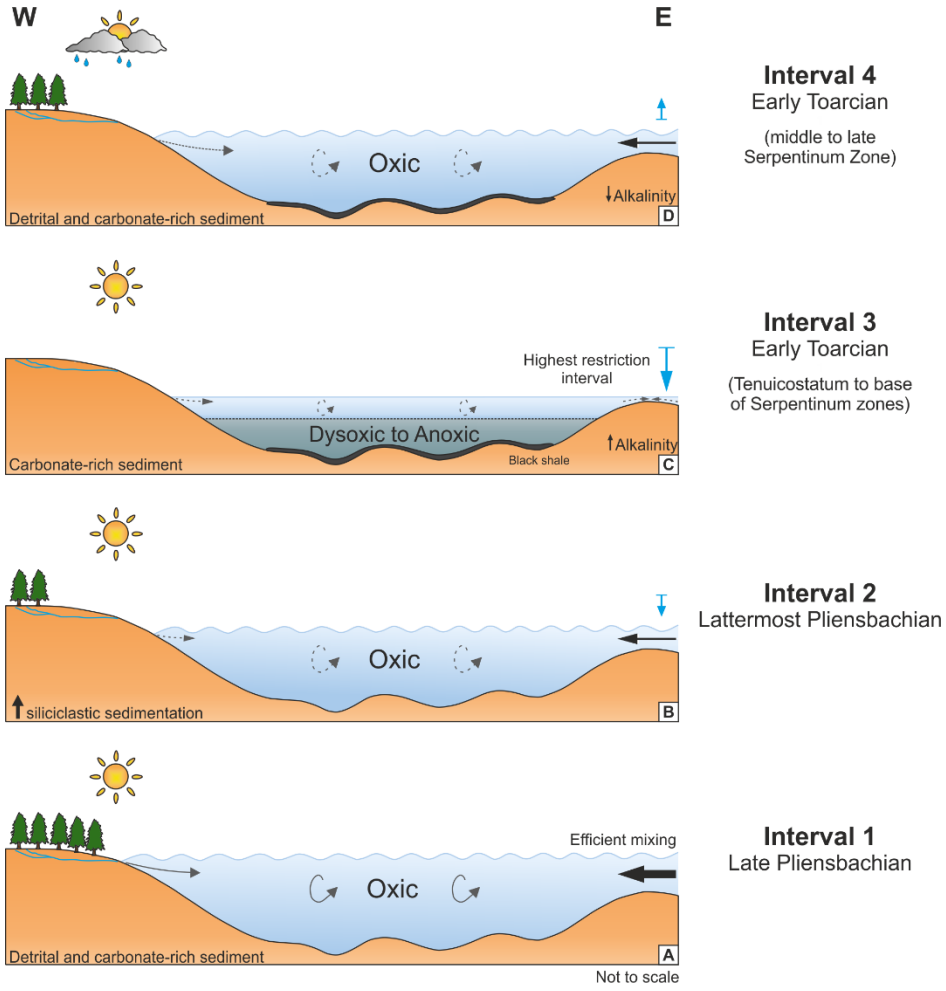

Figure V.3. Diagrammatic sketch illustrating the environmental evolution of the Grands Causses Basin during the late Pliensbachian – early Toarcian. **A -** During the late Pliensbachian, a well oxygenated water body proximal to the terrestrial source area with marine influence under an arid climate; **B -** During the lattermost Pliensbachian, a shallow oxygenated proximal water body separated from the terrestrial source area with a decrease of marine influence under an arid climate; **C -** During the Tenuicostatum to the base of Serpentinum zones (early Toarcian), a restricted and stagnated environment with partial closure of the basin, with the development of dysoxic to anoxic conditions associated with water column stratification under an arid climate; **D -** During the middle to late Serpentinum Zone (early Toarcian), reestablishment of the oxygen levels and of the paleoceanographic circulation patterns, with an increase of water column under a less arid climate.

V.1.2. Caylus section – Quercy Basin

V.1.2.1. Cluster Analysis

Using **R-Mode cluster analysis** the samples were organized in four groups (A to D) according to the degree of similarity of the OM components in relation to origin criterion (Table V.2): **Group A** contains marine components (Foraminiferal Test-Linings, Dinocysts and Acritarchs), the terrestrial palynomorphs (Sporomorph subgroup) and the undifferentiated palynomorphs; **Group B** includes only the amorphous zoomorphs; **Group C** is composed solely by a marine component (Prasinophyte algae), an aquatic continental constituent (Hydrozoan medusae) and AOM; **Group D** is composed by zooclasts (possible Hydrozoan polyp fragments), the higher plants derived components (Phytoclast group and Membrane) and freshwater microplankton (Gloeocapsomorpha).

Table V.2. Caylus section R-Mode cluster analysis description.

Group	Description
A	Foraminiferal test-linings + dinocysts + acritarchs + terrestrial palynomorph + undifferentiated palynomorph
B	Amorphous zoomorph
C	Prasinophyte algae + Hydrozoan medusae + AOM
D	Zooclasts + membrane + phytoclast + gloeocapsomorpha

Q-Mode cluster analysis subdivided the samples into three palynofacies associations, according to the OM abundance of the groups and subgroups (Figure V.4): (i) **Palynofacies Association I**, with a predominance of amorphous zoomorphs and zooclasts; (ii) **Palynofacies Association II**, with a prevalence of amorphous zoomorphs; and, (iii) **Palynofacies Association III**, with a dominance of zoomorph derived AOM.

Samples Cay3 and Cay6 displayed low OM recovery and palynofacies data was not accounted for cluster analysis due to bias, even so an analysis of the components and their preservation state was performed.

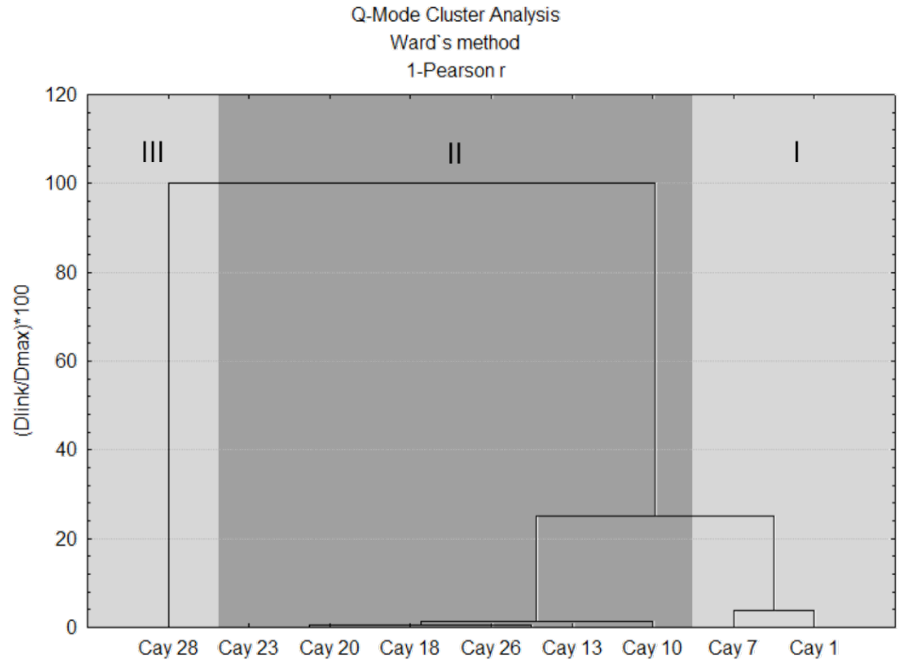

Figure V.4. Q-Mode cluster analysis for samples from the Caylus section.

Palynofacies Association I

The palynofacies assemblage is dominated by **amorphous components from the Zoomorph subgroup**, in this case, possibly Hydrozoans (polyps, medusae, tentacles, unarticulated colonies elements, etc.) with an average percentage of 61.41% and **zooclasts** (possibly hydrozoans' polypoid forms fragments) with an average percentage of 10.32%. The amorphous zoomorphs display features of AOM but with specific morphological characteristics of organic particles of animal origin still recognizable (zoomorphs). TOC (below 0.18 wt.%) and IR (below 17 wt.%) present very low values.

The Phytoclast group presents low percentages (average 1.39%), indicating a low input of terrestrial higher plants (continental contribution). No particle from the Amorphous group was encountered in the association. The Palynomorph group co-dominates the assemblage with the Zoomorph subgroup being the most representative with an average percentage of 66.16%. It is characterized by Foraminiferal Test-Linings, Hydrozoan Medusae and the dominant amorphous zoomorphs referred previously. Marine components were identified in all samples (average 5.97%) as well as terrestrial components with an average percentage of 6.95%, some in the form of agglomerates (dyads, triads and tetrads) and bisaccate pollen grains. Some tetrads and grains were from genus *Classopollis*. Undifferentiated palynomorphs (average 8.87%) were also identified. The Zooclast group also co-dominates the palynological association. According to

Mendonça Filho et al. (2010a, 2011a, 2014a, 2016 *Ineditus in efficiendis*) this OM association is related to a Kerogen Type III.

Palynofacies Association II

The palynofacies assemblage is dominated by **amorphous components from the Zoomorph subgroup**, (probable Hydrozoans – same components as palynofacies association I) with an average percentage of 92.77%. The amorphous zoomorphs display features of AOM but with specific morphological characteristics of organic particles of animal origin still recognizable (zoomorphs). TOC values range between 0.38% and 8.80%, higher than palynofacies association I. IR values vary between 54 wt.% and 82 wt.%, most samples with values >70 wt.%, displaying a lower carbonate content than palynofacies association I.

The Phytoclast group is absent in the majority of samples that correspond to this palynofacies association (only present in sample Cay10 – 4.32%), indicating a low to null input of terrestrial higher plants (continental contribution). The Amorphous group is also absent. The Palynomorph group dominates the assemblage with the Zoomorph subgroup being the most representative. It is characterized by Foraminiferal Test-Linings, Hydrozoan Medusae and the dominant amorphous zoomorphs referred previously. Marine components from all subgroups were identified in most samples. Terrestrial components, such as pollen grains and spores, are present in some samples in low percentages. Freshwater microplankton (Gloeocapsomorpha) is present in some samples. Undifferentiated palynomorphs (average 0.94%) were also identified. Low percentages of zooclasts were also accounted. According to Mendonça Filho et al. (2010a, 2011a, 2014a, 2016 *Ineditus in efficiendis*) this OM association is related to a Kerogen Type II.

Palynofacies Association III

This palynofacies association is dominated by **AOM,** probably derived from microbiological rework of **components from the Zoomorph subgroup** (same components as palynofacies associations I and II), combined with bacterial derived AOM. This association refers only to one sample which TOC percentage is 0.32%, lower than palynofacies association II but slightly higher than palynofacies association I. IR value is 59 wt.%, to which corresponds a higher carbonate content than palynofacies association II and lower than palynofacies association I.

The Phytoclast group is present in low percentages (0.95%), indicating a low input of terrestrial higher plants (continental contribution). The Amorphous group dominates the assemblage being represented by zoomorph derived AOM along with

bacterial AOM (84.18%). The Palynomorph group is represented by marine microplankton (Prasinophyte algae), freshwater microplankton (Gloeocapsomorpha) and zoomorphs (Foraminiferal Test-Linings and Hydrozoan Medusae). A significant percentage of zooclasts is also present (11.39%). According to Mendonça Filho et al. (2010a, 2011a, 2014a, 2016 *Ineditus in efficiendis*) this OM association is related to a Kerogen Type II.

V.1.2.2. Paleoenvironmental characterization and evolution

The Caylus sedimentary succession was subdivided into three intervals based on the palynofacies associations established for this section (Figure V.5).

Interval 1 (samples Cay1, Cay3, Cay6 and Cay7) corresponds to the **Palynofacies Association I** and includes samples from the **Barre à Pecten Fm.** (Figure V.6A). The low TOC content coupled with the presence of amorphous zoomorphs (Hydrozoans) indicate oxic to dysoxic conditions that, in terms of a microbial biofacies, represents an aerobic to dysaerobic system (Mendonça Filho et al., 2016 *Ineditus in efficiendis*). It demonstrates the existence of oxygen level stratification in the water column that presents a more oxygenated upper layer allowing the development of a primary organic productivity (phytoplanktonic), as the food chain base, that would support the primary consumers and ultimately the secondary consumers, Hydrozoan (Mendonça Filho et al., 2016 *Ineditus in efficiendis*). The lower level of the water column is more limited in terms of oxygen availability allowing the amorphization processes through microbiological reworking (anaerobic) of the zoomorph fragments. The presence of Hydrozoans in their medusae form indicates a very shallow water column in very stressful conditions, with high alkalinity, which can be corroborated by the low IR values (high $CaCO_3$ content) of the samples. This value points out to a high concentration of CO_3^{2-} and HCO_3^- ions that could be associated with the OM decomposition processes due to high dissolution of CO_2 originated from the bacterial reworking. The presence of *Classopollis* ssp. indicates an arid climate (hot and dry) that promotes evaporation leading to a shallowing of the water column and an increase in salinity (Srivastava, 1976; Tyson, 1995; Mendonça Filho et al., 2010a, 2011c, 2014c). This fact, coupled with a low percentage of phytoclasts and terrestrial components, indicate a very proximal water body separated from the terrestrial source area, possibly due to the aridity conditions (Tyson, 1995).

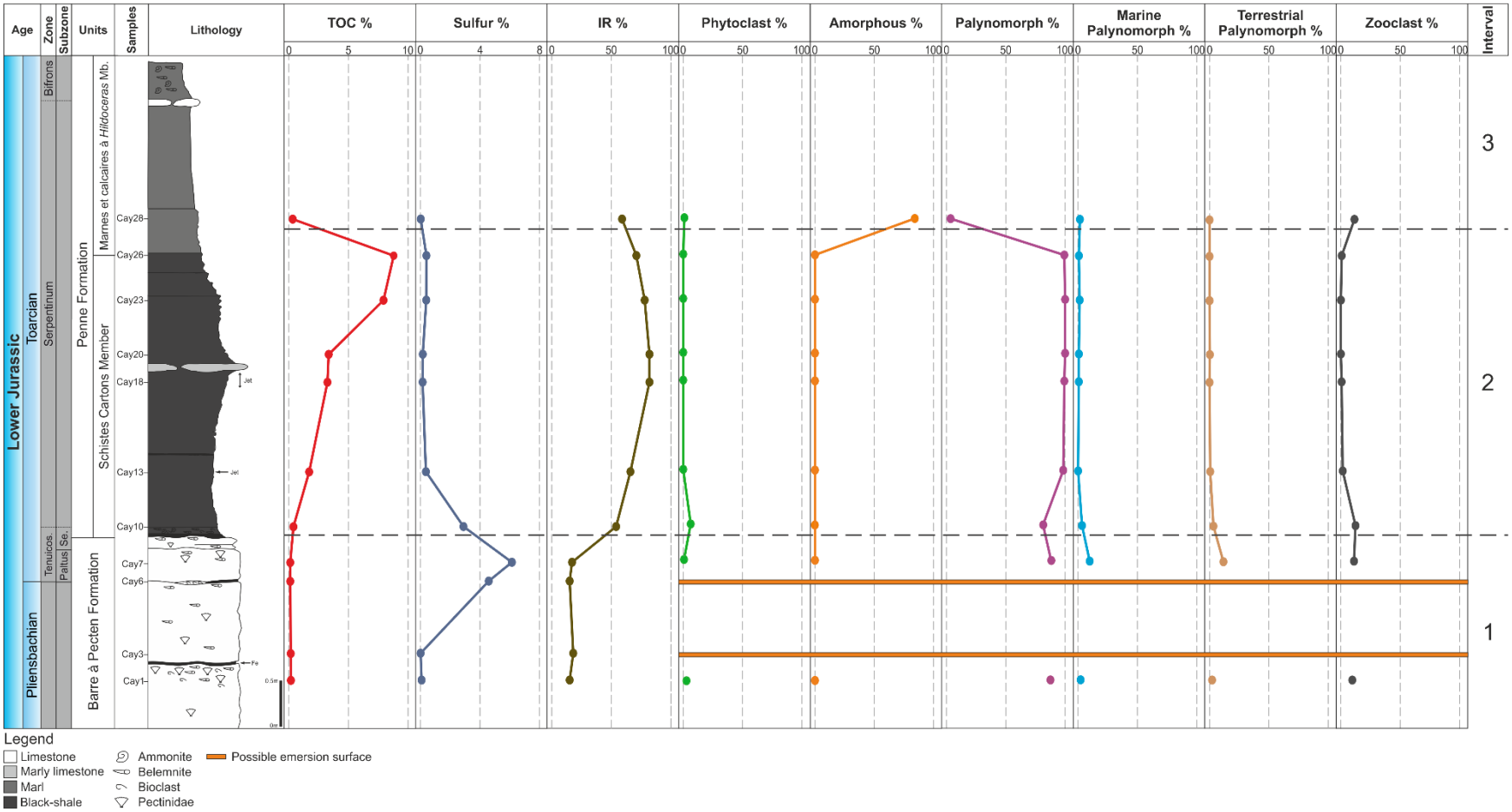

Figure V.5. Palynofacies and geochemical data stratigraphic variation across the Caylus section.

Samples Cay3 and Cay6 presented low recovery for particulate OM. However, some phytoclasts, marine microplankton, sporomorphs and fragments of Hydrozoan polypoid forms and medusoid free-swimming forms (medusae) with different amorphization stages were recognized. A high occurrence of undifferentiated palynomorphs was also noted indicating a low preservation of the particulate components. The organic particles present characteristics of oxidized OM relatable with periods of maximum shallowing, possibly emersion (Mendonça Filho et al., 2016 *Ineditus in efficiendis*). This corroborates the idea of a shallowing of the system that could possibly be registered through macroscopic pedogenetic features in these two surfaces.

Interval 2 (samples Cay10, Cay13, Cay18, Cay20, Cay23 and Cay26) relates to **Palynofacies Association II** and includes samples from the **Schistes Cartons Mb.** of the Penne Fm. (Figure V.6B). This interval is characterized by an abrupt change in the depositional conditions. There is a more effective non-carbonate sedimentation (great contribution of fine siliciclastic deposits) recorded by the IR values (up to 82%). The high IR values coupled with the high TOC contents and the presence of the amorphous zoomorphs (Hydrozoan fauna) can only co-exist in conditions of a high water level with a lower alkalinity (non-saturation in ions) with no precipitation of $CaCO_3$ (Mendonça Filho et al., 2016 *Ineditus in efficiendis*). This leads to infer a freshwater entrance into the system and an oxygen level stratification of the water column indicating oxic to dysoxic conditions which, in terms of a microbial biofacies, represents an aerobic to dysaerobic system. The water column presents a more oxygenated upper level that allows the development of a primary organic productivity (phytoplanktonic) as the food chain base, that supports the primary consumers and ultimately the secondary consumers, the Hydrozoan fauna (Mendonça Filho et al., 2016 *Ineditus in efficiendis*). The lower level of the water column is more limited in terms of oxygen availability allowing the initial stages of the amorphization processes through microbiological reworking (anaerobic) of the zoomorph fragments. Furthermore it is important to emphasize that such high siliciclastic contribution cannot be associated with wind transported sediment entrance, it must represent a freshwater entrance into the system although there is no evidence of terrestrial continental OM (phytoclasts or terrestrial palynomorph) (Mendonça Filho et al., 2016 *Ineditus in efficiendis*). This freshwater influx can possibly be related to the development of a more humid climatic setting and an increase in precipitation or to the influx of freshwater coming from the Arctic through the Laurasian seaway, as has been suggested by several authors for other European basins, namely the Paris and SW German basins (e.g. Bjerrum et al., 2001; Röhl et al., 2001; van de Schootbrugge et al., 2005; Dera et al., 2009; Lézin et al., 2013).

Interval 3 (sample Cay28) represents **Palynofacies Association III** and includes a sample from the **Marnes et calcaires à *Hildoceras* Mb.** of the Penne Fm. (Figure V.6C). Low IR values coupled with high AOM percentage, when compared to interval 1, suggest a shallowing of the water column and an increase of the alkalinity of the system that increased CO_3^{2-} and HCO_3^- ions concentration in the water associated with the OM decomposition processes due to high dissolution of CO_2 originated from the bacterial reworking (Mendonça Filho et al., 2016 *Ineditus in efficiendis*). The presence of oxidized colonial hydrozoan polyp fragments coupled with an increase in the medusae relative proportion and low TOC contents point to a more oxidizing environment that leads to a decrease in preservation (Mendonça Filho et al., 2016 *Ineditus in efficiendis*). This increase of oxygen in the system translates into a proliferation of primary productivity, demonstrated by the presence of bacterial AOM. Although there is an increase in oxygen levels, the contemporary increment of AOM seems to be associated with water column stratification (Mendonça Filho et al., 2016 *Ineditus in efficiendis*).

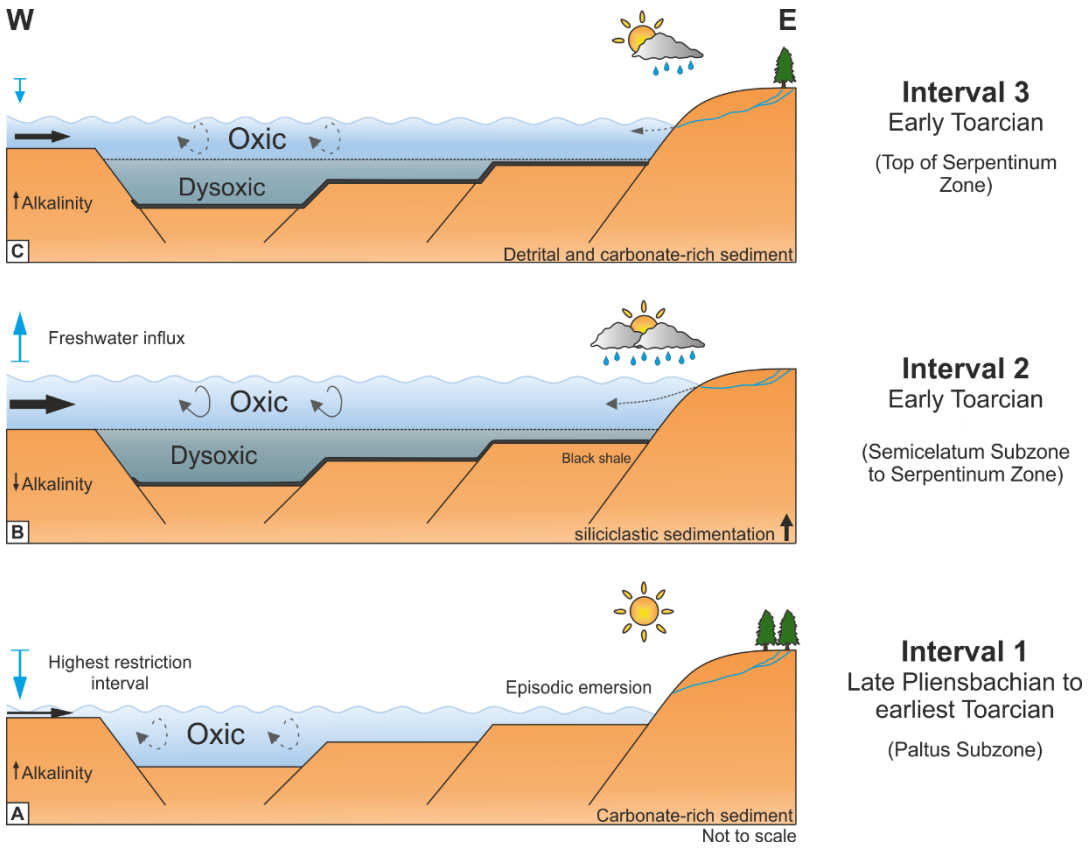

Figure V.6. Diagrammatic sketch illustrating the environmental evolution of the Quercy Basin during the late Pliensbachian – early Toarcian. **A -** From the late Pliensbachian to the Tenuicostatum Zone, Paltus Subzone (earliest Toarcian), a shallow oxygenated proximal water body separated from the terrestrial source area under an arid climate, with episodic emersion; **B -** During Semicelatum Subzone to Serpentinum Zone (ealy Toarcian), freshwater influx lead to the development of dysoxic to anoxic conditions associated with water column stratification and high detrital influx with the increase of water level; **C -** At the top of Serpentinum Zone (early Toarcian), a shallower water body with a more oxidizing environment but stil with water column stratification in terms of oxygen levels.

V.1.3. Pont de Suert section –Pyrenean Basin

V.1.3.1. Cluster Analysis

Using **R-Mode cluster analysis** the samples were organized in three groups (A to C) according to the degree of similarity of the OM components in relation to origin criterion (Table V.3): **Group A** contains marine components (Foraminiferal Test-Linings), aquatic continental constituents (Amorphous Hydrozoan Medusae) and terrestrial palynomorph (Sporomorph subgroup); **Group B** includes the marine microplankton (Acritarchs) and the undifferentiated palynomorph; **Group C** is composed by zooclasts (possible Hydrozoan polyp fragments) and higher plants derived components (Phytoclast group).

Table V.3. Pont Suert section R-Mode cluster analysis description.

Group	Description
A	Foraminiferal test-linings + amorphous Hydrozoan medusae + terrestrial palynomorph
B	Acritarchs + undifferentiated palynomorph
C	Zooclasts + phytoclast

Q-Mode cluster analysis subdivided the samples into two palynofacies associations, according to the OM abundance of the groups and subgroups (Figure V.7): (i) **Palynofacies Association I**, with a predominance of zooclasts (Hydrozoan polyp fragments); and, (ii) **Palynofacies Association II**, with a prevalence of amorphous zoomorph (Hydrozoan medusa) and zooclasts (Hydrozoan polyp fragments).

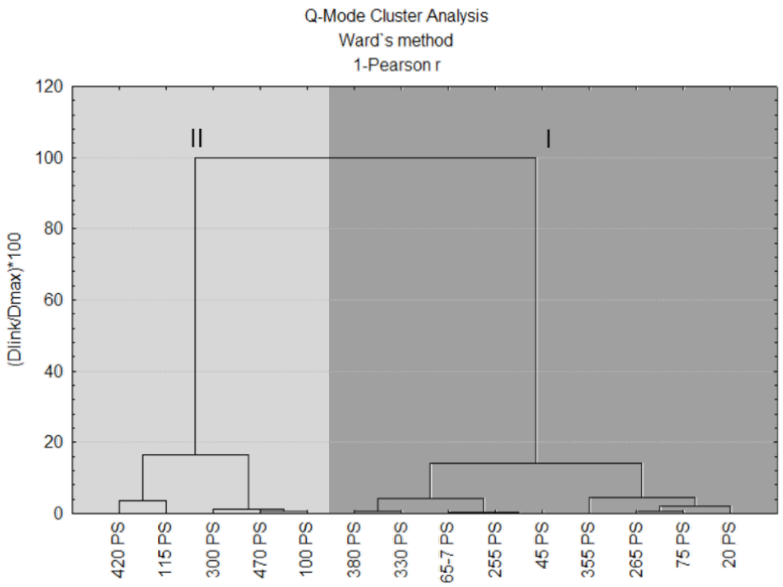

Figure V.7. Q-Mode cluster analysis for samples from the Pont de Suert section.

Palynofacies Association I

The palynofacies is dominated by **zooclasts**, characterized as possible hydrozoan polypoid form fragments, with an average percentage of 79.01%. TOC varies between 0.16 wt.% and 0.40 wt.%. IR values range between 13 wt.% and 67 wt.% with the majority of samples presenting values >55 wt.%.

The Phytoclast group presents very low percentages (average 1.86%), indicating a low input of terrestrial higher (vascular) plants (continental contribution). The Amorphous group is absent in all samples and the Palynomorph group exhibits low values (average 19.13%). It is characterized by Foraminiferal Test-Linings and the dominant amorphous zoomorphs (Hydrozoan Medusae). Marine palynomorphs from all subgroups were identified in most samples. Terrestrial components are present in most samples in low percentages. Undifferentiated palynomorphs (average 7.91%) are also present. The Zooclast group dominates the palynological association.

Palynofacies Association II

The palynofacies is dominated by **amorphous zoomorphs** (Hydrozoan Medusae) with an average percentage of 60.14% and **zooclasts** (possibly the same components as palynofacies association I) with an average percentage of 31.98%. TOC varies between 0.14 wt.% and 0.35 wt.%. IR values fluctuate between 21 wt.% and 53 wt.%, higher carbonate content than palynofacies association I.

The Phytoclast group presents very low percentages (average 0.91%). These values indicate a very low influence of terrestrial higher (vascular) plants components (continental contribution), lower than on palynofacies association I. The Amorphous group is absent. The Palynomorph group exhibits high values (average 67.12%), being mainly characterized by Foraminiferal Test-Linings and the dominant amorphous zoomorphs. Marine palynomorphs (Dinocyst and Acritarch) were identified in all samples. Terrestrial components were recognized in most samples in low percentages. Undifferentiated palynomorphs (average 4.09%) are also present. The Zooclast group co-dominates the palynological association.

In both associations and according to Mendonça Filho et al. (2010a, 2011a, 2014a, 2016 *Ineditus in efficiendis*) the OM is related to a Kerogen Type III.

V.1.3.2. Paleoenvironmental characterization and evolution

The Pont de Suert sedimentary succession was subdivided into five intervals based on the palynofacies associations established for this section (Figure V.8). TOC and TS values were not taken into account for interpretation purposes due to the high maturity of the samples (see V.3). Furthermore, it is important to emphasize that the differentiation of the palynological components was also affected by the maturity level.

Intervals 1, 3 and 5 (samples 20PS, 45PS, 65-7PS, 75PS, 330PS, 355PS, 380PS, 255PS and 265PS) correspond to the **Palynofacies Association I** and include samples from the **Barre a Pecten Fm.** and the **Calcaires argileux à *Spiriférines***, **Calcaires argileux et marnes à *Soaresirhynchia*** and **Calcaires argileux à *Telothyris* members** of the Padrinas Fm. (Figure V.9A). The average IR values of these intervals, coupled with the presence of an Hydrozoan fauna represented in very high proportions of zooclasts (possible Hydrozoan polypoid forms) and low proportions of amorphous zoomorphs (Hydrozoan free-swimming medusoid forms), are indicative of an oxidizing environment which, in terms of the microbial biofacies, represents an aerobic system that would allow the development of a high primary organic productivity (phytoplanktonic) as the food chain base, that would support the primary consumers and ultimately the secondary consumers, Hydrozoan fauna (Mendonça Filho et al., 2016 *Ineditus in efficiendis*).The shallow water body presents some marine influence verified by the presence of marine microplankton (Tyson, 1995).

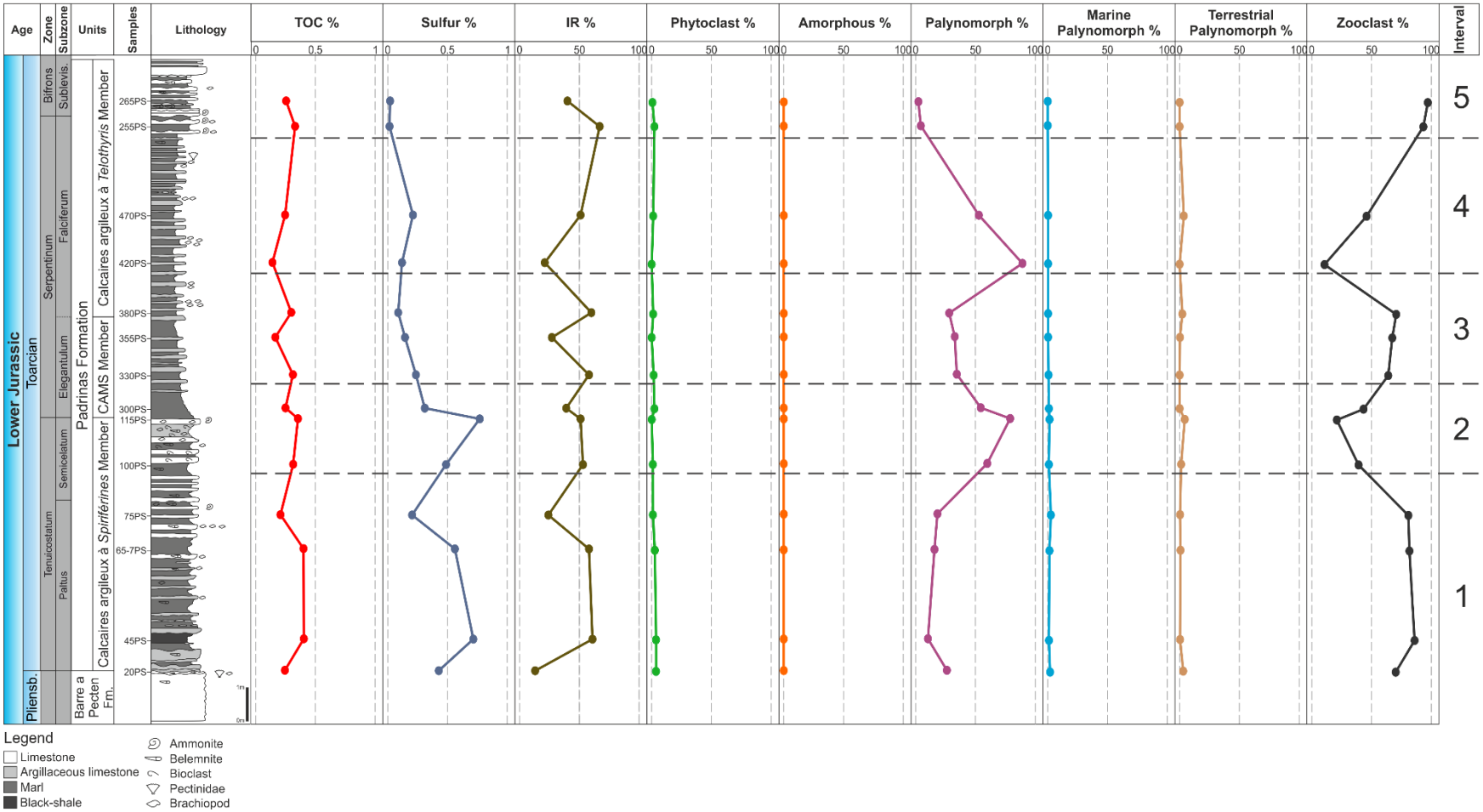

Figure V.8. Palynofacies and geochemical data stratigraphic variation across the Pont de Suert section. Sublevis.=Sublevisoni; CAMS Member=Calcaires argileux et marnes à *Soaresirhynchia* Member

Intervals 2 and 4 (samples 100PS, 115PS 300PS, 420PS and 470PS) represent **Palynofacies Association II** and comprise samples from the **Calcaires argileux à *Spiriférines***, **Calcaires argileux et marnes à *Soaresirhynchia*** and **Calcaires argileux à *Telothyris* members** of the Padrinas Fm. (Figure V.9B). The lower IR values, when compared with intervals 1, 3 and 5, coupled with a decrease in the relative proportion of zooclasts and an increase in the prevalence of amorphous zoomorphs, when compared with interval 1, indicate a shallowing of the water column (Mendonça Filho et al., 2016 *Ineditus in efficiendis*). The development of the Hydrozoan medusoid forms, when compared to the polypoid forms, shows an increase of the stress conditions of the system with a rise in alkalinity derived from higher CO_3^{2-} and HCO_3^- ions concentration in the water associated with the OM decomposition processes due to high dissolution of CO_2 originated from the bacterial reworking (Mendonça Filho et al., 2016 *Ineditus in efficiendis*). The amorphization of the zoomorphs leads to the inference of oxygen level stratification of the water column, indicating oxic to dysoxic conditions which, in terms of the microbial biofacies, represents an aerobic to dysaerobic system. The water column presents a more oxygenated level allowing the development of a primary organic productivity (phytoplanktonic), as the food chain base, that supports the primary consumers and ultimately the secondary consumers, the Hydrozoan fauna (Mendonça Filho et al., 2016 *Ineditus in efficiendis*). The lower level of the water column is more limited in terms of oxygen availability allowing the initial stages of the amorphization processes through microbiological reworking (anaerobic) of the zoomorph fragments. The presence of marine microplankton shows the marine influence of this shallow water body that suffers water level fluctuations possibly due to variations of the precipitation and evaporation rates related with climatic oscillations (Tyson, 1995).

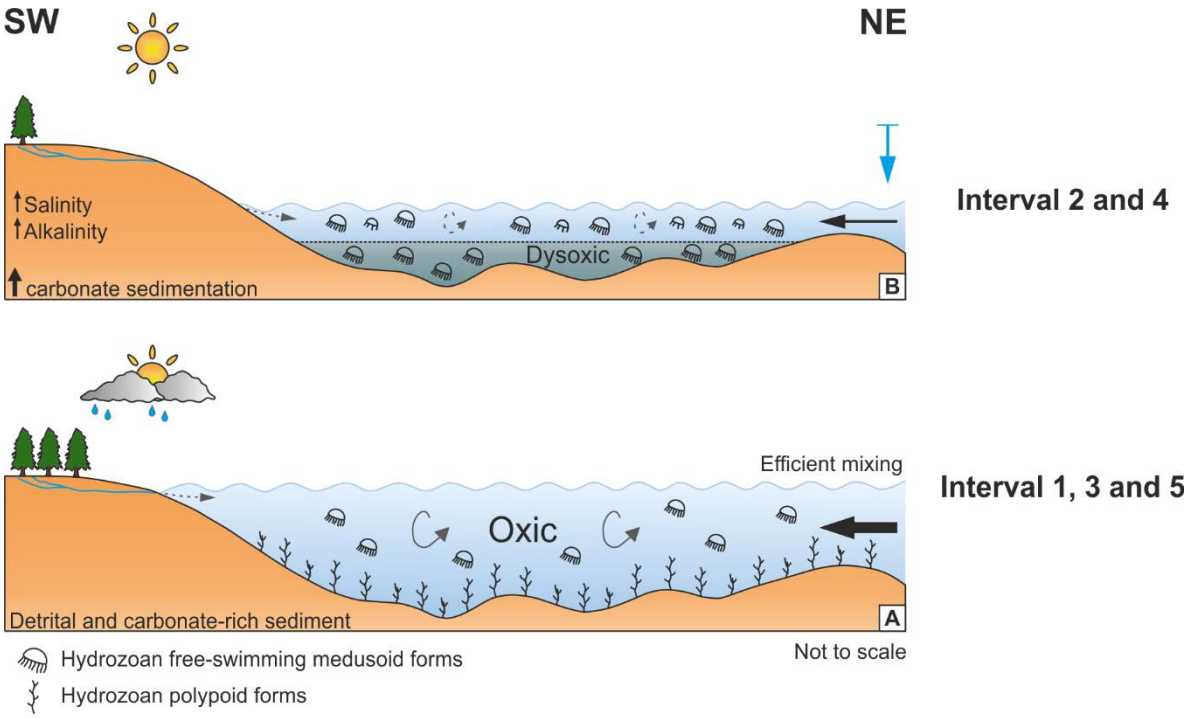

Figure V.9. Diagrammatic sketch illustrating the environmental evolution of the Pyrenean Basin during the late Pliensbachian – earliest middle Toarcian. **A -** During interval 1 (late Pliensbachian to base of Semicelatum Subzone), interval 3 (Elegantum to base of Falciferum subzones) and interval 5 (top of Falciferum to base of Sublevisoni subzones), a well oxygenated proximal water body with marine influence; **B -** During interval 2 (Semicelatum to base of Elegantum subzones) and interval 4 (Falciferum Subzone), a shallowing of the water column lead to a more restricted and stagnated environment, with the development of dysoxic to anoxic conditions associated with water column stratification under a more arid climate.

V.2. Organic matter significance in the T-OAE recorded in southern France

The T-OAE is marked by environmental perturbations that resulted in organic-rich sediments deposition in the epicontinental basins of southern France, namely in the three studied reference sections of GCB, QB and PB (e.g. Jenkyns, 1985, 1988; Emmanuel et al., 2006; Hermoso et al., 2012, 2013; Harazim et al., 2013; Lézin et al., 2013). On the basis of the palynofacies and geochemical analysis data from the Suèges, Caylus and Pont de Suert sedimentary sections was possible to define the depositional paleoenvironment of each basin.

In terms of the OM all studied successions represent a very proximal shallow marine influenced system with various restriction conditions with water column variation, alkalinity, salinity and oxygen availability, being mainly controlled by the climate (arid-humid). Water column shows phases of stratified oxygen regimen, varying from oxic to suboxic and dysoxic to anoxic (from aerobic to quasi-anaerobic). This paleoenvironmental setting has been previously proposed by Schouten et al. (2000),

Röhl and Schmid-Röhl (2005), van de Schootbrugge et al. (2005) and McArthur et al. (2008) for the evolution of the SW German basin and others from the European epicontinental seaway as the “silled-basin transgressive chemocline” model to explain the early Toarcian black shale deposition. This model suggests a Pliensbachian regression that induced stagnant conditions and the onset of black shale deposition during the early Toarcian slow sea level rise. Deep-water conditions were never established. The redox boundary rose progressively onto the basin-margin areas during this slow transgression. Superimposed on the sea-level variation are short-term climatically induced variations, very patent in all three studied basins (Röhl and Schmid-Röhl, 2005).

As above demonstrated, the results of this study fully support this model presenting new evidences for the restriction conditions of these basins, being determined the maximum restriction interval for the Suèges (GCB) and Caylus (QB) successions. In the Suèges section (GCB) this interval presents a synchronicity with the deposition of the OM-rich sediments of the Schistes Cartons Fm. (Tenuicostatum to base of Serpentinum zones). Maillot et al. (2009), in a study of two different sections based on geochemistry and calcareous nannofossil and benthic foraminiferal assemblages, suggest an increase in water level during this time frame contradicting the interpretations established in this study by the organic facies variability. In the Caylus section (QB) the maximum restriction interval (late Pliensbachian to earliest Toarcian - Paltus Subzone) occurs prior to the deposition of OM-rich sediments of the Schistes Cartons Mb. of the Penne Fm.. For the Pont de Suert section (PB) was only possible to determine the water level fluctuations of the shallow proximal system and not its maximum restriction interval due to the influence of the high maturation stage of the OM (influence in the identification of the particulate components and TOC and TS values cannot be taken into account for interpretation proposes; see V.3). The Pyrenean basin seems therefore to have been the less restricted basin of the three, a fact that could be related to its more southern position, such as evidenced by van de Schootbrugge et al. (2005) and McArthur et al. (2008) that demonstrate some geographical variability in the degree of restriction of the Early Toarcian sea (Figure V.10).

This study verifies a shallow-water origin for the deposition of the early Toarcian black shale deposition in the studied basins corroborating the notion that the deposition of organic-rich sediments is not necessarily limited to deep-water environments and therefore black shales cannot be used as deep-water indicators (Röhl and Schmid-Röhl, 2005).

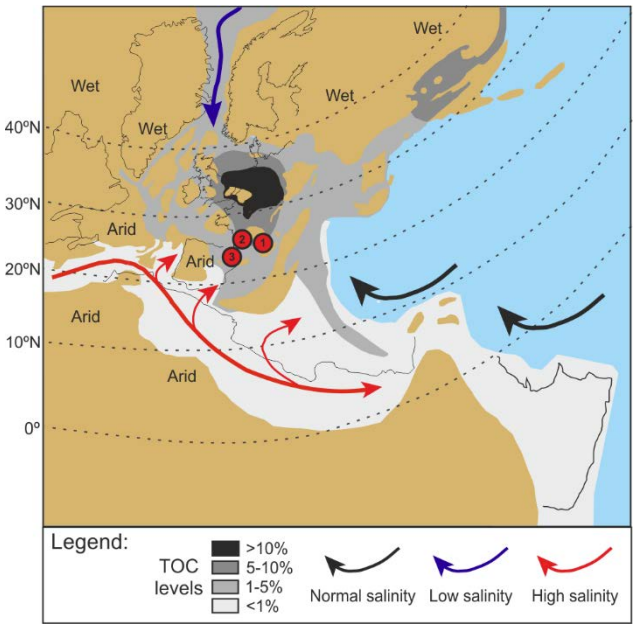

Figure V.10. Paleogeographic map for the early Toarcian with an interpretation of the paleoceanographic conditions, TOC content distribution and location of studied basins: 1 – Grands Causses; 2 – Quercy; 3 – Pyrenean (adapted from van de Schootbrugge et al., 2005).

The three studied sections present slight differences in their paleoenvironmental depositional contexts, such as the water level oscillations, which further demonstrates that although the T-OAE has a global character, in these three basins and in the basins that developed as part of the Toarcian European epicontinental seaway it is strictly controlled by local mechanisms, namely the geomorphology and paleogeography (Schouten et al., 2000; Röhl and Schmid-Röhl, 2005; van de Schootbrugge et al., 2005; McArthur et al., 2008). Global control mechanisms are also evident by the identification of temperature rise proxies and of the negative $\delta^{13}C$ excursion (Emmanuel et al., 2006; Hermoso et al., 2012, 2013; Harazim et al., 2013; Lézin et al., 2013). This paleoclimate framework was already described by several authors (e.g. Jenkyns, 2003; Rosales et al., 2004; Wignall et al., 2005; Gómez et al., 2008; Dera et al., 2009) and could be related to a worldwide greenhouse effect associated with the development of the Large Igneous Province of Karoo-Ferrar (e.g. Duncan et al., 1997; Pálfy and Smith, 2000; Jourdan et al., 2005; Jenkyns, 2010; Percival et al., 2015).

The organic facies of the studied successions display a predominance of polymorphic hydroids (Phylum Cnidaria, Class Hydrozoa, Order Hydroida): colonial (hydroid colonies) and non-colonial sessile polypoid forms (simple polyps), and free-swimming medusoid forms (medusae), with different preservation stages (Figure V.11). The water column level variation, alkalinity, salinity and oxygen availability is represented by the presence of these components. Thus, an oxygenated water column would have allowed the development of a high primary bioproductivity (food-chain producers),

supporting a significant consumer fauna (microcrustaceans, protozoa, etc.) as primary consumers and, therefore, a hydrozoan fauna. In these systems, the hydrozoan fauna is considered as secondary consumers and they are in the top of the low-energy food chain, once microcrustaceans and protozoans compose their main diet (Mendonça Filho et al., 2016 *Ineditus in efficiendis*).

This study represents the description of the first occurrence of organisms from the Phylum Cnidaria, Class Hydrozoa, Order Hydroida, namely its free-swimming medusoid forms, in organopalynological preparations of sediments from the Lower Jurassic (Pliensbachian-Toarcian).

Figure V.11. Schematic drawing showing the possible environment (dominated by organisms from the Phylum Cnidaria, Class Hydrozoa, Order Hydroida) suggested by palynofacies analysis of the Suèges, Caylus and Pont de Suert sedimentary sections (Mendonça Filho et al., 2016 *Ineditus in efficiendis*).

V.3. Thermal Maturity

Several thermal markers such as OM reflectance, λ_{max} and SCI can be used to assess the thermal maturity of the dispersed OM in sediments of the three studied basins. Data obtained through these parameters presented similar values for the Suèges and Caylus sections but entirely different results for the Pont de Suert section, that confirm different thermal maturity evolutions.

V.3.1. Suèges section – Grands Causses Basin

For the Suèges section (GCB), and according to Fisher et al. (1980) and Mukhopadhyay (1994), VR_{eq} shows a good correlation with SCI values for sample S10

(Table IV.4). Spectral fluorescence data for the majority of the samples shows a λ_{max} value of 560nm, demonstrating a good correlation with SCI (Mukhopadhyay, 1994) (Table IV.4). When R_{eq} values determined through SCI (Fisher et al., 1980) are compared with vitrinite reflectance values determined through λ_{max} (Mukhopadhyay, 1994), is observed a shift of the fluorescence spectrum data to red wavelengths. For the majority of samples Q ratio ranges between 0.60 and 0.78 which, according to Taylor et al. (1998), is in agreement with SCI values (Table IV.4). Sample S12 is characterized by a lower λ_{max} value (510nm) which does not match with SCI data (Mukhopadhyay, 1994). The Q ratio for this sample is 0.53, corresponding to a vitrinite reflectance (R_r) value of about 0.45% (Taylor et al., 1998), being therefore in accordance with the R_{eq} value of Fisher et al. (1980). These data indicate that the majority of the samples from the Suèges section are in the immature to early mature evolution stages with the exception of samples S12 and S10 which are in the immature stage, taking into account the OM reflectance and λ_{max} values (Tissot and Welte, 1984; Hartkopf-Fröder et al., 2015). These results are in agreement with Rock-Eval Pyrolysis published data for samples from the Schistes Cartons Fm. of the Rivière-sur-Tarn Group presenting a T_{max} value of 420º-430ºC (Qajoun, 1994) and for the Marnes de Villeneuve and Schistes Cartons formations in the Saint-Paul-des-Fonts and Tournadous sections with average T_{max} values of 425ºC and 426ºC, respectively (Mailliot et al., 2009).

V.3.2. Caylus section – Quercy Basin

For the Caylus section (QB) spectral fluorescence data was only acquired for samples Cay 26 and Cay 28, presenting similar values for both parameters, a λ_{max} value of 560nm and Q ratio ranging between 0.59 and 0.60 (Table IV.5). These values show a good correlation of λ_{max} with SCI according to Mukhopadhyay (1994). When R_{eq} values determined through SCI (Fisher et al., 1980) are compared with vitrinite reflectance values determined through λ_{max} (Mukhopadhyay (1994), is detected a shift of the fluorescence spectrum data to red wavelengths, as observed in samples from the Suèges sections (Table IV.5). SCI and fluorescence spectrum data indicate that the majority of the samples from the Caylus section are in the immature to early mature evolution stages (Tissot and Welte, 1984; Hartkopf-Fröder et al., 2015). These results show a good correlation with Rock-Eval Pyrolysis data of Qajoun (1994) that presents a T_{max} value of 420º-429ºC for samples from the Schistes Cartons Mb. of the Penne Fm.

The discrepancies between λ_{max} and SCI and R_{eq} values for λ_{max} of 560nm observed in both sections maybe related to a shift to red wavelengths already described by Stasiuk (1994) and Araujo et al. (2014). In the former, authors suggest that the proposed correlation

between vitrinite reflectance and λ_{max} of Mukhopadhyay (1994) is flawed at higher thermal maturities for prasinophytes, possibly due to differences in fluorescence changes with increasing maturation for distinct type algae that contribute to alginite. The results of this study seem to support Araujo et al. (2014), although it should be taken into account that OM reflectance was determined in only one sample and that SCI is a very subjective technique. Furthermore, OM reflectance was measured in hydroids and the equivalent vitrinite reflectance was obtained by a correlation determined for OM from Ordovician and Silurian sediments.

V.3.3. Pont de Suert section – Pyrenean Basin

For the Pont de Suert section (PB) VR_{eq} converted from zoomorph reflectance shows lower values than those determined through SCI (Table IV.6) (R_{eq}=0.90%-1.20% according to Fisher et al., 1980). Nevertheless, VR_{eq} is considered reliable and acceptable to set the thermal evolution stage. Furthermore, HR_r values also present a good correlation with SCI (Table IV.6). Equivalent vitrinite reflectance determined through hydroid reflectance (< 1.04% for all samples) presents very low values when compared to SCI according to Mukhopadhyay (1994). SCI and OM reflectance data indicate that all samples from Pont de Suert section are in late mature to post mature evolution stages (Tissot and Welt, 1984; Hartkopf-Fröder et al., 2015).

Suèges and Pont de Suert OM reflectance data seem to show a good correlation between hydroid reflectance and other rank parameters as well as VR_{eq} values determined through the equation for conversion of hydroid reflectance into equivalent vitrinite reflectance proposed by Bertrand and Malo (2012) and Hartkopf-Fröder et al. (2015).

Chapter VI - Final Remarks

VI.1. Conclusions

The results of this study bring new paleoenvironmental evidences for the T-OAE recorded in the Grands Causses, Quercy and Pyrenean basins. The studied sections present slight differences in their paleoenvironmental depositional contexts which further demonstrates that, although the T-OAE has a global character, in these basins that developed as part of the Toarcian European epicontinental seaway, it is controlled by local mechanisms, namely its geomorphology and paleogeography.

In the Grands Causses Basin, the late Pliensbachian is characterized by low TOC content (0.6 wt.%), low percentages of AOM and high percentages of phytoclasts (21.9%) and terrestrial palynomorphs (*Classopollis* ssp.), indicating an oxygenated water body proximal to the terrestrial source area under an arid climate, with some marine influence (marine palynomorphs - 10.0%). The lattermost Pliensbachian presents low TOC content (0.9 wt.%) and a decrease of the marine influence which coupled with high AOM and zooclasts percentages reveal a shallowing of the water column. A decrease in phytoclasts (10.2%) indicates a separation from the terrestrial source area related with aridity conditions. From the Tenuicostatum to the earliest Serpentinum zones (early Toarcian) the palynofacies is dominated by AOM (97.5%) that coupled with high TOC content (5.7 wt.%) indicate a restricted and stagnated environment with partial closure of the basin (highest restriction interval). Dysoxic to anoxic conditions associated with water column stratification develop under an arid climate. From the middle to late Serpentinum Zone (early Toarcian) occurs the reestablishment of the oxygen levels and of the paleoceanographic circulation (decrease in TOC content and AOM and proliferation of marine palynomorphs) under a less arid climate.

In the Quercy Basin, late Pliensbachian to the earliest Toarcian (Paltus Subzone) is characterized by low TOC content (0.2 wt.%) that together with high percentage of amorphous zoomorphs (hydrozoans) and hydrozoans in their medusae form indicate that sedimentation occurred in a shallow proximal water body in oxic to dysoxic conditions (oxygen level stratification), with high alkalinity. Low percentage of phytoclasts and terrestrial components indicate a very proximal water body separated from the terrestrial source area related with aridity conditions (highest restriction interval), with episodic emersion. From the Semicelatum Subzone to Serpentinum Zone occurs a more effective non-carbonate sedimentation (maximum CaCO3 content of 18.0%) that together with high TOC content (4.2 wt.%) and presence of amorphous hydrozoans (92.8%) indicate a high water level and the development of dysoxic to anoxic conditions associated with water column stratification. The lattermost Serpentinum Zone is

characterized by higher $CaCO_3$ content that coupled with high AOM percentage demonstrate a shallowing of the water column with higher alkalinity. The presence of oxidized zooclasts together with low TOC content (0.3 wt.%) indicate the development of a more oxidizing environment. This increase in oxygen is demonstrated by the presence of bacterial AOM (primary productivity). The contemporary increment of AOM percentage and oxygen levels is due to a stratification of the restricted water body in terms of oxygen levels.

In the Pyrenean Basin, from the late Pliensbachian to the base of Semicelatum Subzone, from the Elegantum to the base of the Falciferum subzones and from the top of the Falciferum to the base of the Sublevisoni subzones, the palynofacies is characterized by very high percentages of zooclasts (possible Hydrozoan polypoid forms) and low proportion of amorphous zoomorphs (Hydrozoan free-swimming medusoid forms), which are indicative of an oxidizing environment indicating a well oxygenated proximal water body with marine influence (marine microplankton). From the Semicelatum to the base of the Elegantum subzones and in the Falciferum Subzone, occurs a decrease in the relative proportion of zooclasts and an increase in the prevalence of amorphous zoomorphs indicating a shallowing of the water column leading to a more restricted and stagnated environment. This water level fluctuations are possibly due to variations of the precipitation and evaporation rates according to climatic oscillations.

The record of particulate OM in the upper Pliensbachian – lowermost middle Toarcian sedimentary successions of the Grands Causses, Quercy and Pyrenean basins revealed the presence of components from the Phylum Cnidaria, Class Hydrozoa, Order Hydroida. Therefore, this study represents the description of the first occurrence of these organisms in organopalynological preparations, namely the medusoid forms, in sediments from the Lower Jurassic.

These organisms represent shallow, freshwater, oxygenated continental systems, with a significant contribution of primary bioproductivity (primary producers, bottom of the food chain), primary consumers (microcrustaceans, protozoa, etc., middle of the food chain), and secondary consumers (hydroids) at the top of the low energy food chain for this system. They occur as the most predominant constituent in all studied samples. Fragments of colonial and non-colonial sessile polypoid forms and free-swimming medusoid forms at all stages of development (embryo stage, young and adult polyps, mature forms) represent them.

The predominance of this kind of particulate constituent of the organic matter, through palynofacies analysis (Zoomorph Subgroup), confirms the character related to

the development environment of these organisms (shallow, oxygenated, variable alkalinity and salinity: fresh-brackish water, reaching saline levels). Nevertheless, changing conditions in the depositional environment seem to be more related to climate influence and the geomorphological framework (restriction conditions) of each basin. Changes in palynofacies assemblages are mainly associated to the organic components preservation state and the polymorphic aspect of these organisms life cycle (alternation between polypoid and medusae forms). Thus, changes in the oxygen regimen, mainly at the bottom of the water column are a consequence of evaporative processes (arid climate) and freshwater inflow (humid climate), inducing variations in the salinity levels that lead to the establishment of a stratified water column. In this sense, temperature and humidity could have been the main factors to influence the environmental conditions.

Exposure surface feature is another contributing important factor for paleoenvironmental characterization. The presence of organic matter displaying oxidation aspects can be related to pedogenic alteration. This attribute can represent a maximum shallowing system, supporting the idea of a cyclical shallowing-deepening behavior for this system, namely in the Caylus section from the QB.

The thermal maturity assessment study shows that the majority of the samples from the Suèges (GCB) and Caylus (QB) sections are in the immature to early mature evolution stages and that all samples from Pont de Suert section (PB) are in late mature to post mature evolution stages. Therefore, this study supports a very similar thermal evolution for the Grands Causses and Quercy basins and an entirely different thermal history for the Pyrenean basin. Furthermore, it is presented the first OM reflectance measurements performed in Jurassic hydroids showing a good correlation with other rank parameters as well as VR_{eq} values determined through the equation for conversion of hydroid reflectance into equivalent vitrinite reflectance proposed by Bertrand and Malo (2012).

VI.2. Future Works

This work presents new evidences for the organic facies characterization of sediments from the T-OAE of the three studied basins of southern France. Nonetheless, further studies are needed to improve the knowledge and discussion of these subjects.

To validate the paleoenvironmental reconstruction is recommended the comparison of the results obtained in this study with mineralogical (clay assemblages), palaeontological and inorganic geochemical data.

To determine the Hydroid chemical composition is proposed the use of the Laser Micropyrolysis-Gas Chromatography/Mass Spectrometry technique in order to identify the specific chemical biomarkers of these animal components.

Hydroid polypoid form fragments were recorded reaching more than 1000 μm (1.0 mm) in length. Thus, these organisms could possibly be identified in microscopic examination of thin sections.

For the Pyrenean Basin study is recommended a more detailed sampling pattern for the determination of lower ranking sea level cycles of the succession.

New palynofacies studies in the Paris and German basins in the light of the more recent classification system for particulate OM, especially due to the incorporation and identification of Hydroids. This could lead to new evidences for the geodynamic evolution model of the European epicontinental seaway during the upper Pliensbachian – lowermost middle Toarcian (Lower Jurassic).

References

Alpern, B., Cheymol, D., 1978. Réflectance et fluorescence des organoclastes du Toarcien du Bassin de Paris en fonction de la profondeur et de la temperature. Rev. Inst. Fr. Pet. 33, 515-535.

Al-Suwaidi, A.H., Angelozzi, G.N., Baudin, F., Damborenea, S.E., Hesselbo, S.P., Jenkyns, H.C., Manceñido, M.O., Riccardi, A.C., 2010. First record of the Early Toarcian Oceanic Anoxic Event from the Southern Hemisphere, Neuquén Basin, Argentina. Journal of the Geological Society 167, 633-636.

Andreu, B., Qajoun, A., Cubaynes, R., 1995. Ostracodes du Toarcien du Quercy (Bassin d'Aquitaine, France): Systématique, Biostratigraphie et Paleobiogeographie. Geobios 28, 2: 209-240.

Araujo, C.V., Barbanti, S.M., Condé, V.C., Kalkreuth, W., Macedo, A.C., Newman, J., Pickel, W., Stasiuk, L., Volk, H., 2003. Thermal Indices Working Group: Summary of the 2002 Round Robin Exercise. ICCP News 29, 5–12. ISSN 1445-4858. http://www.iccop.org/publications/iccpnews/ (accessed 13th March 2016)

Araujo, C.V., Borrego, A.G., Cardott, B., Chagas, R.B.A., Flores, D., Gonçalves, P., Hackley, P.C., Hower, J.C., Kern, M.L., Kus, J., Mastalerz, M., Mendonça Filho, J.G., Mendonça, J.O., Menezes, T.R., Newman, J., Suarez-Ruiz, I., Silva, F.S., Souza, I.V., 2014. Petrographic maturity parameters of a Devonian shale maturation series, Appalachian Basin, USA. ICCP Thermal Indices Working Group interlaboratory exercise. International Journal of Coal Geology 130, 89-101.

Araujo, C.V., Kalkreuth, W., Stasiuk, L., Pickel, W., Newman, J., Condé, V.C., 2002. Interlaboratory Studies on Thermal Indices of Torbanite Samples from Australia. 8th Latin American Congress on Organic Geochemistry, Cartagena, Colombia, 31–34.

Arthaud, F., Matte, P., 1975. Les décrochements tardi-hercyniens du Sud-Ouest de l'Europe. Géométrie et essai de reconstitution des conditions de la déformation. Tectonophysics 25, 139–171.

ASTM D4239, 2008. Standard Test Methods for Sulfur in the Analysis Sample of Coal and Coke Using High-Temperature Tube Furnace Combustion Methods, ASTM International, West Conshohocken, PA, 8 pp.

ASTM D7708, 2014. Standard Test Method for Microscopical Determination of Reflectance of Vitrinite Dispersed in Sedimentary Rocks. ASTM International, West Conshohocken, PA, 10 pp.

Baranger, R., Martinez, L., Pittion, J.L., Pouleau, J., 1991. A new calibration procedure for fluorescence measurements of sedimentary organic matter. Org. Geochem. 17 (4), 467–475.

Bernadou, S., 2015. La série du passage Lias-Dogger dans les Pyrénées: Organisation géométrique, variations faciologiques et paléoenvironnementales, facteurs de contrôle. Mémoire de Master 2 Terre et Planète, Toulouse (France).

Bertrand, R., 1987. Maturation thermique et potentiel pétroligène des séries post-taconiennes du nord-est de la Gaspésie et de l'île d'Anticosti (Canada). Thèse de doctorat en sciences, Faculté des Sciences de l'Université de Neuchâtel.

Bertrand, R., 1990. Maturation thermique et histoire de l'enfouissement et de la génération des hydrocarbures du bassin de l'archipel de Mingan et de l'île d'Anticosti, Canada. Can. J. Earth Sci. 27, 731–741.

Bertrand, R., 1993. Standardization of solid bitumen reflectance to vitrinite in some Paleozoic sequences of Canada. Energy Sources 15, 269–287.

Bertrand, R., Chagnon, A., Malo, M., Duchaine, Y., Lavoie, D., Savard, M.M., 2003. Sedimentologic, diagenetic and tectonic evolution of the Saint-Flavien gas reservoir at the structural front of the Quebec Appalachians. Bulletin of Canadian Petroleum Geology 51, 126–154.

Bertrand, R., Malo, M., 2005. Maturation thermique, potentiel roche mère des roches ordoviciennes à dévoniennes du Nord-Ouest du Nouveau-Brunswick. Commission Géologique du Canada, Dossier Public 4886, 1–85.

Bertrand, R., Malo, M., 2012. Dispersed organic matter reflectance and thermal maturation in four hydrocarbon exploration wells in the Hudson Bay Basin: regional implications. Geological Survey of Canada Open File 7066, 1–52.

Bjerrum, C.J., Surlyk, F., 2001. Numerical Paleoceanographic Study of the Early Jurassic Transcontinental Laurasian Seaway. Paleoceanography 16 (4), 390-404.

Boix, C., Perez, R., 2003. The Position of the South Pyrenean Margin in the Late Cretaceous: Evidence for Larger Foraminifera. AAPG International Conference, Barcelona, Spain, 5 pp.

Bordenave, M.L., Espitalié, L., Leplat, P., Oudin, J.L., Vandenbroucke, M., 1993. Screening techniques for source rock evaluation, in: Bordenave, M.L. (Ed.), Applied Petroleum Geochemistry. Editions Technip, Paris, pp. 217 - 278.

Bostick, N.H., 1971. Thermal alteration of clastic organic particles as an indicator of contact and burial metamorphism in sedimentary rocks. Geoscience and Man, Baton Roude, 3, 83-92.

Bouillon, J., Gravili, C., Pagès, F., Gili, J.M., Boero, F., 2006. An Introduction to Hydrozoa. Paris, France: Publications Scientifiques du Muséum, 194, pp. 1-593.

Brusca, R., Brusca, G., 2003. Invertebrates. Sunderland, Massachusetts, USA: Sinauer Associates, Inc.

Caruthers, A.H., Gröcke, D.R., Smith, P.L., 2011. The significance of an Early Jurassic (Toarcian) carbon-isotope excursion in Haida Gwaii (Queen Charlotte Islands), British Columbia, Canada. Earth and Planetary Science Letters 307, 19-26.

Caswell, B.A., Coe, A.L., 2012. A high-resolution shallow marine record of the Toarcian (Early Jurassic) Oceanic Anoxic Event from the East Midlands Shelf, UK. Palaeogeography, Palaeoclimatology, Palaeoecology 365-366, 124-135.

Cohen, A.S., Coe, A.L., Harding, S.M., Schwark, L., 2004. Osmium isotope evidence for the regulation of atmospheric CO_2 by continental weathering. Geology 32 (2), 157-160.

Combaz, A., 1964. Les palynofaciès. Revue de Micropaléontologie 7, 205-218.

Cubaynes, R., 1986. Le Lias du Quercy méridional. Etude litholgique, biostratigraphie, paléoécologie et sédimentologie. Strata (2), 6, 574 pp.

Cubaynes, R., Faure, P., Hantzpergue, P., Pelissie, T., Rey, J., 1989. Le Jurassique du Quercy: unités lithostratigraphiques, stratigraphie et organisation séquentielle, évolution sédimentaire. Géologie de la France 3, 33-62.

Dera, G., Pucéat, E., Pellenard, P., Neige, P., Delsate, D., Joachimski, M.M., Reisberg, L., Martinez, M., 2009. Water mass exchange and variations in seawater temperature in the NW Tethys during the Early Jurassic: Evidence from neodymium and oxygen isotopes of fish teeth and belemnites. Earth and Planetary Science Letters 286, 198-207.

Disnar, J.R., 1996. A comparison of mineralization histories for two MVT deposits, Trèves and Les Malines (Causses basin, France), based on the geochemistry of associated organic matter. Ore Geology Reviews 11, 133-156.

Disnar, J.R., Strat, P.L., Farjanel, G., Fikri, A., 1996. Sédimentation de la matière organique dans le nord-est du Bassin de Paris: conséquences sur le dépôt des argilites carbonées du Toarcien inférieur. Chemical Geology 131, 15-35.

Dumont, T., 1988. Late Triassic-early Jurassic evolution of the western Alps and of their European foreland; initiation of the Tethyan rifting. Bull. Soc. Géol. France 4, 601-611.

Duncan, R.A., Hooper, P.R., Rehacek, J., Marsh, J.S., Duncan, A.R., 1997**.** The timing and duration of the Karoo igneous event, southern Gondwana. Journal of Geophysical Research 102 (B8), 18127-18138.

Dunn, C., 2009. Siphonophores. Current Biology 19 (6), 233-234.

Durand, B., 1980. Sedimentary organic matter and kerogen. Definition and quantitative importance of kerogen. Chapter 1, in: Durand, B. (Ed.), Kerogen - Insoluble organic matter from sedimentary rocks. Editions Technip, Paris, pp. 13 - 34.

Durand, B., Espitalié, J., Nicaise, G., Combaz, A., 1972. Etudes de la matière organique insoluble (kérogène) des argiles du Toarcien. Rev. Inst. Fr. Pét. 27, 865-884.

Eisenack, A., 1932. Neue Mikrofossilien des Baltischen Silurs II. Ibidem 14 (4), 257-277.

Eisenack, A., 1934. Neue Mikrofossilien des baltischen Silurs III und neue Mikrofossilien des böhmischen Silurs I. Paläeontologische Zeitschrift 16 (1-2), 52-76.

Eisenack, A., 1935. Mikrofossilien aus Doggergeschieben Ostpreussens. Zeitschrift für Geschiebeforschung 11, 167-184.

Emmanuel, L., Renard, M., Cubaynes, R., de Rafelis, M., Hermoso, M., Lecallonnec, L., Le Solleuz, A., Rey, J., 2006. The “Schistes Carton” of Quercy (Tarn, France): a lithological signature of a methane hydrate dissociation event in the early Toarcian. Implications for correlations between Boreal and Tethyan realms. Bull. Soc. Géol. France 177 (5), 239- 249.

Fauré, F., 2002. Le Lias des Pyrénées. Strata (2), 39, 761 pp.

Fisher, M.J., Barnard, P.C., Cooper, B.S., 1980. Organic maturation and hydrocarbon generation in the Mesozoic sediments of the Sverdrup Basin, Arctic Canada. Proceedings IV International Palynological Conference, Lucknow (1976–77), 2, 581–588.

Frimmel, A., Oschmann, W., Schwark, L., 2004. Chemostratigraphy of the Posidonia Black Shale, SW Germany I. Influence of sea-level variation on organic facies evolution. Chemical Geology 206, 199-230.

Gómez, J.J., Goy, A., Canales, M.L., 2008. Seawater temperature and carbon isotope variations in belemnites linked to mass extinction during the Toarcian (Early Jurassic) in Central and Northern Spain. Comparison with other European sections. Palaeogeography, Palaeoclimatology, Palaeoecology 258 (1-2), 28-58.

Gonçalves, P.A., Mendonça Filho J.G., Mendonça, J.O., Flores, D., 2014. The presence of zooclasts and zoomorphs in the carbonate Candeeiros formation (Arruda sub-basin, Lusitanian Basin, Portugal): paleoenvironmental evidence. Comunicações Geológicas 101, Especial I, 439-442.

Graciansky, P.C., Dardeau, G., Dommergues, J.L., Durlet, C., Marchand, D., Dumont, T., Hesselbo, S.P., Jacquin, T., Goggin, V., Meister, C., Mouterde, R., Rey, J., Vail, P., 1998. Ammonite biostratigraphic correlation and early Jurassic sequence stratigraphy in France: comparisons with some UK sections, in*:* de Graciansky, P.C., Hardenbol, J., Jacquin, T., Vail, P.R. (Eds.), Mesozoic and Cenozoic Sequence Stratigraphy of European Basins, SEPM Special Publication 60, 583–621.

Gröcke, D.R., Hori, R.S., Trabucho-Alexandre, J., Kemp, D.B., Schwark, L., 2011. An open ocean record of the Toarcian oceanic anoxic event. Solid Earth 2, 245-257.

Grohmann, P.A., 2008. Bioincrustation caused by a hydroid species in the turbine cooling system at the Funil Hydroeletric power plant, Itatiaia, Rio de Janeiro, Brazil. Naturalia 31, 1-7.

Guex, J., Morard, A., Bartolini, A., 2001. Découverte d'une importante lacune stratigraphique à la Domérien-Toarcien: implications paléo-océanographiques. Bulletin de la Société Vaudoise des Sciences Naturelles 87.3, 277-284, http://dx.doi.org/10.5169/seals-28140.

Gutierre, S.M.M., 2012. pH tolerance of the biofouling invasive hydrozoan *Cordylophora caspia*. Hydrobiologia 679(1), 91-95.

Harazim, D., van de Schootbrugge, B., Sorichter, K., Fiebig, J., Weug, A., Suan, G., Oschmann, W., 2013. Spatial variability of watermass conditions within the European Epicontinental Seaway during the Early Jurassic (Pliensbachian-Toarcian). Sedimentology 60, 359-390, http://dx.doi.org/10.1111/j.1365-3091.2012.01344.x.

Hartkopf-Fröder, C., Königshof, P., Littke, R., Schwarzbauer, J., 2015. Optical thermal maturity parameters and organic geochemical alteration at low grade diagenesis to anchimetamorphism: A review. International Journal of Coal Geology 150-151, 74-119, http://dx.doi.org/10.1016/j.coal.2015.06.005.

Hermoso, M., Minoletti, F., Pellenard, P., 2013. Black shale deposition during Toarcian super-greenhouse driven by sea level. Climate of the Past 9, 2703-2712.

Hermoso, M., Minoletti, F., Rickaby, R.E.M., Hesselbo, S.P., Bausin, F., Jenkyns, H.C., 2012. Dynamics of a stepped carbon-isotope excursion: Ultra high-resolution study of Early Toarcian environmental change. Earth and Planetary Science Letters 319-320, 45-54.

Héroux, Y., Chagnon, A., 1994. Pétrographie de la matière organique et assemblages des minéraux des argiles du district minier et de la région de Pine Point, Canada: une caractérisation des anomalies associées aux gîtes. Exploration and Mining Geology 3, 53–65.

Héroux, Y., Chagnon, A., Savard, M., 1996. Organic matter and clay anomalies associated with base-metal sulfide deposits. Ore Geology Reviews 11, 157–173.

Héroux, Y., Chagnon, A., Dewing, K., Rose, H.R., 2000. The carbonate-hosted base-metal sulphide Polaris deposit in the Canadian Arctic: Organic matter alteration and clay diagenesis, in: Glikson, M., Mastalerz, M. (Eds.), Organic Matter and Mineralisation: Thermal Alteration, Hydrocarbon Generation and Role in Metallogenesis. Kluwer Academic Publishers, Dordrecht, pp. 260–295.

Hesselbo, S.P., Gröcke, D.R., Jenkyns, H.C., Bjerrum, C.J., Farrimond, P., Morgans Bell, H.S., Green, O.R., 2000. Massive dissociation of gas hydrate during a Jurassic oceanic event. Nature 406, 392–395.

Hesselbo, S.P., Jenkyns, H.C., Duarte, L.V., Oliveira, L.C.V., 2007. Carbon-isotope record of the Early Jurassic (Toarcian) Oceanic Anoxic Event from fossil wood and marine carbonate (Lusitanian Basin, Portugal). Earth Planetary Science Letters 253, 455–470.

Hollander, D.J., Bessereau, G., Belin, S., Huc, A.Y., Houzay, J.P., 1991. Organic Matter in the Early Toarcian Shales, Paris Basin, France: a Response to Environmental Changes. Rev. Inst. Fr. Pet. 46, 543-562.

Huc, A.Y., 1977. Contribution de la géochemie organique à une esquisse paléoécologique des schistes bitumineux de Toarcien de l'est du bassin de Paris. Étude de la matiére organique insoluble (kérogène). Rev. Inst. Fr. Pét. 32 (5), 703-718.

Huchriede, H., Meischner, D., 1996. Origin and environment of manganese-rich sediments within black-shale basins. Geochimica et Cosmochimica Acta 60 (8), 1399-1413.

Hunt, J.M., 1995. Petroleum geochemistry and geology. W.H. Freeman and Company, New York, 743 pp.

ISO 7404-5, 2009. Methods for the petrographic analysis of coals – Part 5: Method of determining microscopically the reflectance of vitrinite, International Organization for Standardization, 14 pp.

Izumi, K., Miyaji, T., Kazushige, T., 2012. Early Toarcian (Early Jurassic) oceanic anoxic event recorded in the shelf deposits in the northwestern Panthalassa: Evidence from the Nishinakayama Formation in the Toyora area, west Japan. Palaeogeography, Palaeoclimatology, Palaeoecology 315-316, 100-108.

Jankowski, T., Collins, A., Campbell, R., 2008. Global diversity of inland water cnidarians, in: Balian, E., Lévêque, C., Segers, H., Martens K. (Eds.), Freshwater Animal Diversity Assessment. Dordrecht. The Netherlands: Springer Netherlands, pp. 35-40.

Jarvie, D.M., 1991. Total Organic Carbon (TOC) analysis, in: Merril, R.K. (Ed.), Source and Migration Processes and Evaluation Techniques, Tulsa, Treatise of Petroleum Geology. American Association of Petroleum Geologists, pp. 113 - 118.

Jenkyns, H.C., 1985. The Early Toarcian and Cenomanian-Turonian anoxic events in Europe: comparisons and contrasts. Geologische Rundschau 74, 505-18.

Jenkyns, H.C., 1988. The Early Toarcian (Jurassic) Anoxic Event: stratigraphic, Sedimentary and Geochemical Evidence. American Journal of Science 288, 101-151.

Jenkyns, H.C., 2003. Evidence for rapid climate change in the Mesozoic-Palaeogene greenhouse world. Philosophical Transaction of the Royal Society of London A 361, 1885-1916.

Jenkyns, H.C., 2010. Geochemistry of oceanic anoxic events. Geochemistry, Geophysics, Geosystems 11, Q03004, http://dx.doi.org/10.1029/2009GC002788.

Jenkyns, H.C., Géczy, B., Marshall, J.D., 1991. Jurassic manganese carbonates of Central Europe and the Early Toarcian anoxic event. Journal of Geology 99 (2), 197-149.

Johnson, J.A., Hall, C.A., 1989. The structural and sedimentary evolution of the Cretaceous North Pyrenean Basin, southern France. Geological Society of America Bulletin 101, 231- 247.

Jourdan, F., Féraud, G., Bertrand, H., Kampunzu, A.B., Tshoso, G., Watkeys, M.K., Gall, B.L., 2005. Karoo large igneous province: Brevity, origin, and relation to mass extinction questioned by new $^{40}Ar/^{39}Ar$ age data. Geology 33 (9), 745-748.

Kozlowski, R., 1959. Les hydroïdes ordoviciens à squelette chitineux. Acta Palaeontologica Polonica 4 (3), 14-271.

Küspert, W., 1982. Environmental Changes During Oil Shale Deposition as Deduced from Stable Isotope Ratios, in: Einsele, G., Seilacher, A. (Eds.), Cyclic and Event Stratification, Springer Berlin Heidelberg, Part III, pp. 482-501.

Lemoine, M., de Graciansky, P.C., 1988. History of a passive continental-margin – The Eastern Alps in the Mesozoic. Bull. Soc. Géol. France 4, 597-600.

Lézin, C., Andreu, B., Pellenard, P., Bouchez, J., Emmanuel, L., Fauré, P., Landrein, P., 2013. Geochemical disturbance and paleoenvironmental changes during the Early Toarcian in NW Europe. Chemical Geology 341, 1-15, http://dx.doi.org/10.1016/j.chemgeo.2013.01.003.

Lézin, C., Fauré, P. (unpublished). Caylus section stratigraphic log.

Lézin, C., Fauré, P. (unpublished). Pont de Suert section stratigraphic log.

Lézin, C., Fauré, P. (unpublished). Suèges section stratigraphic log.

Lézin, C., Rey, J., Faure, P., Cubaynes, R., Pelissie, T., Durlet, C., Deconinck, J., 2007. Tectono-biosedimentary recordings at the Lias-Dogger transition: example of the Quercy carbonate platform (Aquitaine Basin, France). Bull. Soc. Géol. France 178 (4), 275-291.

Littke, R., Baker, D.R., Leythaeuser, D., 1987. Microscopic and sedimentologic evidence for the generation and migration of hydrocarbons in Toarcian source rocks of different maturities. Org. Geochem. 13 (1-3), 549-559.

Littke, R., Baker, D.R., Leythaeuser, D., Rullkötter, J., 1991. Keys to the depositional history of the Posidonia Shale (Toarcian) in the Hils Syncline, northern Germany, in: Tyson, R.V., Pearson, T.H. (Eds.), Modern and Ancient Continental Shelf Anoxia, Geological Society Special Publication 58, pp. 311-333.

Mailliot, S., Mattioli, E., Bartolini, A., Baudin, F., Pittet, B., Guex, J., 2009. Late Pliensbachian-Early Toarcian (Early Jurassic) environmental changes in an epicontinental basin of NW Europe (Causses area, central France): A micropaleontological and geochemical approach. Palaeogeography, Palaeoclimatology, Palaeoecology 273, 346-364, http://dx.doi.org/10.1016/j.palaeo.2008.05.014.

Mazzini, A., Svensen, H., Leanza, H.A., Corfu, F., Planke, S., 2010. Early Jurassic shale chemostratigraphy and U-Pb ages from the Neuquén Basin (Argentina): Implications for the Toarcian Oceanic Anoxic Event. Earth and Planetary Science Letters 297, 633-645 http://dx.doi.org/10.1016/j.epsl.2010.07.017.

McArthur, J.M., Algeo, T.J., van de Schootbrugge, B., Li, Q., Howarth, R.J., 2008. Basinal restrictions, black shales, Re-Os dating, and the Early Toarcian (Jurassic) oceanic anoxic event. Paleoceanography 23, PA4217, http://dx.doi.org/10.1029/2008PA001607.

Mendonça Filho, J.G., 1999. Aplicação de estudos de palinofácies e fácies Orgânica em rochas do Paleozoico da Bacia do Paraná, Sul do Brasil, Universidade Federal do Rio Grande do Sul, PhD Thesis, 338 pp.

Mendonça Filho, J.G. Menezes, T.R., Mendonça, J.O., Oliveira, A.D., Carvalho, M.A., Sant'Anna, A.J.; Souza, J.T., 2010a. Palinofácies, in: Carvalho, I.S. (Ed.), Paleontologia, Rio de Janeiro, Interciência 2, pp. 379-413.

Mendonça Filho, J.G., Chagas, R.B.A., Menezes, T.R., Mendonça, J.O., Silva, F.S., Sabadini-Santos, E., 2010b. Organic facies of the Oligocene lacustrine system in the Cenozoic Taubaté basin, Southern Brazil. International Journal of Coal Geology 84, 166-178, http://dx.doi.org/10.1016/j.coal.2010.07.004.

Mendonça Filho, J.G., Menezes, T.R., Mendonça, J.O., Oliveira, A.D., Santanna, A.J., 2011a. Kerogen: Composition and Classification, in: Flores, D., Marques, M. (Org.), 4th ICCP Training Course on Dispersed Organic Matter, (ISBN nº 978-989-8265-67-8) ed. Plenimagem. 2011, Chapter 3, pp. 17-23.

Mendonça Filho, J.G., Menezes, T.R., Mendonça, J.O., Chagas, R.B.A., 2011b. Techniques used in the Kerogen Study, in: Flores, D., Marques, M. (Org.), 4th ICCP Training Course on dispersed Organic Matter, (ISBN nº 978-989-8265-67-8) ed. Plenimagem. 2011, Chapter 4, pp. 25-31.

Mendonça Filho, J.G., Menezes, T.R., Mendonça, J.O., 2011c. Organic Composition (Palynofacies Analysis), in: Flores, D., Marques, M. (Org.), 4th ICCP Training Course on Dispersed Organic Matter, (ISBN nº 978-989-8265-67-8) ed. Plenimagem. 2011, Chapter 5, pp. 33-81.

Mendonça Filho, J.G., Menezes, T.R., Mendonça, J.O., Oliveira, A.D., Silva, T.F., Rondon, N.F., Silva, F.S., 2012. Organic facies: Palynofacies and organic geochemistry approaches, in: Panagiotaras, D., (Ed.) Geochemistry - Earth's system processes. InTech, Rijeka, pp 211–248.

Mendonça Filho, J.G., Menezes, T.R., Mendonça, J.O., Oliveira, A.D., 2014a. Kerogen: Composition and Classification. 7th ICCP Training Course on Dispersed Organic Matter, GFZ (Deutsches GeoForschungsZentrum), Potsdam, Germany. 2014, Chapter 3, pp. 17- 24.

Mendonça Filho, J.G., Menezes, T.R., Mendonça, J.O., 2014b. Techniques used in the Kerogen Study. 7th ICCP Training Course on Dispersed Organic Matter, GFZ (Deutsches GeoForschungsZentrum), Potsdam, Germany. 2014, Chapter 4, pp. 25-35.

Mendonça Filho, J.G., Menezes, T.R., Mendonça, J.O., 2014c. Organic Composition (Palynofacies Analysis). 7th ICCP Training Course on Dispersed Organic Matter, GFZ (Deutsches GeoForschungsZentrum), Potsdam, Germany. 2014, Chapter 5, pp. 36-89.

Mendonça Filho, J.G., Oliveira, A.D., Souza, J.T., Mendonça, J.O., Barbosa, T.S., 2016. First occurrence of polypoid and medusoid forms of cnidarians (Class Hydrozoa, Order Hydroida) in organic matter concentrate: a case study for carbonate systems (*Ineditus in efficiendis*).

Mills, C.E., 1999-2009. Bioluminescence of Aequorea, a hydromedusa. Electronic internet document. Available at published by the author, web page established June 1999, last updated 11 January 2009 (http://faculty.washington.edu/cemills/Aequorea.html).

Morard, A., 2004. Les événements du passage Domérien-Toarcien entre Téthys occidentale et Europe du Nord-Ouest. Thèse, Université Lausanne, Géologie - Paléontologie, 158 pp.

Morard. A., Guex, J., Bartolini, A., Morettini, E., de Wever, P., 2003. A new scenario for the Domerian-Toarcian transition. Bull. Soc. Géol. Fr. 174 (4), 351-356.

Morris, K.A., 1980. Comparison of major sequences of organic-rich mud deposits in the British Jurassic. J. Geol. Soc. London 137, 157-170.

Mukhopadhyay, P.K., 1994. Vitrinite reflectance as a maturity parameter: petrographic and molecular characterization and its applications to basin modeling, in: Mukhopadhyay, P.K., Dow, W.D. (Eds.), Vitrinite reflectance as a maturity parameter: applications and limitations. American Chemical Society, Washington, pp. 1-24.

Müller, G., Blaschke, R., 1969. Zur Entstehung des Posidonienschiefers (Lias epsilon). Naturwiss. 12, 635-636.

NCEA-C-1282, 2002**.** Methods for the Determination of Total Organic Carbon (TOC) in Soils and Sediments. Ecological Risk Assessment Support Center. NCEA-C-1282. Office of Research and Development, Las Vegas.

Oliveira, A.D., Mendonça Filho, J.G., Carvalho, M.A., Menezes, T.R., Lana, C.C., Brenner, W.W., 2004. Novo método de preparação palinológica para aumentar a recuperação de dinoflagelados. Revista Brasileira de Paleontologia 7 (2), 169-175.

Oliver, W.A. Jr., A.G. Coates, 1987. Phylum Cnidaria, in: Boardman, R.S., Cheetham, A.H., Rowell, A.J. (Eds.), Fossil Invertebrates. Blackwell Scientific Publications, pp. 140-193.

Ottenjahn, K., 1975. Spectral fluorescence measurements of sporinites in reflected light and other applicability for coalification studies, in: Alpern, B. (Ed.), Petrographie Organic et Potentiel Pétrolier. Centre Nationale Recherche Scientifique, Paris, pp. 49–65.

Ottenjahn, K., 1980. Spektrale Fluoreszenz-Mikrophotometrievo n Kohlen und Olschiefern. Leitz. Mitt. Wiss. Tech. 7, 262–273.

Ottenjahn, K., Teichmüller, M., Wolf, M., 1974. Spektrale fluoreszenzmessungen an sporiniten mit Auflicht–Anregung, eine mikroskopische methode zur bestimmung des inkohlungsgrades gering inkohlter kohlen. Fortschritte in der Geologie von Rheinland und Westfalen 24, 1–36.

Ottenjahn, K., Wolf, M., Wolf-Fischer, E., 1981. Beziehungen zwischen der Fluoreszenz von Vitriniten and den Technologischen Eigenschaften von Kohlen. International Conference on Coal Science, Dusseldorf, Germany: IEA, 86–91.

Pálfy, J., Smith, P.L., 2000. Synchrony between Early Jurassic extinction, oceanic anoxic event, and the Karoo-Ferrar flood basalt volcanism. Geology 28 (8), 747-750.

Pearson, D.L., 1990. Pollen / spore color “standard,” version 2: Phillips Petroleum Company Geology Branch, Bartlesville, Oklahoma.

Pelissié, T., 1982. Le Causse jurassique de Limoge-Quercy Stratigraphique, Sédimentologie, Structure. Thèse de Doctorat 3º cycle, Université P. Sabatier, Toulousse, 281 pp.

Percival, L.M.E., Witt, M.L.I., Mather, T.A., Hermoso, M., Jenkyns, H.C., Hesselbo, S.P., Al-Suwaidi, A.H., Storm, M.S., Xu, W., Ruhl, M., 2015. Globally enhanced mercury deposition during the end-Pliensbachian extinction and Toarcian OAE: A link to the Karoo-Ferrar Large Igneous Province. Earth and Planetary Science Letters 428, 267-280.

Pina, B., 2015. Geoquímica orgânica da série carbonatada da base da Formação do Cabo Carvoeiro (Toarciano inferior) da região de Peniche – Ambiente deposicional e preservação da matéria orgânica. Unpublished master’s thesis, University of Coimbra, Coimbra, Portugal.

Pinard, J., Weis, R., Neige, P., Mariotti, N., Cencio, A.D., 2014. Belemnites from the Upper Pliensbachian and the Toarcian (Lower Jurassic) of Tournadous (Causses, France). N. Jb. Geol. Paläont. Abh. 273/2, 155–177, http://dx.doi.org/10.1127/0077-7749/2014/0421.

Portella, K.F., Joukoski, A., Silva, A.S., Brassac, N.M., Belz, C.E., 2009. Biofouling e biodeterioração química de argamassa de cimento portland em reservatório de usina hidroelétrica. Química Nova 32(4), 1047-1051.

Prauss, M., Ligouis, B., Luterbacher, H., 1991. Organic matter and palynomorphs in the 'Posidonienschiefer' (Toarcian, Lower Jurassic) of southern Germany, in: Tyson, R.V., Pearson, T.H. (Eds.), Modern and Ancient Continental Shelf Anoxia, Geological Society Special Publication 58, pp. 335-351.

Purcell, J.E., 1997. Pelagic cnidarians and ctenophores as predators: selective predation, feeding rates, and effects on prey populations. Annales de l'Institute Oceanograph 72(2), 125-137.

Qajoun, A., 1994. Le Toarcien du Quercy Septentrional: stratigraphie et micropaléontologie. Strata (2), 22, 236 pp.

Rey, J., Bonnet, L., Cubaynes, R., Qajoun, A., Ruget, C., 1994. Sequence stratigraphy and biological signals: statistical studies of benthic foraminifera from Liassic series. Palaeogeography, Palaeoclimatology, Palaeoecology 111, 149-171.

Rey J., Cubaynes R., Fauré P., Brunel F., Qajoun A., 1995. Les séquences de dépôt et Cycles Transgressifs-Régressifs du Lias moyen et supérieur du Quercy (Aquitaine oriental). Strata (1), 7, 60-62.

Rey, J., Cubaynes, R., Fauré, P., Hantzpergue, P., Pélissié, T., 1988. Stratigraphie séquentielle et évolution d'une plate-forme carbonatée: le Jurassique du Quercy (Sud-Ouest de la France). C.R. Acad. Sci. Fr. (II) 306, 1009-1015.

Riera, V., Oms, O., Gaete, R., Galobart, A., 2009. The end-Cretaceous dinosaur succession in Europe: The Tremp Basin record (Spain). Palaeogeography, Palaeoclimatology, Palaeoecology 283, 160-171, http://dx.doi.org/10.1016/j.palaeo.2009.09.018.

Rodrigues, B., Duarte, L.V., Mendonça Filho, J.G., Santos, L., 2015a. Contribuição da geoquímica orgânica na caracterização paleoambiental da base da Formação de S.Gião (Toarciano inferior) da região de Coimbra (Bacia Lusitânica, Portugal). X Congresso Ibérico de Geoquímica – XVIII Semana de Geoquímica, LNEG, Portugal, 262-265.

Rodrigues, B., Duarte, L.V., Mendonça Filho, J.G., Santos, L.G., 2015b. Palaeoenvironmental significance of organic facies variation cross the Lower Toarcian in the northeastern sector of the Lusitanian Basin, Portugal. Geophysical Research Abstracts 17, EGU2015-3044-1.

Rodrigues, B., Duarte, L.V., Mendonça Filho, J.G., Santos, L.G., Oliveira, A.D., 2015c. Organofaciological evidences of terrestrial organic matter deposition across the Toarcian Oceanic Anoxic Event recorded in the Coimbra region, northern Lusitanian Basin, Portugal, in: Kus, J., David, P., Kalaitzidis, S., Schulz, H-M., Sachsenhofer, R.F. (Eds.), ICCP Program & Abstract Book. 67th Annual Meeting of the International Committee for Coal and Organic Petrology, September 5-11. 2015, Potsdam, Germany. Schriftenreihe der Deutschen Gesellschaft für Geowissenschaften Heft 87, 145-146.

Rodrigues, B., Mendonça Filho, J.G., Duarte, L.V., Comas-Rengifo, M.J., Goy, A., Mendonça, J.O., 2015d. Estudo organofaciológico ao longo do Pliensbachiano terminal – Toarciano inferior de Rodiles (Astúrias, Espanha). X Congresso Ibérico de Geoquímica – XVIII Semana de Geoquímica, LNEG, Portugal, 266-269.

Röhl, H., Schmid- Röhl, A., 2005. Lower Toarcian (Upper Liassic) black shales of the Central European epicontinental basin: a sequence stratigraphic case study from the SW German Posidonia Shale, in: Harris, N. (Ed.), The Deposition of Organic Carbon-Rich Sediments: Models, Mechanisms and Consequence, SEPM Special Publication 82, 165– 189.

Röhl, H., Schmid- Röhl, A., Oschmann W., Frimmel, A., Schwark, L., 2001. The Posidonia Shale (Lower Toarcian) of SW-Germany: an oxygen-depleted ecosystem controlled by sea level and palaeoclimate. Palaeogeography, Palaeoclimatology, Palaeoecology 165, 27-52.

Rosales, I., Quesada, S., Robles, S., 2004. Paleotemperature variations of Early Jurassic seawater recorded in geochemical trends of belemnites from the Basque-Cantabrian basin, northern Spain. Palaeogeography, Palaeoclimatology, Palaeoecology 203, 253-275, http://dx.doi.org/10.1016/S0031-0182(03)00686-2.

Ruppert, E.E., Barnes, R.D., 1994. Invertebrate Zoology, Sixth Edition. Saunders College Publishing, Harcourt Brace and Company, Orlando, Florida.

Schmid-Röhl, A., Röhl, H., Oschmann, W., Frimmel, A., Schwark, L., 2002. Palaeoenvironmental reconstruction of Lower Toarcian epicontinental black shales (Posidonia Shale, SW Germany): global versus regional control. Geobios 35, 13-20.

Schouten, S., van Kaam-Peters, H.M.E., Rijpstra, W.I.C., Schoell, M., Damste, J.S.S., 2000. Effects of an oceanic anoxic event on the stable carbon isotopic composition of Early Toarcian carbon. American Journal of Science 300, 1-22.

Sellés, A.G., Vila, B., 2015. Re-evaluation of the age of some dinosaur localities from the southern Pyrenees by means of megaloolithid oospecies. Journal of Iberian Geology 41 (1), 125-139, http://dx.doi.org/10.5209/rev_JIGE.2015.v41.n1.48659.

Sissingh, W., 2006. Syn-kinematic palaeogeographic evolution of the West European Platform: correlation with Alpine plate collision and foreland deformation. Netherlands Journal of Geosciences –Geologie en Mijnbouw 85 (2), 131-180.

Song, J., Littke, R., Maquil, R., Weniger, P., 2014. Organic facies variability in the Posidonia Black Shale from Luxembourg: Implications for thermal maturation and depositional environment. Palaeogeography, Palaeoclimatology, Palaeoecology 410, 316-336, http://dx.doi.org/10.1016/j.palaeo.2014.06.002.

Srivastava, S.K., 1976. The fossil pollen genus *Classopollis*. Lethaia 9, 1-78.

Staplin, F.L., 1969. Sedimentary organic matter, organic metamorphism and oil and gas occurrence. Bulletin of Canadian Petroleum Geology 17, 47-66.

Stasiuk, L.D., 1994. Fluorescence properties of Paleozoic oil-prone alginite in relation to hydrocarbon generation, Williston basin, Saskatchewan, Canada. Marine and Petroleum Geology 11(2), 219-231.

Suan, G., Rogov, M.A., Spangenberg, J.E., Nikitenko, B.L., Föllmi, K.B., Adatte, T., 2010. Response of Arctic climate and hydrology to the Toarcian Oceanic Anoxic Event. Geophysical Research Abstracts 12, EGU2010-3612.

Suárez-Ruiz, I.; Flores, D.; Mendonça Filho, J.G.; Hackley, P.C., 2012. Review and update of the applications of organic petrology: Part 1, Geological Applications. International Journal of Coal Geology 99, 54-112, http://dx.doi.org/10.1016/j.coal.2012.02.004.

Taylor, G.H., Teichmüller, M., Davis, A., Diessel, C.F.K., Littke, R., Robert, P., 1998. Organic Petrology. Gebrüder Borntraeger, Berlin.

Teichmüller, M., 1974. Generation of petroleum-like substances in coal seams as seen under the microscope, in: Tissot, B., Bienner, F. (Eds.), Advances in Organic Geochemistry. Editions Technip, Paris, pp. 321-349.

Teichmüller, M., Ottenjann, K., 1977. Liptinite und lipoid Stoffe in einen Erdölmuttergestein. Erdöl ind Kohle 30, 387-398.

Thierry, J. et al., 2000. Middle Toarcian, in: Dercourt, J., Gaetani, M., Vrielynck, B., Barrier, E., Biju-Duval, B., Brunet, M.-F., Cadet, J.P., Crasquin, S., Sandulescu, M. (Eds.), Atlas Peri-Tethys Paleogeographical Maps, vol. I–XX.CCGM/CGMW, Paris, map 8, (40 co-authors).

Tissot, B.P., Durand, B., Espitalié, J., Combaz, A., 1974. Influence of nature and diagenesis of organic matter in formation of petroleum. Bull. Am. Assoc. Pet. Geol. 58, 499-506.

Tissot, B., Welte, D.H., 1984. Petroleum Formation and Occurrence, 2nd Revised and Enlarged Edition, Springer-Verlag, Berlin.

Traverse, A., 1988. Paleopalynology. Unwin Hyman, London.

Trümpy, D.M., 1983. Le Lias Moyen et Supérieur des Grands Causses et de la région de Rodez: contributions stratigraphiques, sédimentologiques et géochimiques à la connaissance d'un bassin à sédimentation marneuse. Cahiers de l'Université, Université de Pau et des Pays de l'Adour, 19, 1-363.

Tschudy, R.H., 1961. Palynomorphs as indicators of facies environments in Upper Cretaceous and Lower Tertiary strata, Colorado and Wyoming. Wyoming Geological Society, 16th Annual Field Conference, Guidebook, 53-9.

Tyson, R.V., 1995. Sedimentary Organic Matter. Organic facies and palynofacies. Chapman and Hall, London.

Valentin, J.L., 2000. Ecologia numérica. Interciência, Rio de Janeiro. 62.

van Breugel, Y., Baas, M., Schouten, S., Mattioli, E., Damsté, J.S.S., 2006. Isorenieratane record in black shales from the Paris Basin, France: Constraints on recycling of respired CO_2 as a mechanism for negative carbon isotope shifts during the Toarcian oceanic anoxic event. Paleoceanography 21, PA4220, http://dx.doi.org/10.1029/2006PA001305.

van de Schootbrugge, B., Bachan, A., Suan, G., Richoz, S., Payne, J.L., 2013. Microbes, mud and methane: cause and consequence of recurrent Early Jurassic anoxia following the end-Triassic mass extinction. Palaeontology, 1-25, http://dx.doi.org/10.1111/pala.12034.

van de Schootbrugge, B., Harazim, D., Sorichter, K., Oschmann, W., Fiebig, J., Püttmann, W., Peinl, M., Zanella, F., Teichert, B.M.A., Hoffmann, J., Stadnitskaia, A., Rosenthal, Y., 2010. The enigmatic ichnofossil *Tisoa siphonalis* and widespread authigenic seep carbonate formation during the Late Pliensbachian in southern France. Biogeosciences 7, 3123-3138, http://dx.doi.org/10.5194/bg-7-3123-2010.

van de Schootbrugge, B., McArthur, J.M., Bailey, T.R., Rosenthal, Y., Wright, J.D., Miller, K.G., 2005. Toarcian oceanic anoxic event: An assessment of global causes using belemnite C isotope records. Paleoceanography 20, PA3008, http://dx.doi.org/10.1029/2004PA001102.

Vanderhaeghe, O., Grabkowiak, A., 2014. Tectonic accretion and recycling of the continental lithosphere during the Alpine orogeny along the Pyrenees. Bull. Soc. Géol. France 185 (4), 257-277.

Vincent, A.J., 1995. Palynofacies analysis of Middle Jurassic sediments from the Inner Hebrides. PhD Thesis, University of Newcastle upon Tyne. 475 pp.

Wignall, P.B., Newton, R.J., Little, C.T.S., 2005. The timing of paleoenvironmental change and cause-and-effect relationships during the Early Jurassic mass extinction in Europe. American Journal of Science 305, 1014-1032.

Appendix A. Palynofacies Percentages

Sampling Distribution			Phytoclast Group														Amorphous Group			Palynomorph Group																							
			Opaque	Non-Opaque																																							
				Biostructured										Non-biostructured		Cuticle		Membrane	Total Phytoclast Group		AOM	Total Amorphous Group	Undifferentiated	Marine Microplankton			Fresh. Micropl.	Sporomorph							Zoomorph			Total Palynomorph Group	Zooclast Group	Palynofacies Association	Interval
				Striped		Striate		Banded		Pitted																	Pollen Grains															
Units		Samples	Lath	Degraded	Undegraded	Degraded	Undegraded	Degraded	Undegraded	Degraded	Undegraded	Degraded	Undegraded	Degraded	Undegraded			Resin	Fluorescent Heter. AOM			Dinocysts	Prasinophyte	Acritarchs	Gloeocapsomorpha	Single Grain	Dyads	Tetrads	Polyads	Bisaccate	Spores	Foraminiferal Test-Linings	Medusae	Amorphous						
Rivière-sur-Tarn Group	Marnes de Fontaneilles Fm.	S69	0.00	0.00	0.00	0.00	0.00	0.00	0.00	0.00	0.00	0.97	0.00	0.00	0.00	0.00	0.97	0.65	51.29	51.94	0.00	0.00	0.65	0.00	0.32	3.55	0.00	0.32	0.00	0.32	0.97	0.00	0.65	0.00	6.77	40.32	II	4
		S64	0.00	1.58	0.00	0.00	0.00	1.27	0.00	0.95	0.00	1.90	0.63	0.00	0.00	0.00	6.33	0.00	44.62	44.62	0.00	0.32	0.00	0.95	12.03	3.16	0.00	0.32	0.00	0.00	0.32	0.00	4.11	0.00	21.20	27.85	II	
		S61	0.00	0.00	0.00	0.00	0.00	0.00	0.00	0.00	0.00	0.00	0.00	0.00	0.00	0.00	0.00	0.00	79.33	79.33	0.00	0.00	0.00	0.00	0.00	0.33	0.00	0.00	0.00	0.00	0.00	0.00	0.33	0.00	0.67	20.00	II	
	Schistes Cartons Formation	S55	0.00	0.00	0.00	0.00	0.00	0.00	0.00	0.00	0.00	0.00	0.00	0.00	0.00	0.00	0.00	0.00	67.44	67.44	0.00	0.00	0.00	0.00	1.00	0.00	0.00	0.00	0.00	0.00	0.00	0.00	0.00	0.00	1.00	31.56	II	
		S52	0.00	0.33	0.00	0.00	0.00	0.00	0.00	0.33	0.00	0.33	0.33	0.00	0.00	0.00	1.33	0.00	97.67	97.67	0.00	0.00	0.66	0.00	0.00	0.00	0.00	0.00	0.00	0.00	0.00	0.00	0.00	0.00	0.66	0.33	III	3
		S50	0.00	0.00	0.00	0.00	0.00	0.00	0.00	0.00	0.00	0.33	0.00	0.00	0.00	0.00	0.33	0.00	99.34	99.34	0.00	0.00	0.33	0.00	0.00	0.00	0.00	0.00	0.00	0.00	0.00	0.00	0.00	0.00	0.33	0.00	III	
		S22	0.00	0.00	0.00	0.00	0.00	0.00	0.00	0.00	0.00	0.65	0.00	0.00	0.00	0.00	0.65	0.00	98.39	98.39	0.00	0.00	0.32	0.00	0.00	0.00	0.00	0.00	0.00	0.00	0.00	0.00	0.00	0.00	0.32	0.65	III	
		S19	0.00	0.00	0.00	0.00	0.00	0.00	0.00	0.00	0.00	1.31	0.00	0.00	0.00	0.00	1.31	0.00	96.72	96.72	0.00	0.00	0.33	0.00	0.33	0.00	0.00	0.00	0.00	0.00	0.00	0.00	0.00	0.00	0.66	1.31	III	
		S17	0.00	0.00	0.00	0.00	0.00	0.00	0.00	0.00	0.00	1.30	0.00	0.00	0.00	0.00	1.30	0.98	94.46	95.44	0.00	0.00	0.00	0.00	0.00	0.33	0.00	0.00	0.00	0.00	0.33	0.00	0.00	0.00	0.65	2.61	III	
		S15	0.00	0.00	0.00	0.00	0.00	0.00	0.00	0.00	0.00	0.31	0.00	0.00	0.00	0.00	0.31	0.00	97.17	97.17	0.00	0.00	0.00	0.63	0.00	0.00	0.00	0.00	0.00	0.00	0.00	0.00	0.00	0.00	0.63	1.89	III	
	Marnes de Villeneuve Fm.	S12	0.00	2.23	0.32	0.00	0.00	0.96	0.00	0.32	0.00	5.41	0.96	0.00	0.00	0.00	10.19	0.64	34.71	35.99	0.00	6.05	0.00	3.18	0.64	3.50	0.00	0.32	0.00	0.00	0.64	0.00	5.10	0.00	19.43	34.39	II	2
		S11	0.00	5.63	0.00	0.00	0.00	0.00	0.00	2.65	0.00	10.93	0.66	0.00	0.00	0.00	19.87	1.32	11.92	14.57	0.00	10.60	0.33	2.32	0.00	5.30	0.00	0.00	0.00	0.00	0.66	0.33	11.59	0.00	31.13	34.44	I	1
		S10	0.00	4.32	0.00	0.00	0.00	1.00	0.33	2.33	0.00	12.96	2.99	0.00	0.00	0.00	23.92	1.99	15.28	17.28	0.00	2.33	0.00	4.32	0.00	5.98	1.00	0.00	0.33	0.00	0.66	1.33	9.97	0.00	25.91	32.89	I	

Appendix A.1. Relative percentages of the particulate organic compounds identified in the palynofacies analysis of samples from the Suèges section (Grands Causses Basin).

Sampling Distribution			Phytoclast Group														Amorphous Group			Palynomorph Group																										
			Opaque	Non-Opaque																																										
				Biostructured											Non-biostructured		Cuticle																														
				Striped		Striate		Banded		Pitted																																					
Units		Samples	Lath	Degraded	Undegraded	Degraded	Undegraded	Degraded	Undegraded	Degraded	Undegraded	Degraded	Undegraded	Degraded	Undegraded	Membrane	Total Phytoclast Group	Resin	Fluorescent Heter. AOM	Total Amorphous Group	Undifferentiated	Dinocysts	Prasinophyte	Acritarchs	Gloeocapsomorpha	Single Grain	Dyads	Tetrads	Polyads	Bisaccate	Spores	Foraminiferal Test-Linings	Medusae	Amorphous	Total Palynomorph Group	Zooclast Group	Palynofacies Association	Interval
																		AOM			Marine Microplankton			Fresh. Micropl.	Sporomorph						Zoomorph												
																										Pollen Grains						Hydrozoan												
Penne Formation	MCH Mb.	Cay28	0.00	0.00	0.00	0.00	0.00	0.00	0.00	0.32	0.00	0.63	0.00	0.00	0.00	0.00	0.95	0.00	84.18	84.18	0.00	0.00	1.58	0.00	0.63	0.00	0.00	0.00	0.00	0.00	0.00	0.32	0.95	0.00	3.48	11.39	III	3
	Schistes Cartons Member	Cay26	0.00	0.00	0.00	0.00	0.00	0.00	0.00	0.00	0.00	0.00	0.00	0.00	0.00	0.00	0.00	0.00	0.00	0.00	0.00	0.00	0.65	0.00	0.00	0.00	0.00	0.00	0.00	0.00	0.00	0.00	0.00	98.70	99.35	0.65	II	2
		Cay23	0.00	0.00	0.00	0.00	0.00	0.00	0.00	0.00	0.00	0.00	0.00	0.00	0.00	0.00	0.00	0.00	0.00	0.00	0.00	0.00	1.29	0.00	0.00	0.00	0.00	0.00	0.00	0.00	0.00	0.00	0.65	98.06	100.00	0.00	II	
		Cay20	0.00	0.00	0.00	0.00	0.00	0.00	0.00	0.00	0.00	0.00	0.00	0.00	0.00	0.00	0.00	0.00	0.00	0.00	0.00	0.00	0.65	0.00	0.00	0.00	0.00	0.00	0.33	0.00	0.00	0.00	0.33	98.69	100.00	0.00	II	
		Cay18	0.00	0.00	0.00	0.00	0.00	0.00	0.00	0.00	0.00	0.00	0.00	0.00	0.00	0.00	0.00	0.00	0.00	0.00	0.00	0.00	0.63	0.00	0.00	0.00	0.00	0.00	0.00	0.00	0.00	0.00	0.00	98.75	99.37	0.63	II	
		Cay13	0.00	0.00	0.00	0.00	0.00	0.00	0.00	0.00	0.00	0.00	0.00	0.00	0.00	0.00	0.00	0.00	0.00	0.00	0.63	0.00	0.00	0.00	1.25	0.63	0.00	0.00	0.00	0.00	0.00	0.00	0.31	95.61	98.43	1.57	II	
		Cay10	0.00	0.33	0.00	0.00	0.00	0.00	0.00	0.66	0.00	3.32	0.00	0.00	0.00	1.99	6.31	0.00	0.00	0.00	4.98	0.66	1.00	1.66	1.33	2.33	0.00	0.00	0.00	0.00	1.00	1.66	0.00	66.78	81.40	12.29	II	
Barre à Pecten Formation		Cay7	0.00	0.00	0.00	0.00	0.00	0.00	0.00	0.00	0.00	0.00	0.00	0.00	0.00	0.65	0.65	0.00	0.00	0.00	14.33	4.56	0.00	5.21	0.00	8.14	0.00	0.00	0.00	0.65	2.93	5.54	0.33	46.58	88.27	11.07	I	1
		Cay6	Low Recovery																																		I	
		Cay3																																			I	
		Cay1	0.00	0.00	0.00	0.00	0.00	0.00	0.00	0.00	0.00	2.47	0.31	0.00	0.00	0.00	2.78	0.00	0.00	0.00	3.40	0.31	0.00	1.85	0.00	1.85	0.00	0.00	0.00	0.00	0.31	1.85	1.85	76.23	87.65	9.57	I	

Appendix A.2. Relative percentages of the particulate organic compounds identified in the palynofacies analysis of samples from the Caylus section (Quercy Basin).

Units	Samples	Phytoclast Group – Opaque – Lath	Phytoclast Group – Non-Opaque – Biostructured – Striped – Degraded	Striped – Undegraded	Striate – Degraded	Striate – Undegraded	Banded – Degraded	Banded – Undegraded	Pitted – Degraded	Pitted – Undegraded	Non-biostructured – Degraded	Non-biostructured – Undegraded	Cuticle – Degraded	Cuticle – Undegraded	Membrane	Total Phytoclast Group	Amorphous Group – Resin	Amorphous Group – AOM – Fluorescent Heter. AOM	Total Amorphous Group	Palynomorph Group – Undifferentiated	Marine Microplankton – Dinocysts	Marine Microplankton – Prasinophyte	Marine Microplankton – Acritarchs	Fresh. Micropl. – Gloeocapsomorpha	Sporomorph – Pollen Grains – Single Grain	Pollen Grains – Dyads	Pollen Grains – Tetrads	Pollen Grains – Polyads	Pollen Grains – Bisaccate	Sporomorph – Spores	Zoomorph – Foraminiferal Test-Linings	Zoomorph – Hydrozoan – Medusae	Hydrozoan – Amorphous	Total Palynomorph Group	Zooclast Group	Palynofacies Association	Interval
Padrinas Formation – Calcaires argileux à Telothyris Mb.	265PS	0.00	0.00	0.00	0.00	0.00	0.00	0.00	0.33	0.00	0.33	0.00	0.00	0.00	0.00	0.65	0.00	0.00	0.00	1.95	0.00	0.00	0.00	0.00	0.00	0.00	0.00	0.00	0.00	0.00	0.00	0.00	0.33	2.28	97.07	I	5
	255PS	0.29	0.00	0.00	0.00	0.00	0.00	0.00	0.58	0.00	0.58	0.00	0.86	0.00	0.00	2.31	0.00	0.00	0.00	1.15	0.00	0.00	0.00	0.00	0.00	0.00	0.00	0.00	0.00	0.00	0.00	0.00	3.17	4.32	93.37	I	
	470PS	0.00	0.00	0.00	0.00	0.00	0.00	0.00	0.00	0.00	1.27	0.00	0.00	0.00	0.00	1.27	0.00	0.00	0.00	7.32	0.00	0.00	0.32	0.00	1.59	0.96	0.00	0.00	0.00	0.64	0.00	0.00	41.72	52.87	45.86	II	4
	420PS	0.00	0.00	0.00	0.00	0.00	0.00	0.00	0.00	0.00	0.00	0.00	0.00	0.00	0.00	0.00	0.00	0.00	0.00	1.29	0.00	0.00	0.32	0.00	0.00	0.00	0.00	0.00	0.00	0.00	0.00	0.00	87.74	89.35	10.65	II	
Padrinas Formation – Calcaires argileux et marnes à Soaresirhynchia Mb.	380PS	0.00	0.00	0.00	0.00	0.00	0.00	0.00	0.00	0.00	0.32	0.00	0.97	0.00	0.00	1.29	0.00	0.00	0.00	7.74	0.00	0.00	0.32	0.00	0.32	0.65	0.00	0.97	0.00	0.32	0.97	0.00	16.77	28.06	70.65	I	3
	355PS	0.00	0.00	0.00	0.00	0.00	0.00	0.00	0.00	0.00	0.00	0.00	0.00	0.00	0.00	0.00	0.00	0.00	0.00	5.18	0.00	0.00	0.32	0.00	0.00	0.00	0.00	0.00	0.00	0.32	0.32	0.00	26.54	32.69	67.31	I	
	330PS	0.00	0.00	0.00	0.00	0.00	0.00	0.00	0.32	0.00	1.30	0.00	0.00	0.00	0.00	1.62	0.00	0.00	0.00	4.55	0.00	0.32	0.32	0.00	0.00	0.00	0.00	0.00	0.00	0.00	0.00	0.00	29.22	34.42	63.96	I	
	300PS	0.00	0.00	0.00	0.00	0.00	0.00	0.00	0.00	0.00	1.65	0.00	0.66	0.00	0.00	2.31	0.00	0.00	0.00	3.63	0.00	0.00	0.99	0.00	0.00	0.00	0.00	0.00	0.00	0.00	0.99	0.00	48.84	54.46	43.23	II	2
Padrinas Formation – Calcaires argileux à Spiriférines Mb.	115PS	0.00	0.00	0.00	0.00	0.00	0.00	0.00	0.00	0.00	0.00	0.00	0.00	0.00	0.00	0.00	0.00	0.00	0.00	1.82	0.61	0.00	0.91	0.00	1.82	0.00	0.30	0.00	0.00	1.52	0.30	0.00	71.12	79.03	20.97	II	
	100PS	0.00	0.00	0.00	0.00	0.00	0.00	0.00	0.32	0.00	0.64	0.00	0.00	0.00	0.00	0.96	0.00	0.00	0.00	6.37	0.00	0.00	0.96	0.00	0.64	0.00	0.00	0.32	0.00	0.32	0.00	0.00	51.27	59.87	39.17	II	
	75PS	0.00	0.00	0.00	0.00	0.00	0.00	0.00	0.33	0.00	0.66	0.00	0.00	0.00	0.00	0.99	0.00	0.00	0.00	10.60	0.00	0.00	2.65	0.00	0.00	0.00	0.00	0.00	0.33	0.00	0.33	0.00	4.30	18.21	80.79	I	1
	65-7PS	0.37	0.00	0.00	0.00	0.00	0.00	0.00	0.73	0.00	1.47	0.00	0.00	0.00	0.00	2.56	0.00	0.00	0.00	13.55	0.37	0.00	1.10	0.00	0.00	0.00	0.00	0.00	0.00	0.73	0.00	0.00	0.00	15.75	81.68	I	
	45PS	0.66	0.33	0.00	0.00	0.00	0.00	0.00	1.00	0.00	1.66	0.00	0.00	0.00	0.00	3.65	0.00	0.00	0.00	7.640	0.00	0.00	1.00	0.00	0.00	0.00	0.00	0.00	0.00	0.33	0.00	0.00	1.33	10.30	86.05	I	
Barre a Pecten Fm	20PS	0.00	0.00	0.00	0.00	0.00	0.00	0.00	1.32	0.00	2.32	0.00	0.00	0.00	0.00	3.64	0.00	0.00	0.00	18.87	0.00	0.00	1.99	0.00	1.32	0.00	0.00	0.00	0.00	1.66	0.00	0.00	2.32	26.16	70.20	I	

Appendix A.3. Relative percentages of the particulate organic compounds identified in the palynofacies analysis of samples from the Pont de Suert section (Pyrenean Basin).

Appendix B. Petrographic Atlas

The aim of this atlas is to present microscopic aspects, on transmitted and reflected white, incident blue and UV lights, of the studied samples that were not included in Chapter IV – Results.

The petrographic atlas includes five parts that correspond to the main groups of kerogen in transmitted transmitted white and incident blue lights – Phytoclast, Amorphous, Palynomorph and Zooclast. The last part is dedicated to petrographic aspects observed in plugs of kerogen concentrate in reflected white and incident blue and UV lights.

The characterization of the kerogen assemblage on transmitted and incident blue and UV lights follows the classification system proposed by Tyson (1995), Vincent (1995), Mendonça Filho (1999), and Mendonça Filho et al. (2010a; 2011c; 2012; 2014c; 2016, *Ineditus in efficiendis*). The photomicrographs were taken using a Carl Zeiss Axio Imager A1 microscope at the Laboratory of Palynofacies and Organic Facies of the Federal University of Rio de Janeiro (LAFO-UFRJ).

B.1. Phytoclast Group

Phytoclasts correspond to fragments of tissues derived from highly lignified mechanical support tissue of higher plants and fungi (Bostick, 1971). For more information about nomenclature and/or petrographic features see section 1.2.1.1. on Chapter II of this thesis.

B.1.1. Suèges section – Grands Causses Basin

A. Non-opaque biostructured phytoclast, pitted (S11; TWL).

B. Non-opaque biostructured phytoclast, pitted (S64; TWL).

C. Non-opaque phytoclast, cuticle layer fragments associated with innermost part of epidermis (S12; TWL).

D. Non-opaque phytoclast, cuticle layer fragments associated with innermost part of epidermis (S12; FM, UV light).

E. Non-opaque phytoclast, cuticle layer fragments associated with innermost part of epidermis (S64; TWL).

F. Non-opaque phytoclast, cuticle layer fragments associated with innermost part of epidermis (S64; FM, UV light).

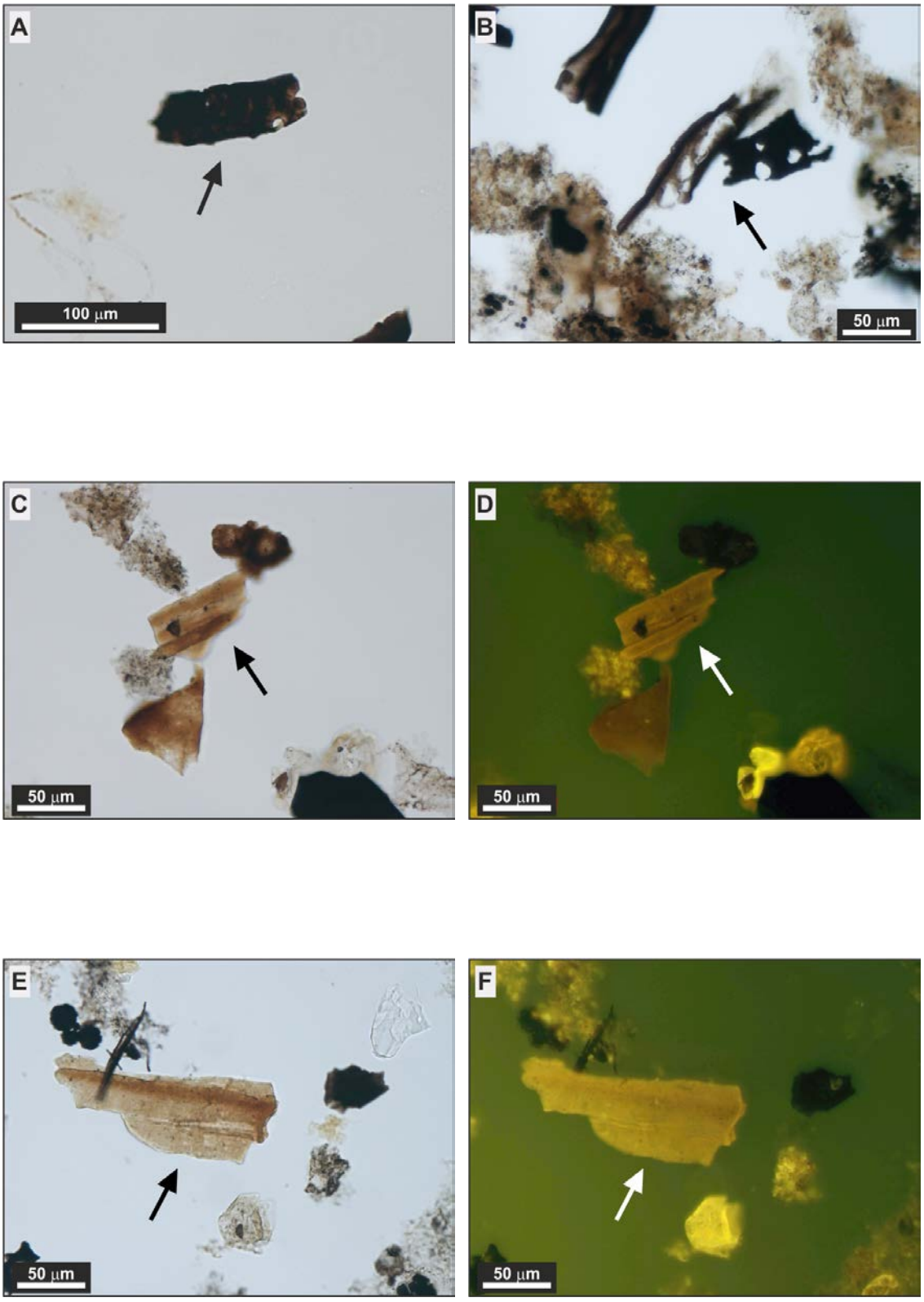
A
100 µm
B
50 µm
C
50 µm
D
50 µm
E
50 µm
F
50 µm

B.1.2. Caylus section – Quercy Basin

A. Non-opaque biostructured phytoclast, pitted (Cay28; TWL).

B. Non-opaque biostructured phytoclast, stripped (Cay6; TWL).

C. Non-opaque non-biostructured phytoclast (Cay3; TWL).

D. Non-opaque phytoclast, membrane (Cay10; TWL).

E. Non-opaque phytoclast, cuticle (Cay10; TWL).

F. Non-opaque phytoclast, cuticle (Cay10; FM, UV light).

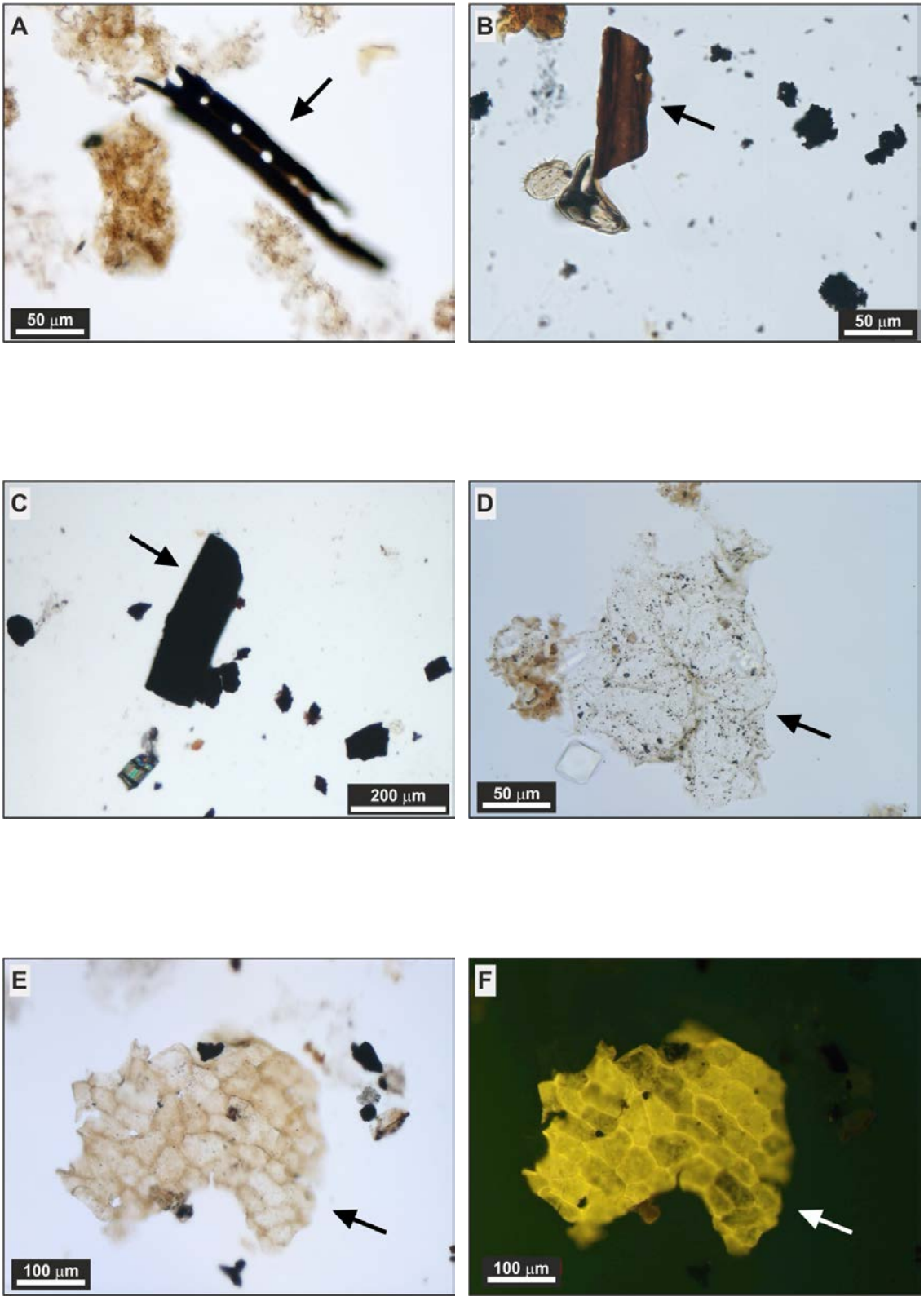
A
50 µm
B
50 µm
C
200 µm
D
50 µm
E
100 µm
F
100 µm

B.1.3. Pont de Suert section – Pyrenean Basin

A. Non-opaque biostructured phytoclast, pitted (20PS; TWL).

B. Non-opaque biostructured phytoclast, pitted (255PS; TWL).

C. Non-opaque biostructured phytoclast, pitted (255PS; Dark field).

D. Non-opaque non-biostructured phytoclast (45PS; TWL).

E. Opaque phytoclast, lath (45PS; TWL)


A
50 µm

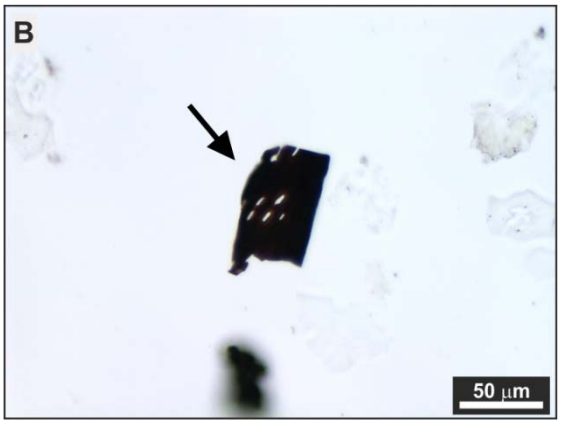
B
50 µm

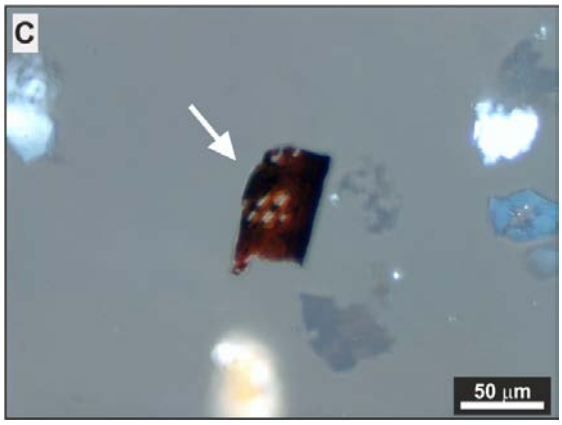
C
50 µm

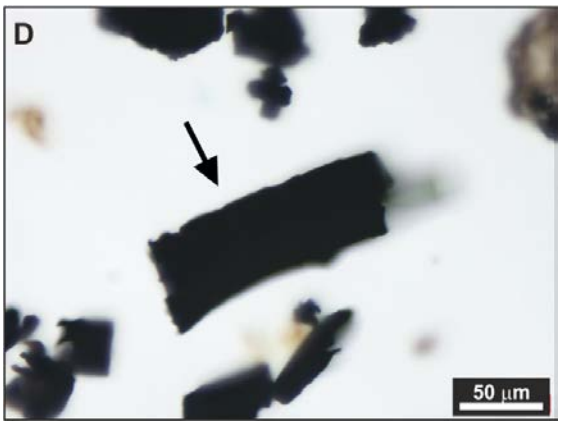
D
50 µm

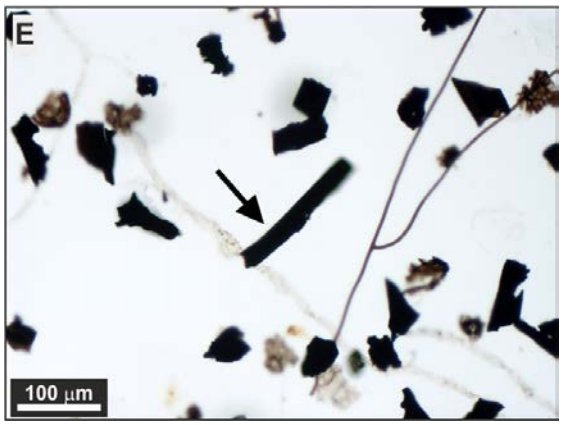
E
100 µm

B.2. Amorphous Group

The Amorphous group includes all particulate organic components that appear structureless at the scale of the optical microscopy (Tyson, 1995). For more information about nomenclature and/or petrographic features see section 1.2.1.2. on Chapter II of this thesis.

B.2.1. Suèges section – Grands Causses Basin

A. Hydrozoan derived AOM (S15; TWL).

B. Hydrozoan derived AOM (S15; FM, UV light).

C. Hydrozoan derived AOM (S15; FM, UV light).

D. Hydrozoan derived AOM (S15; FM, UV light).

E. Resin (S10; TWL).

F. Resin (S10; FM, UV light).

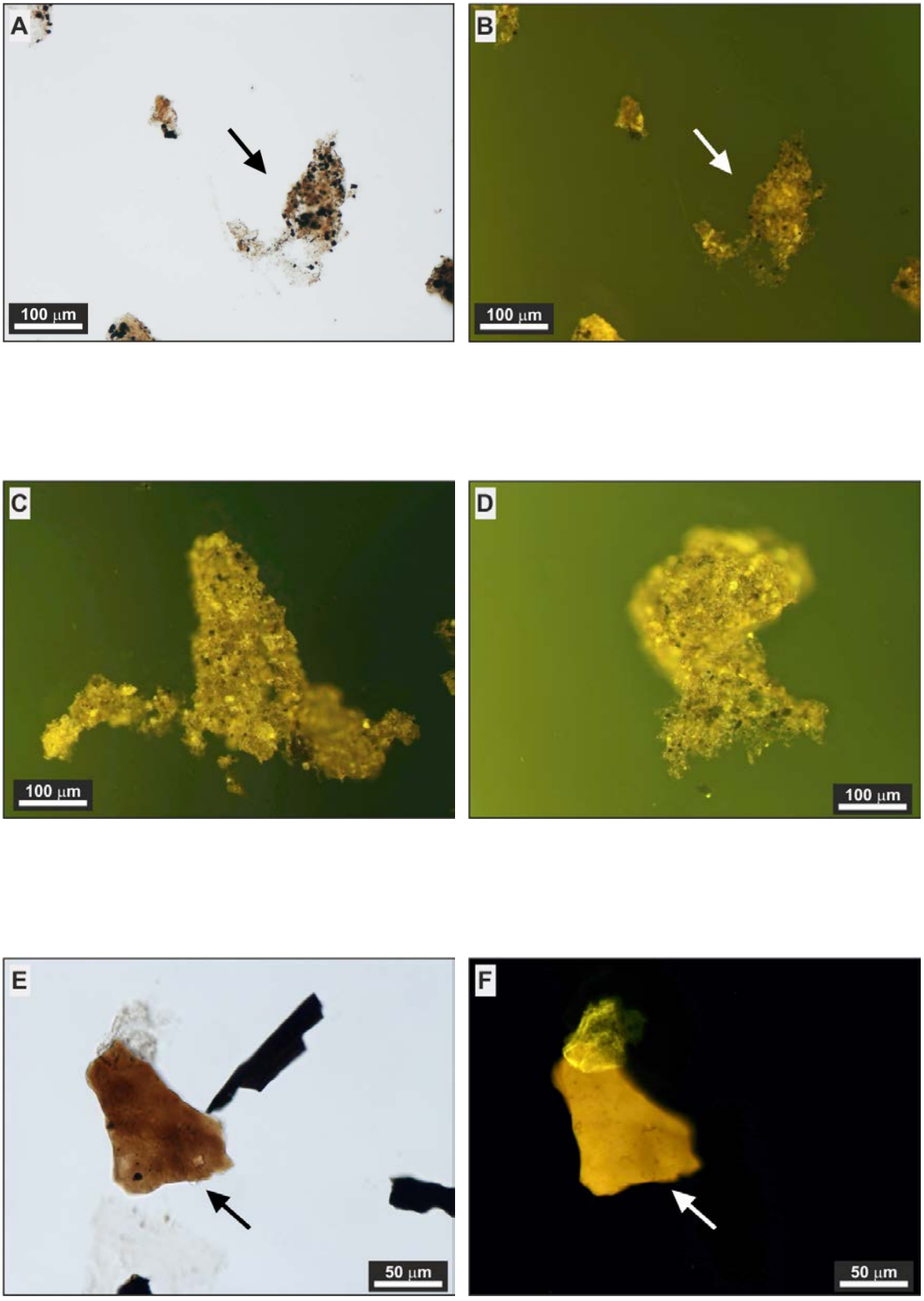
A
100 µm
B
100 µm
C
100 µm
D
100 µm
E
50 µm
F
50 µm

B.2.2. Caylus section – Quercy Basin

A. Bacterial and Hydrozoan derived AOM (Cay28; TWL).

B. Bacterial and Hydrozoan derived AOM (Cay28; FM, UV light).

C. Bacterial and Hydrozoan derived AOM (Cay28; TWL).

D. Bacterial and Hydrozoan derived AOM (Cay28; Dark Field).

E. Bacterial and Hydrozoan derived AOM (Cay28; FM, UV light)

F. Bacterial and Hydrozoan derived AOM (Cay28; FM, blue light).

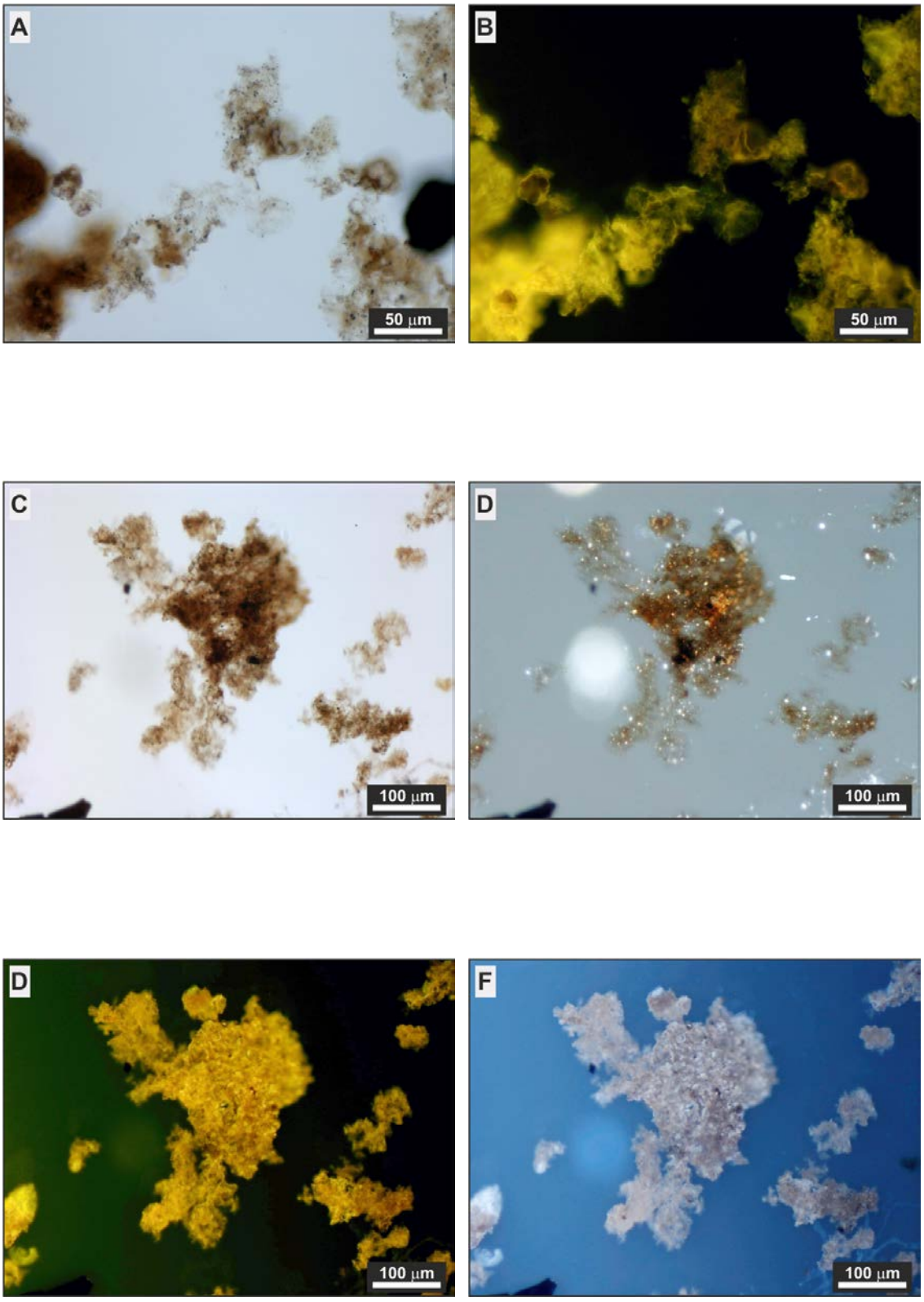
A
50 µm
B
50 µm
C
100 µm
D
100 µm
D
100 µm
F
100 µm

B.3. Palynomorph Group

Palynomorph group includes all organic-walled microfossils (HCl and HF resistant) (Tchudy, 1961). For more information about nomenclature and/or petrographic features see section 1.2.1.3. on Chapter II of this thesis.

B.3.1. Suèges section – Grands Causses Basin

B.3.1.1. Sporomorph subgroup

A. Pollen grain (S10; TWL).

B. Pollen grain (S10; FM, UV light).

C. Spore with visible trilete (S69; TWL).

D. Spore with visible trilete (S69; FM, UV light).

E. Bisaccate pollen (S12; FM, UV light).

F. Tetrad of the genus *Classopollis* (S12; FM, UV light).

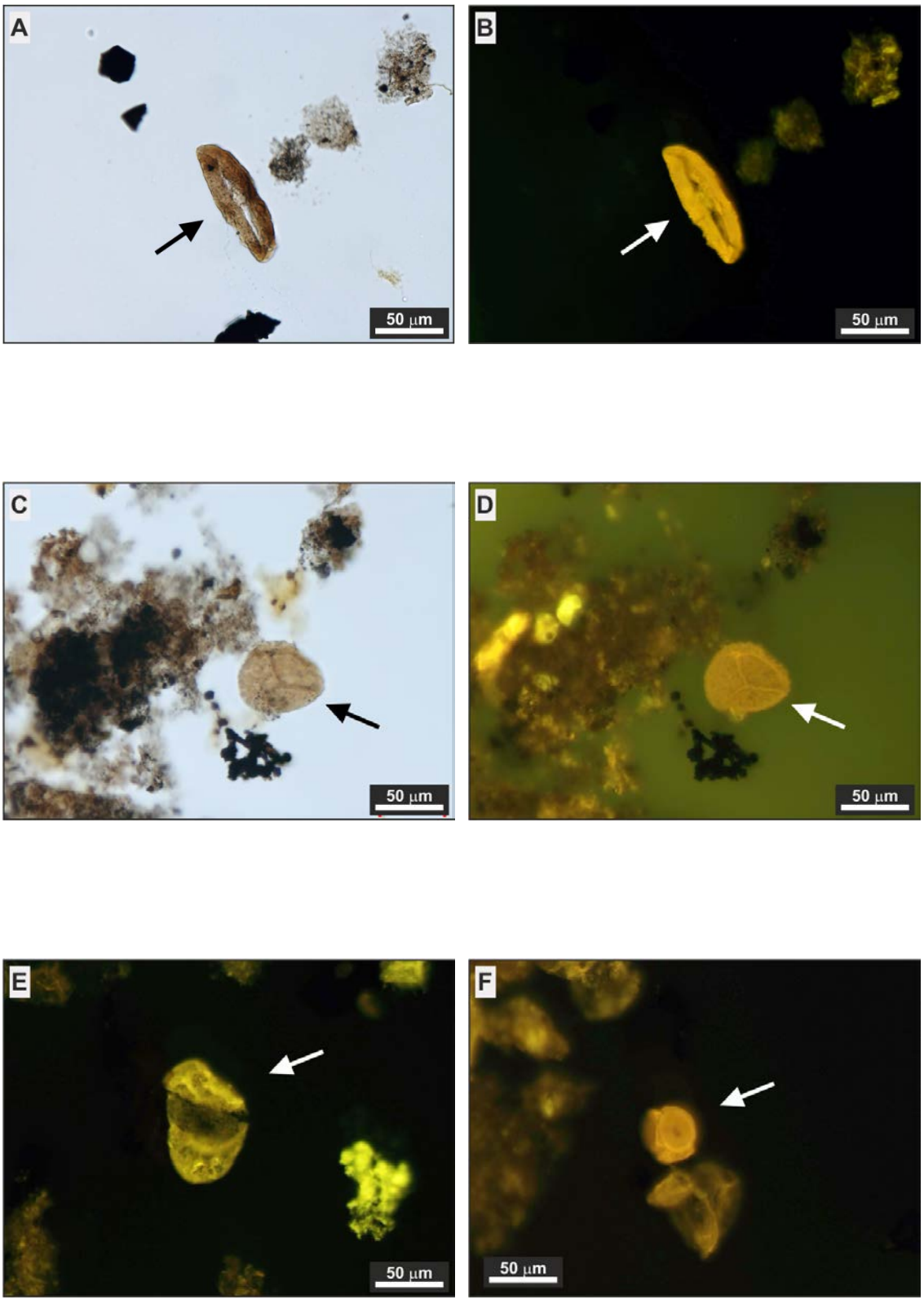
A
50 µm
B
50 µm
C
50 µm
D
50 µm
E
50 µm
F
50 µm

B.3.1.2. Freshwater microplankton subgroup

A. Gloeocapsomorpha (S10; TWL).

B. Gloeocapsomorpha (S10; FM, UV light).

B.3.1.3. Marine Microplankton subgroup

C. Dinoflagellate Cyst (S12; TWL).

D. Dinoflagellate Cyst (S12; FM, UV light).

E. Dinoflagellate Cyst (S12; TWL).

F. Dinoflagellate Cyst (S12; FM, UV light).

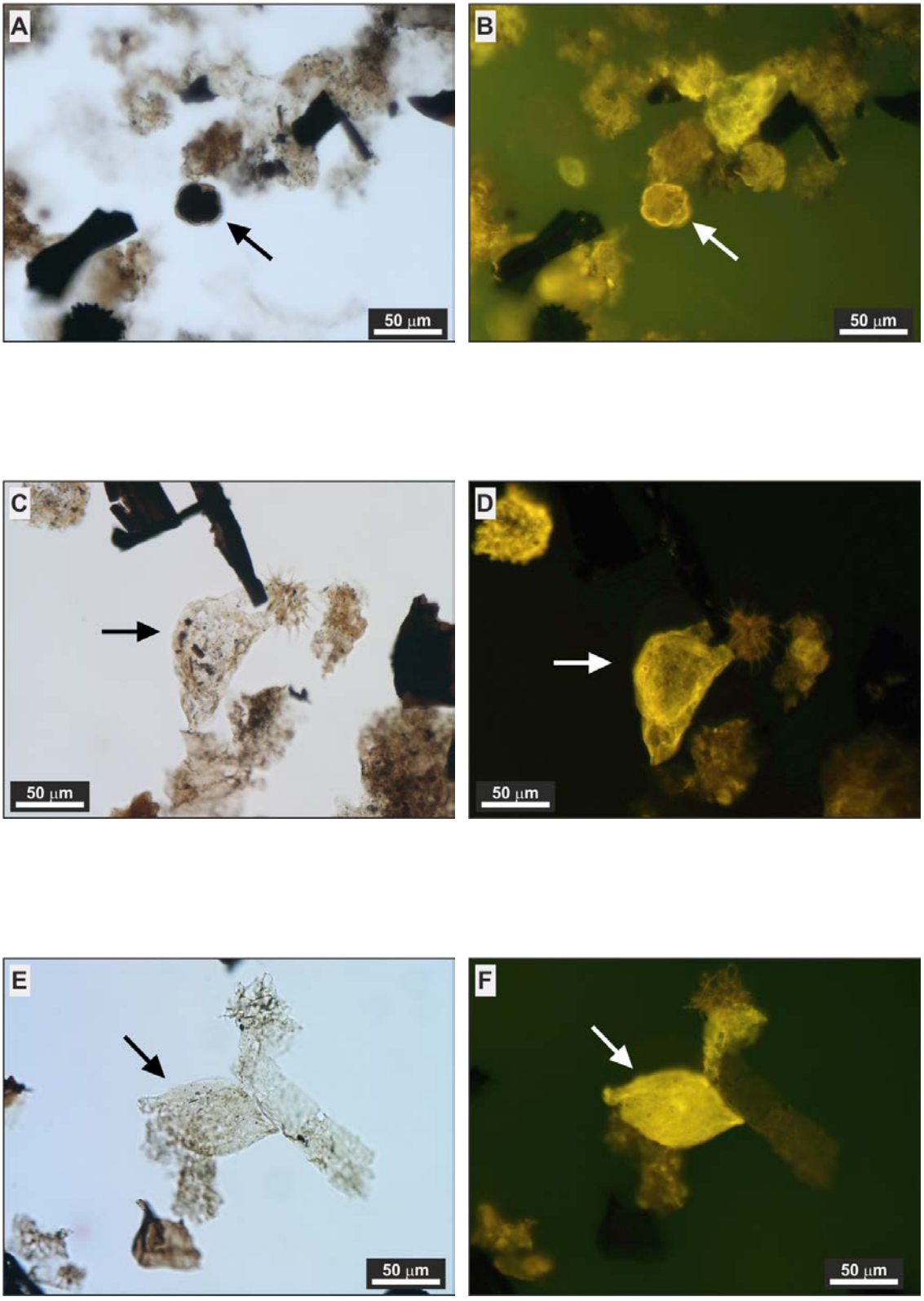
A
50 μm
B
50 μm
C
50 μm
D
50 μm
E
50 μm
F
50 μm

G. Acritarch (S10; FM, UV light).

H. Acritarch (S10; FM, blue light).

I. Prasinophyte algae, *Tasmanites* genus (S61; TWL).

J. Prasinophyte algae, *Tasmanites* genus (S61; FM, UV light).

B.3.1.4. Zoomorph subgroup

K. Foraminiferal Test-lining (S10; TWL).

L. Foraminiferal Test-lining (S12; TWL).

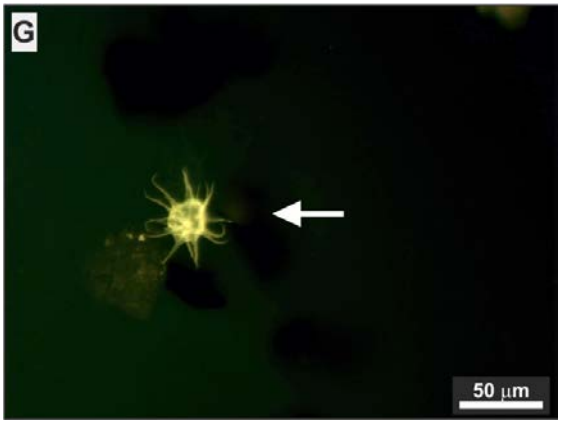
G
50 µm

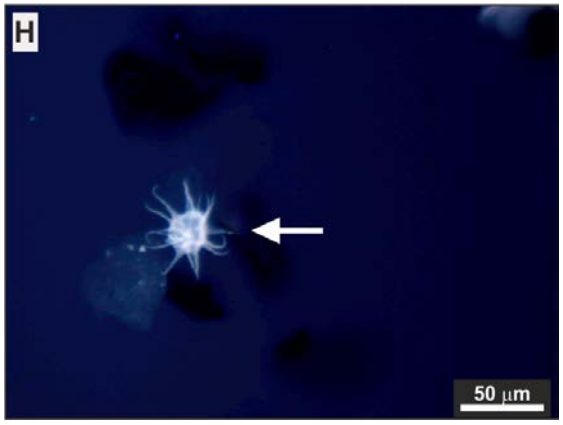
H
50 µm

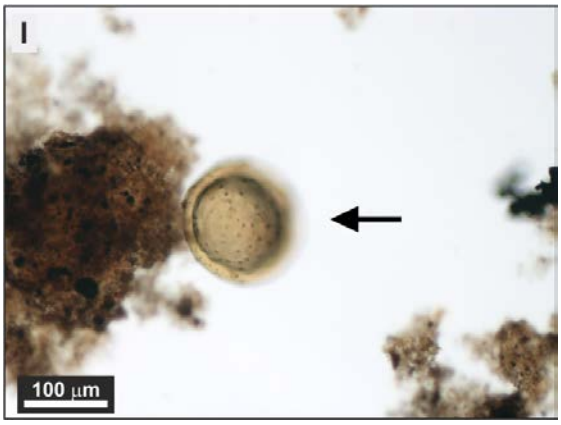
I
100 µm

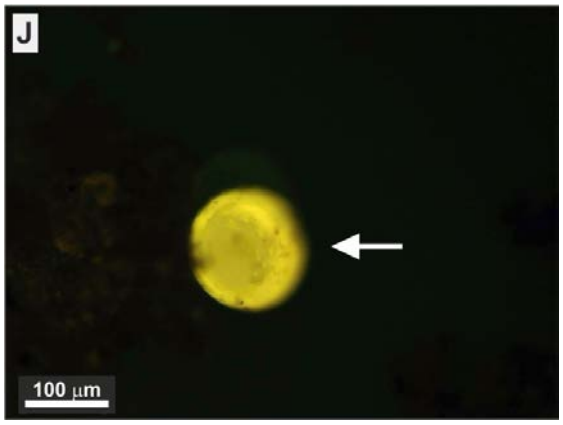
J
100 µm

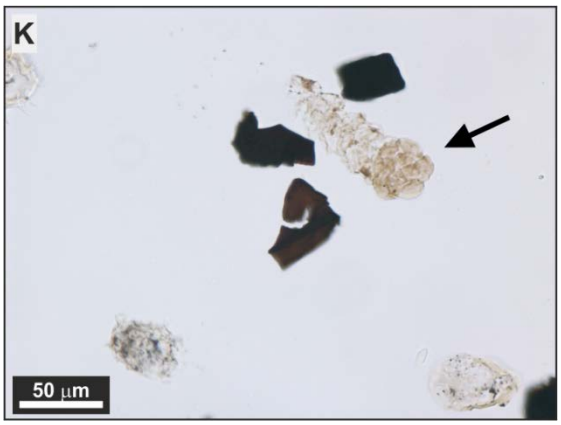
K
50 µm


L
50 µm

B.3.2. Caylus section – Quercy Basin

B.3.2.1. Sporomorph subgroup

A. Pollen grain of the genus *Classopollis* (Cay6; TWL).

B. Pollen grain of the genus *Classopollis* (Cay6; FM, UV light).

C. Spore with visible trilete (Cay7; TWL).

D. Spore with visible trilete (Cay7; FM, UV light).

E. Bisaccate pollen (Cay1; FM, UV light).

F. Polyad (Cay13; FM, UV light).

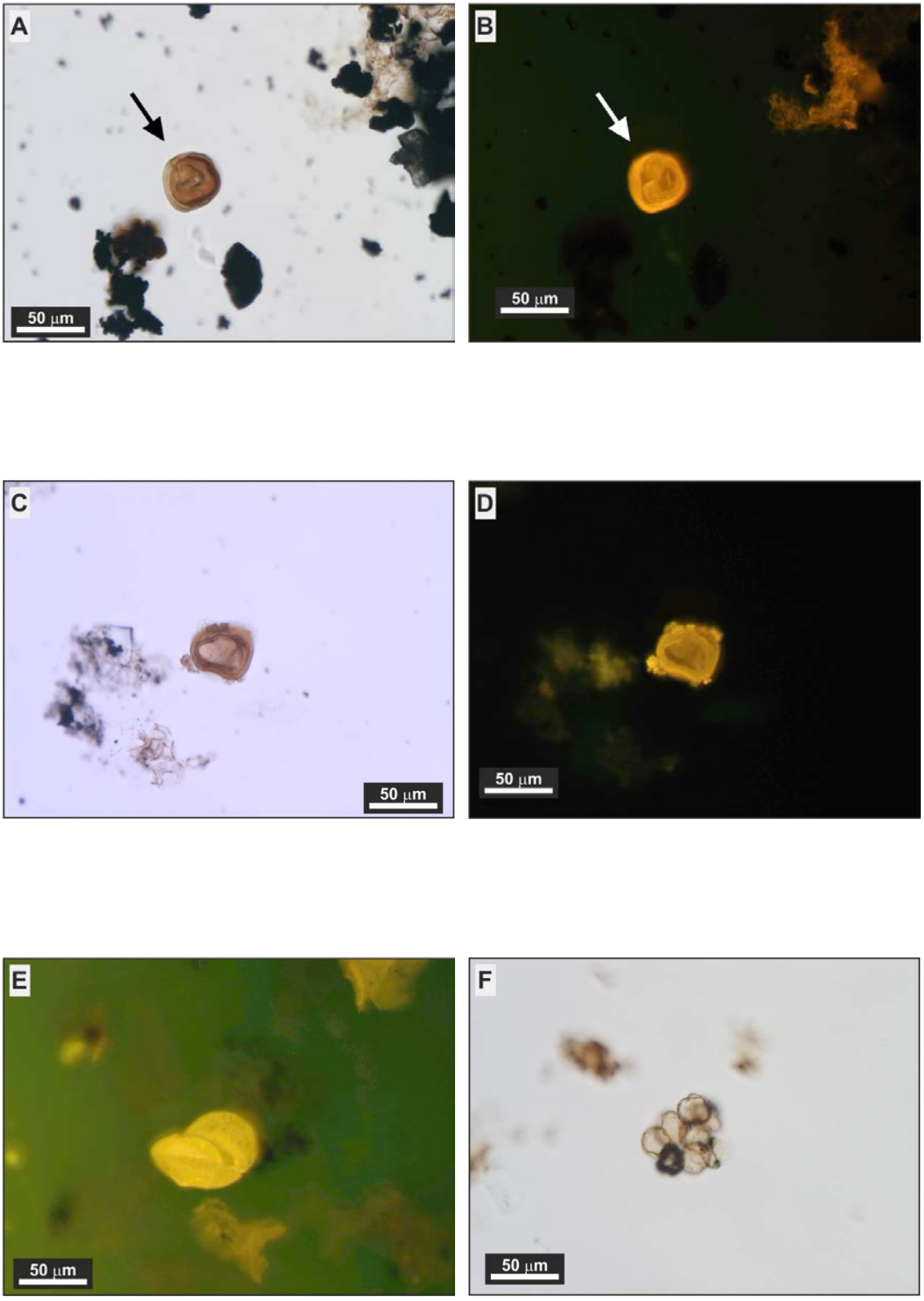
A
50 μm
B
50 μm
C
50 μm
D
50 μm
E
50 μm
F
50 μm

B.3.2.2. Freshwater microplankton subgroup

A. Gloeocapsomorpha (Cay10; TWL).

B. Gloeocapsomorpha (Cay10; FM, UV light).

B.3.2.3. Marine Microplankton subgroup

C. Dinoflagellate Cyst (Cay1; TWL).

D. Dinoflagellate Cyst (Cay1; FM, UV light).

E. Dinoflagellate Cyst (Cay7; TWL).

F. Dinoflagellate Cyst (Cay7; Dark field).

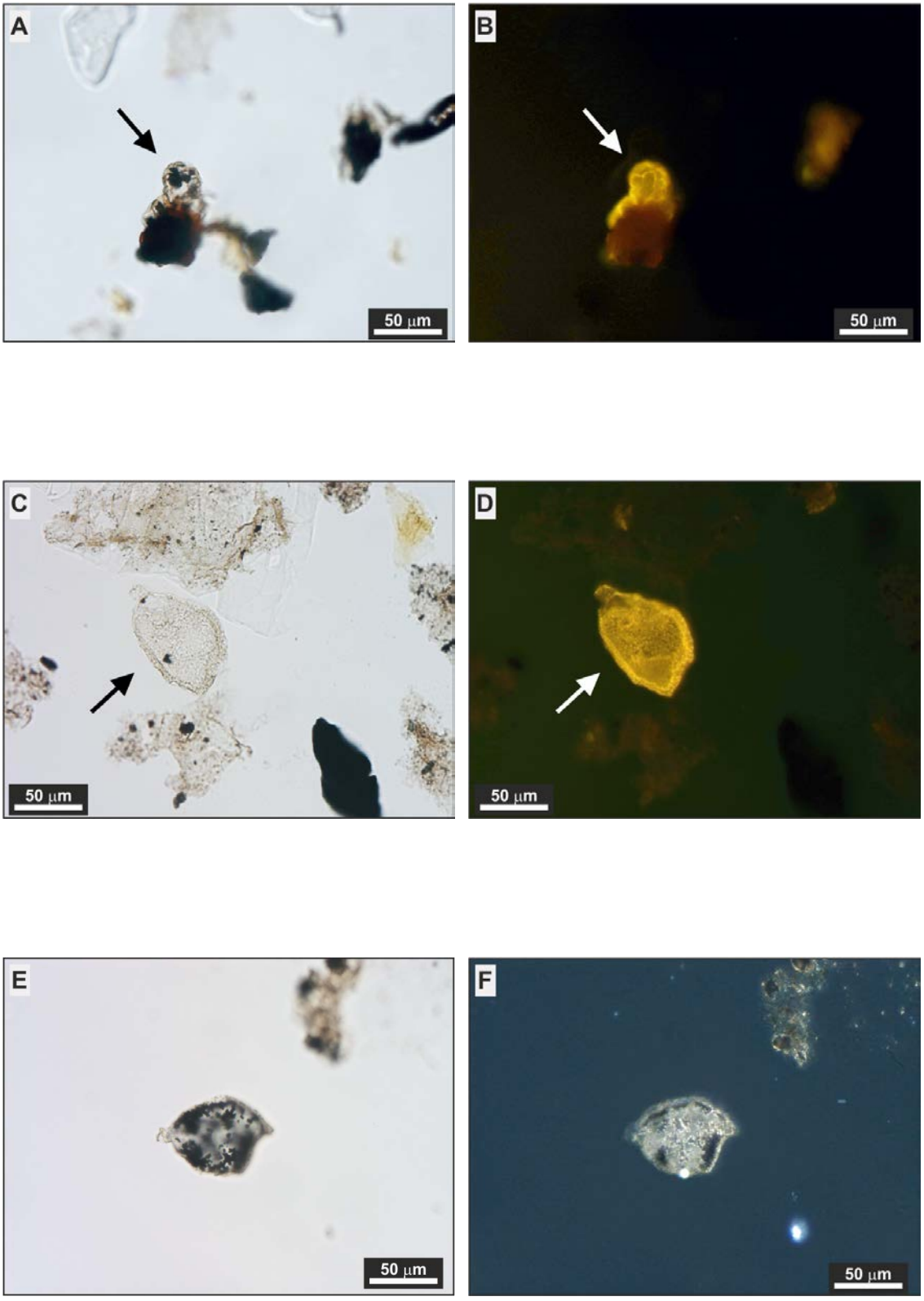
A
50 µm
B
50 µm
C
50 µm
D
50 µm
E
50 µm
F
50 µm

G. Acritarch (Cay6; TWL).

H. Prasinophyte algae, *Tasmanites* genus (Cay26; TWL).

I. Prasinophyte algae, *Cymatiosphaera* genus (Cay28; TWL).

J. Prasinophyte algae, *Cymatiosphaera* genus (Cay28; FM, blue light).

B.3.2.4. Zoomorph subgroup

K. Foraminiferal Test-lining (Cay6; TWL).

L. Foraminiferal Test-lining (Cay10; TWL).

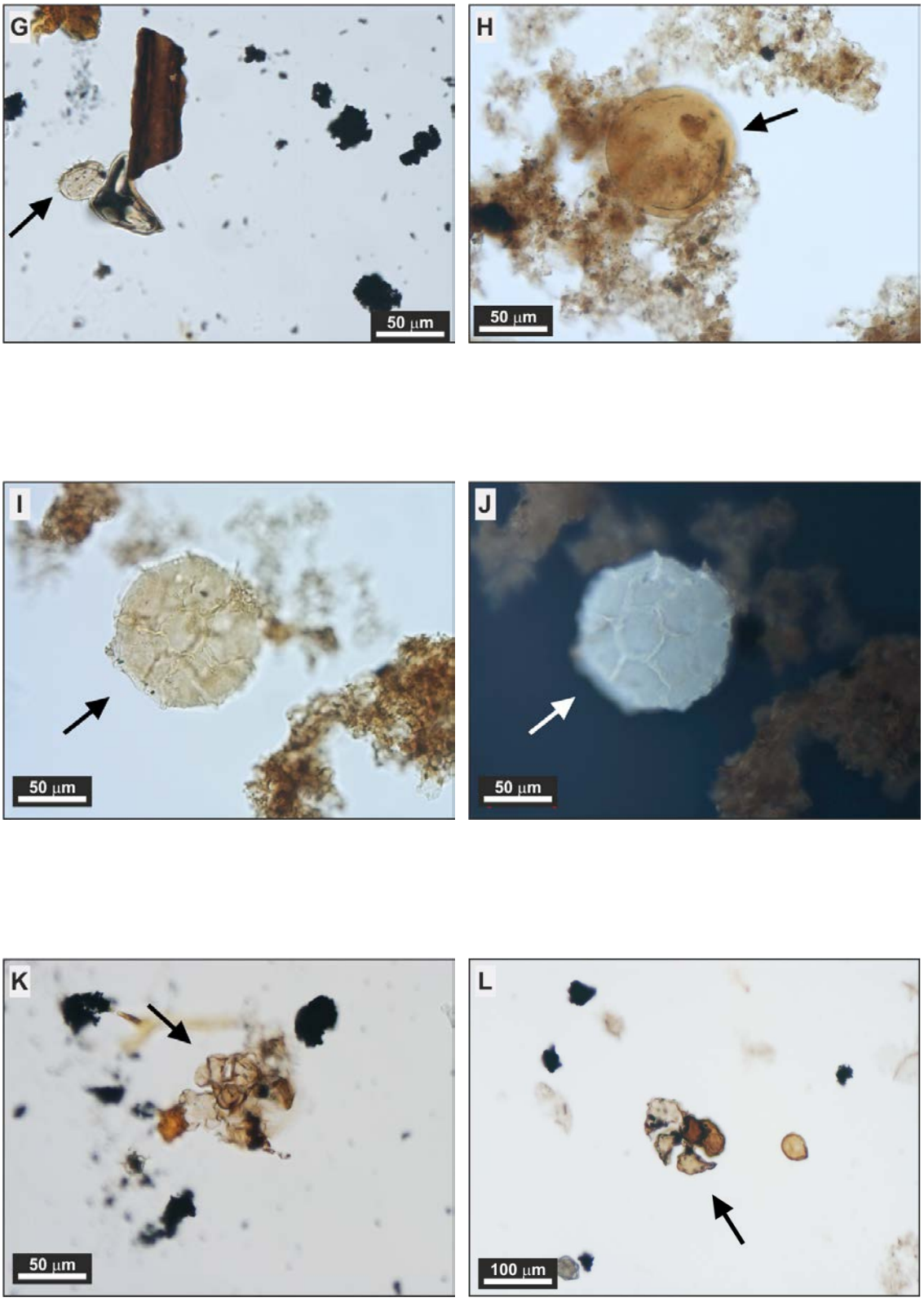
G
50 µm
H
50 µm
I
50 µm
J
50 µm
K
50 µm
L
100 µm

M. Amorphous Hydrozoan (Cay18; TWL).

N. Amorphous Hydrozoan (Cay18; FM, UV light).

O. Amorphous Hydrozoan (Cay20; TWL).

P. Amorphous Hydrozoan (Cay20; FM, UV light).

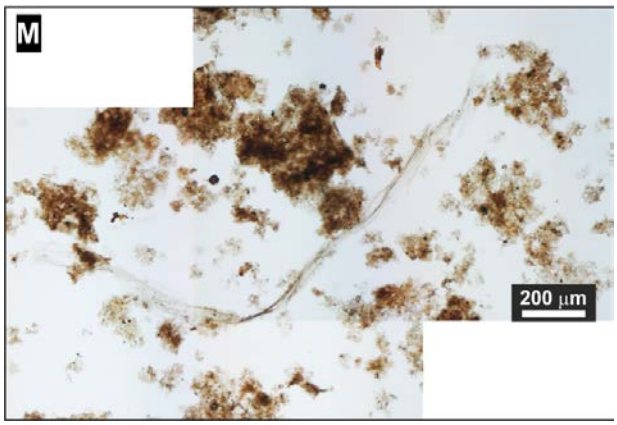
M
200 µm

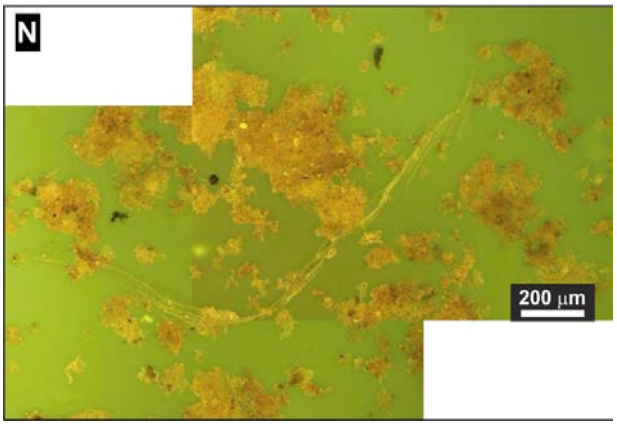
N
200 µm


O
200 µm

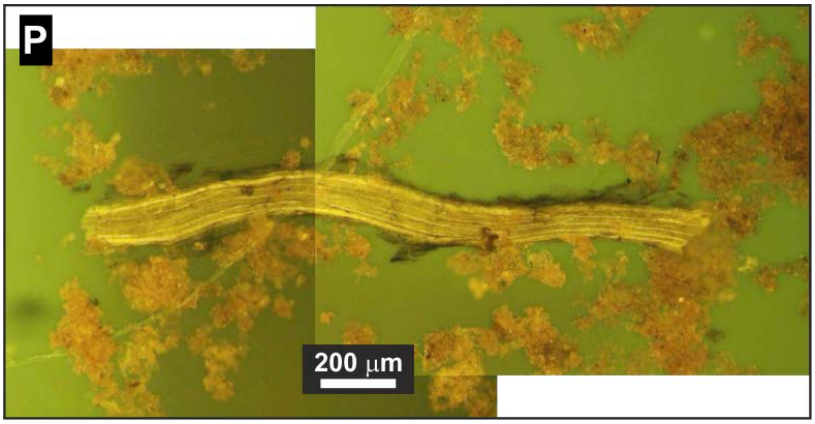
P
200 µm

B.3.3. Pont de Suert section – Pyrenean Basin

B.3.3.1. Sporomorph subgroup

A. Dyad (45PS; TWL).

B. Dyads (470PS; TWL).

C. Spore with visible trilete (100PS; TWL).

D. Spore with visible trilete (355PS; TWL).

E. Bisaccate pollen (75PS; TWL).

F. Polyad (380PS; TWL).

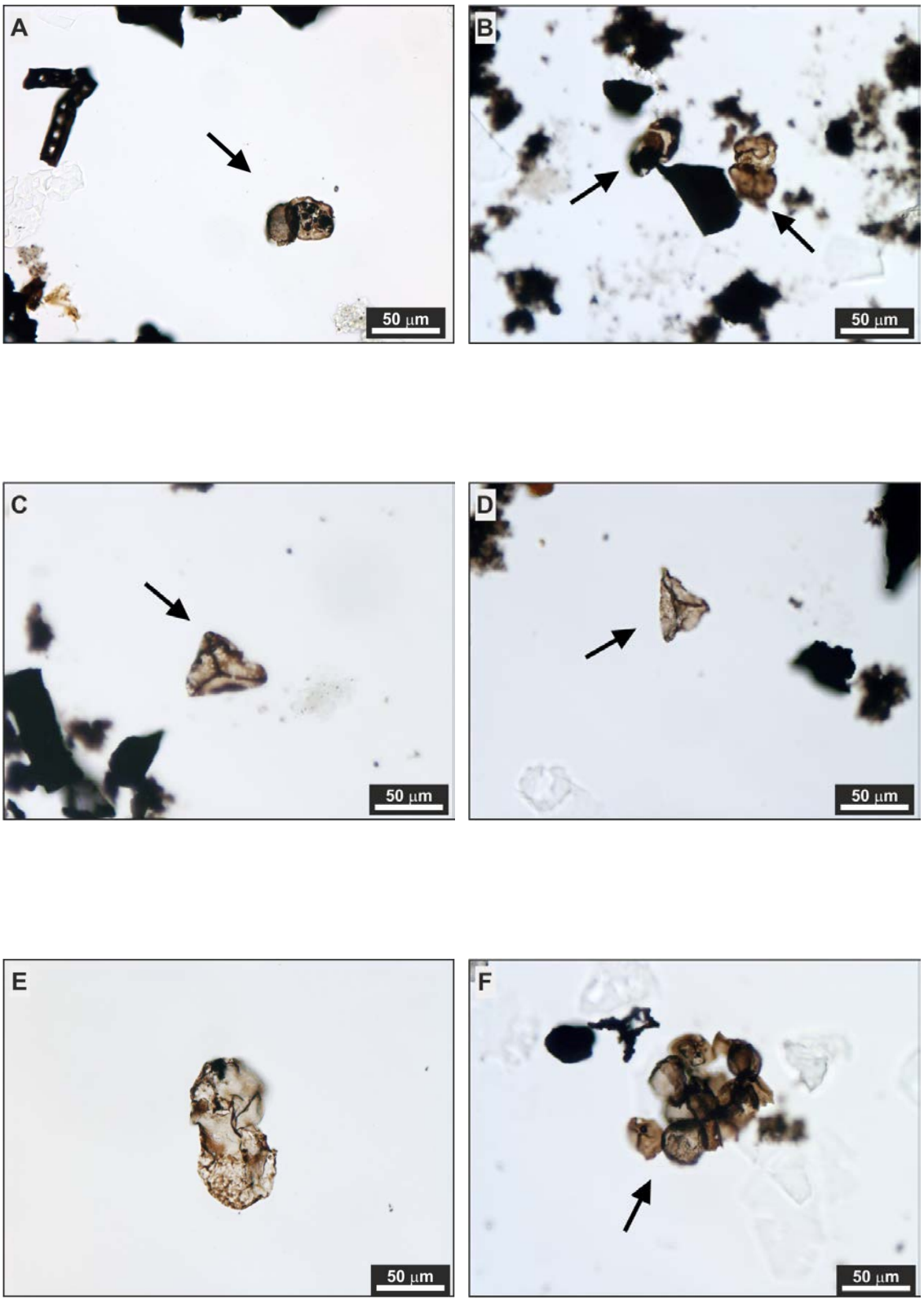
A
50 µm
B
50 µm
C
50 µm
D
50 µm
E
50 µm
F
50 µm

B.3.3.2. Marine Microplankton subgroup

A. Acritarch (20PS; TWL).

B. Acritarch (65-7PS; TWL).

C. Acritarch (115PS; TWL).

D. Dinoflagellate Cyst (65-7PS; TWL).

E. Prasinophyte algae, *Tasmanites* genus (115PS; TWL).

B.3.3.3. Zoomorph subgroup

F. Foraminiferal Test-lining (300PS; TWL).

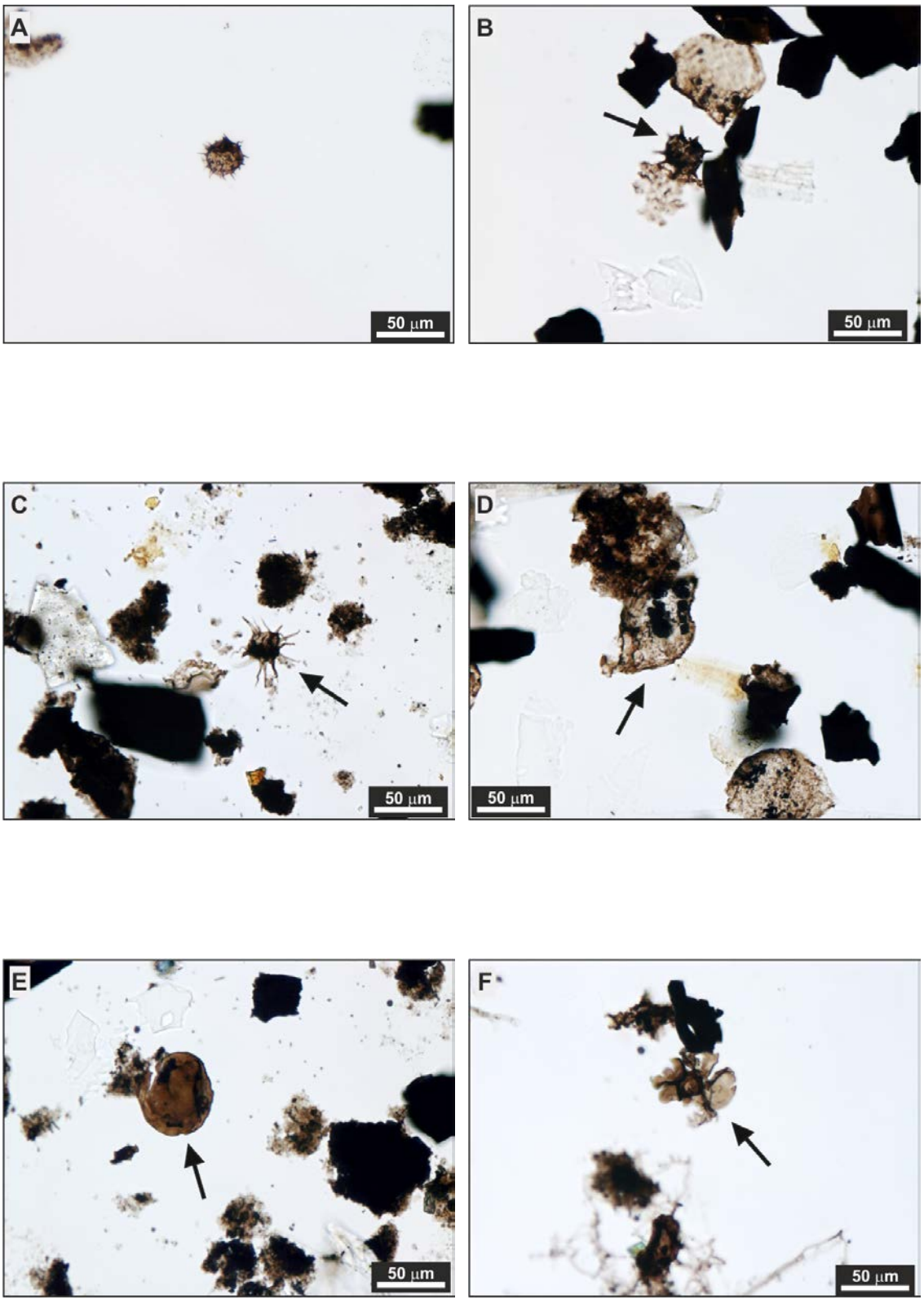
A
50 µm
B
50 µm
C
50 µm
D
50 µm
E
50 µm
F
50 µm

B.4. Zooclast Group

Zooclast Group is comprises animal-derived organic particles (e.g. graptolites, crustacean eggs, tintinnids, insect cuticle fragments, and other arthropod cuticle fragments) (Tyson, 1995). For more information about nomenclature and/or petrographic features see section 1.2.1.3. on Chapter II of this thesis.

B.4.1. Suèges section – Grands Causses Basin

A. Possible Hydrozoan polypoid form fragment showing lateral budding (S10; TWL).

B. Possible Hydrozoan polypoid form fragment showing lateral budding (S10; TWL).

C. Possible feature of tentacle form of hydrozoan polyp showing cells of cnidocytes (S10; TWL).

D. Possible Hydrozoan polypoid form fragment showing lateral budding (S10; TWL).

E. Possible Hydrozoan polypoid form fragment (S10; TWL).

F. Possible Hydrozoan polypoid form fragment showing lateral budding (S10; TWL).

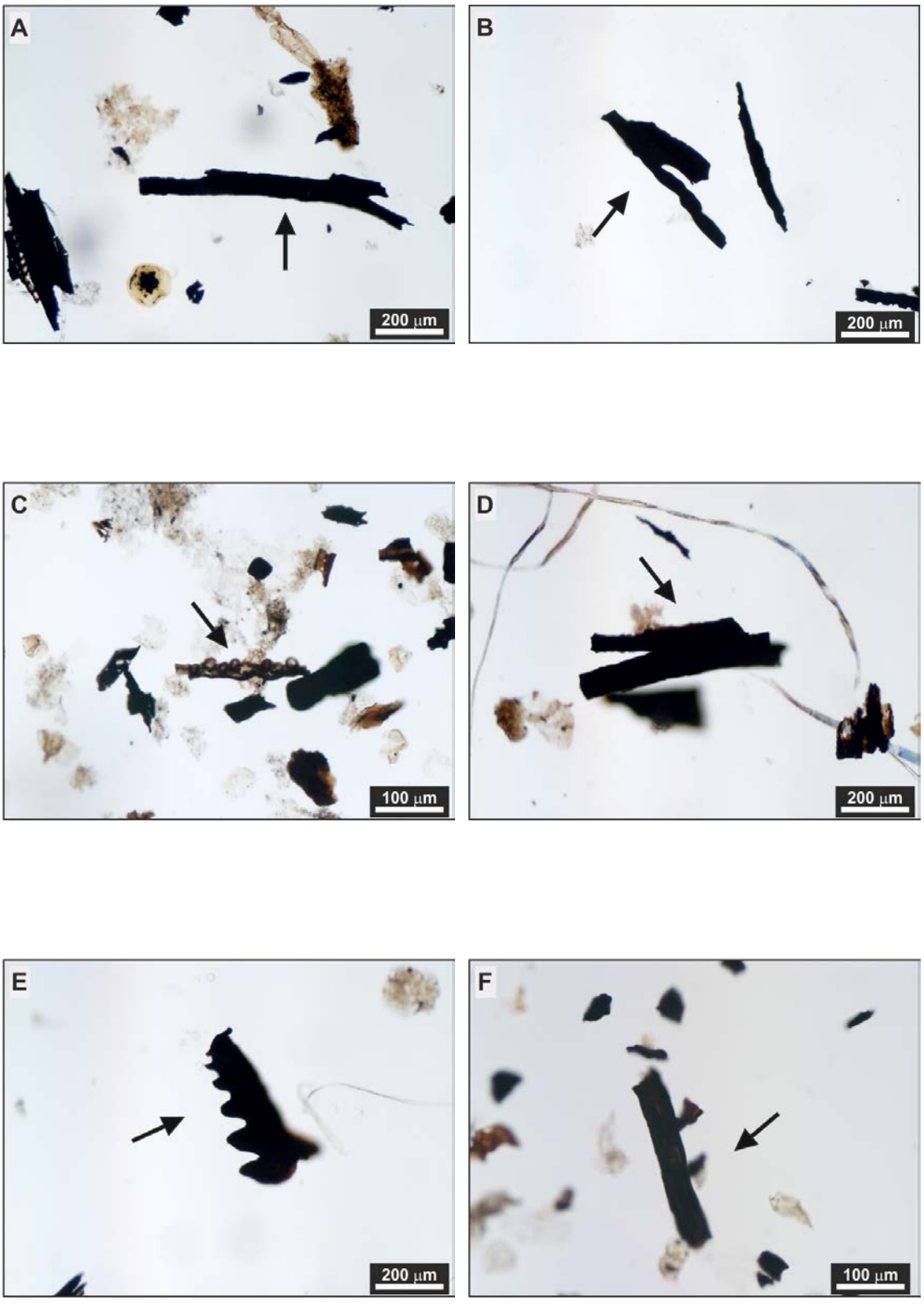
A
200 µm
B
200 µm
C
100 µm
D
200 µm
E
200 µm
F
100 µm

B.4.2. Caylus section – Quercy Basin

A. Possible Hydrozoan polypoid form fragment showing lateral budding (Cay28; TWL).

B. Possible Hydrozoan polypoid form fragment showing lateral budding (Cay28; FM, UV light).

C. Possible Hydrozoan polypoid form fragment showing lateral budding (Cay28; TWL).

D. Possible Hydrozoan polypoid form fragment showing lateral budding (Cay28; FM, UV light).

E. Detail of possible Hydrozoan polypoid form fragment showing lateral budding (Cay28; TWL).

F. Detail of possible Hydrozoan polypoid form fragment showing lateral budding (Cay28; FM, UV light).

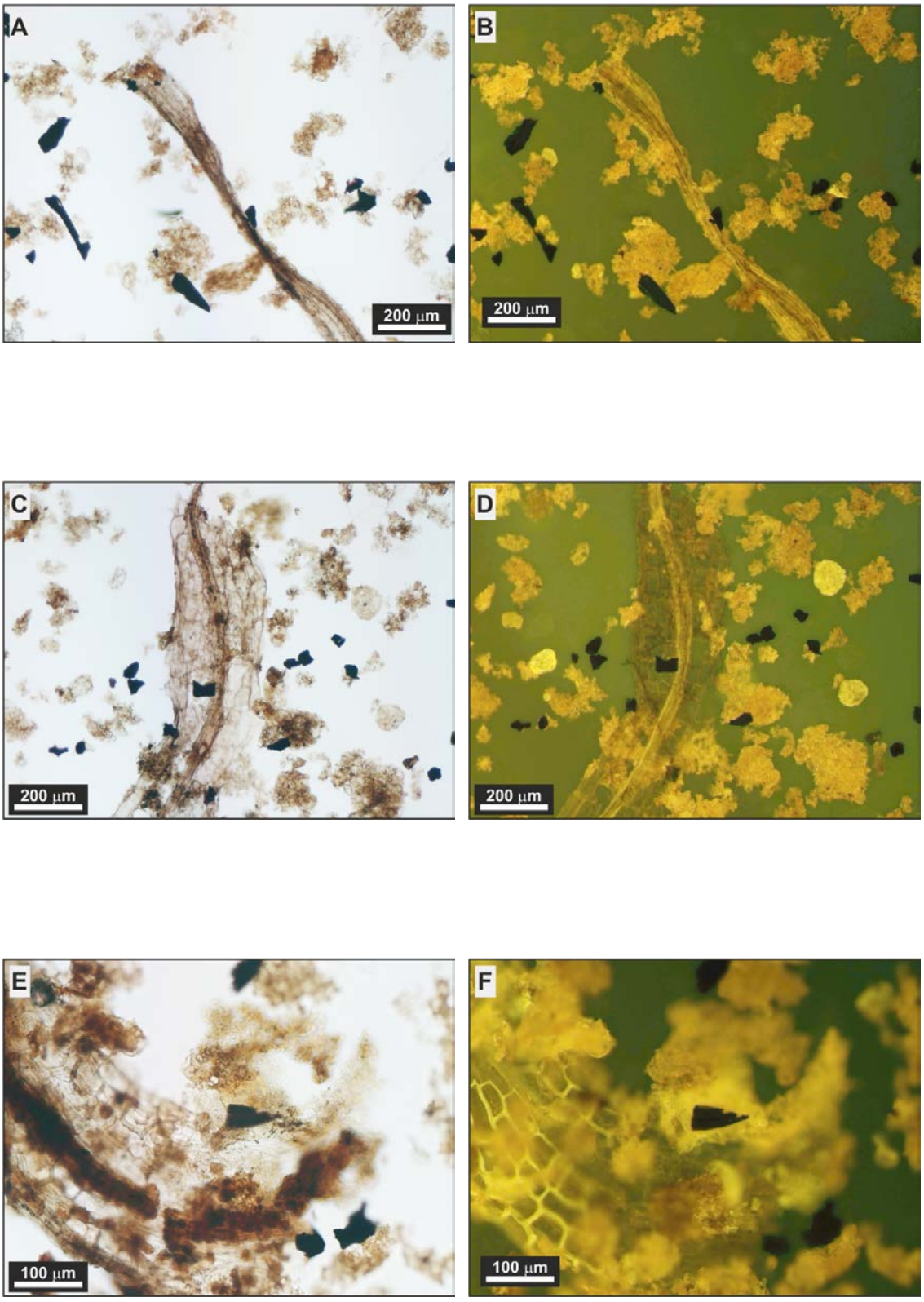
A
200 µm
B
200 µm
C
200 µm
D
200 µm
E
100 µm
F
100 µm

B.5. Kerogen concentrate aspects

A. Gloeocapsomorpha (S64; FM, blue light).

B. Gloeocapsomorpha (S64; RWL).

C. Hydrozoan medusae basal view (Cay28; FM, blue light).

D. Hydrozoan medusae lateral view (Cay28; FM, blue light).

E. Colonial Hydrozoan (S12; FM, blue light).

F. Colonial Hydrozoan (S12; FM, UV light).

G. Colonial Hydrozoan (S12, RWL).

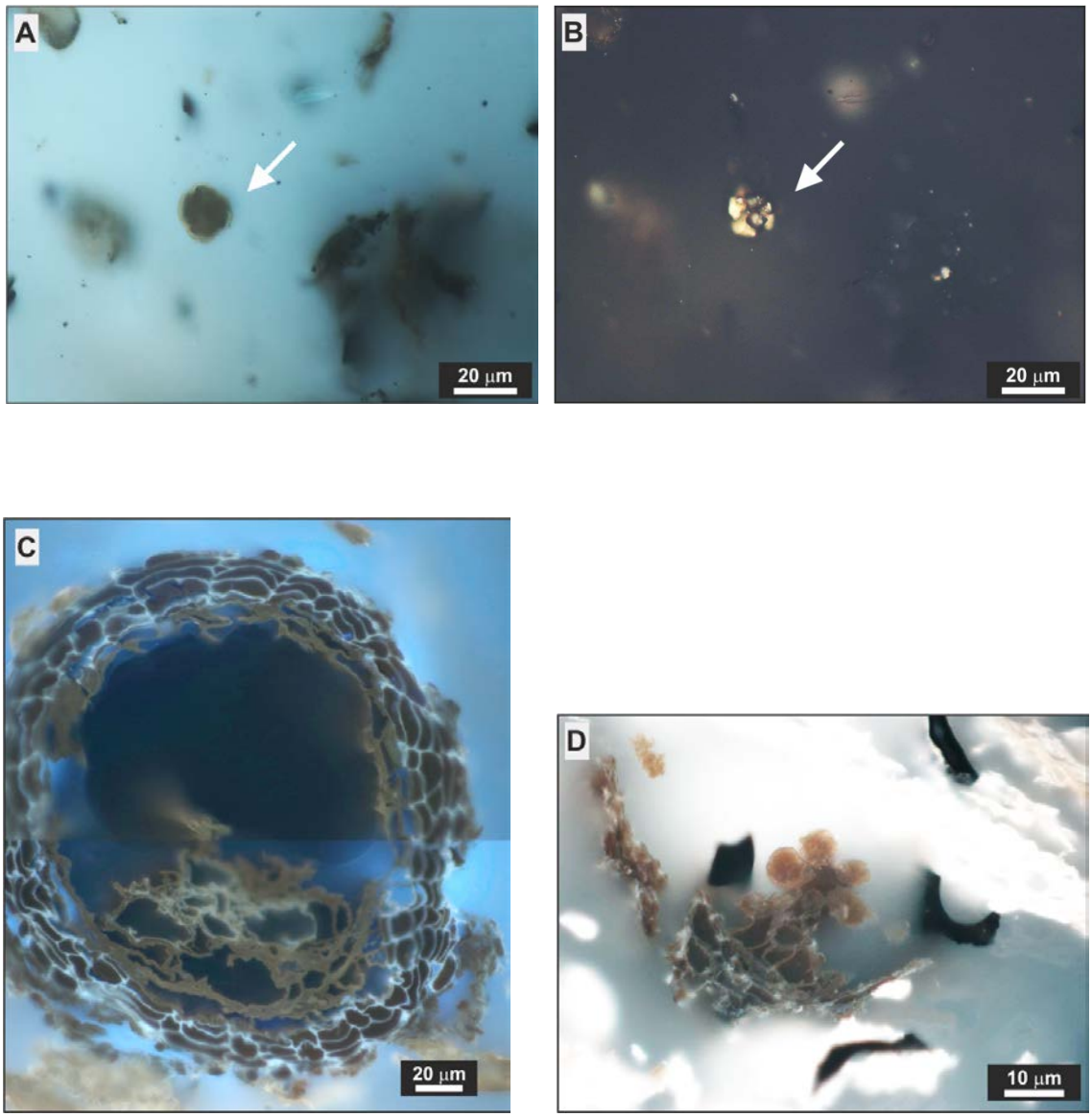
A
20 µm
B
20 µm
C
20 µm
D
10 µm

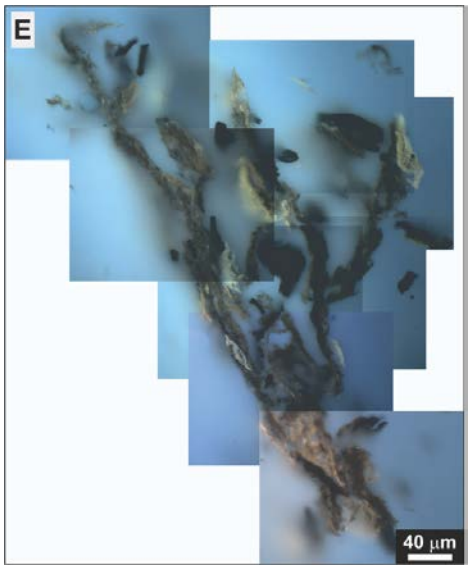
E
40 µm

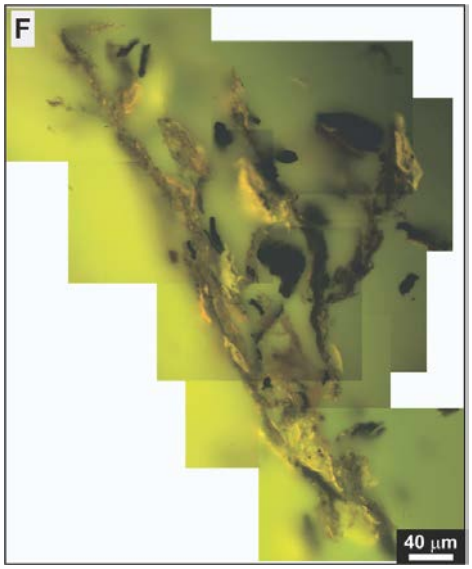
F
40 µm

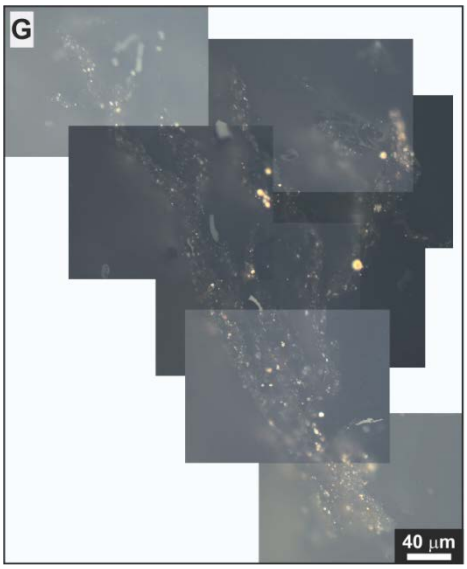
G
40 µm